BIOLOGICAL FUNCTIONS OF DOT1L, THE HISTONE H3 LYSINE 79 METHYLTRANSFERASE

By
Anh Tram Nguyen

A dissertation submitted to the faculty of the University of North Carolina at Chapel Hill in partial fulfillment of the requirements for the degree of Doctor of Philosophy in the School of Medicine Department of Biochemistry and Biophysics.

Chapel Hill
2011

Approved by

Yi Zhang
Brian Strahl
Leslie Parise
Henrik Dohlman
Da-zhi Wang

©2011
Anh Tram Nguyen
ALL RIGHTS RESERVED

ABSTRACT

Anh Tram Nguyen
Biological functions of DOT1L, the histone H3 lysine 79 methyltransferase
(Under the direction of Dr. Yi Zhang)

The enzymes responsible for epigenetic modifications are key regulators of gene expression, ultimately influencing cell fate and function during normal and oncogenic biological processes. These modifications can occur on histone proteins of the nucleosome to dynamically regulate chromatin structure at active and silenced gene loci. Methylation of histone H3 lysine 79 by Dot1 (disruptor of telomeric silencing) was first observed in yeast and serves as a marker for active transcription. Yeast Dot1 is a regulator of telomeric silencing, DNA damage repair, and the meiotic pachytene checkpoint. Additionally, Dot1 activity is regulated by the PAF complex, Rad6-Bre1 ubiquitination of H2B, and charge-based interaction with histone H4. Despite extensive research on Dot1, the role and regulation of mammalian homolog DOT1L (Like) is unclear. In this dissertation, I aim to understand the biological functions of DOT1L in both normal development and cancer.

In mouse, DOT1L has been linked to embryogenesis and erythropoeisis; however, the molecular mechanisms underlying these two processes require further elucidation. Germ-line disruption of DOT1L resulted in embryonic lethality with cardiovascular defects. In these studies, I demonstrate that DOT1L is required for normal heart function. Cardiac-specific knockout of DOT1L causes dilated cardiomyopathy (DCM), which can be rescued

by ectopic expression of minidystrophin. Mechanistically, DOT1L directly regulates transcription of dystrophin, which is critical for maintaining sarcolemma integrity and proper heart function. Finally, I provide evidence suggesting that malfunction of DOT1L activity may be a contributing factor in human DCM.

Previously, DOT1L has been linked to leukemogenesis caused by chromosomal rearrangements of the *MLL* gene, encoding a histone H3 lysine 4 methyltransferase. Specifically, DOT1L enzymatic activity is required for MLL-AF10, MLL-ENL, and MLL-AF4 *in vitro* leukemic transformation. In these studies, I sought to expand the repertoire of MLL-fusion oncoproteins that utilize DOT1L by investigating MLL-AF9 leukemogenesis. Through *in vitro* and *in vivo* assays, I demonstrate that initial transformation by MLL-AF9 and maintenance of leukemic stem cell identity require DOT1L activity. These data support a universal mechanism involving mis-targeting of DOT1L and H3K79 hypermethylation for the up-regulation of leukemia-associated genes. Thus, DOT1L serves as a promising candidate for targeted therapeutics to treat MLL-related leukemias.

To my family for their unwavering support

ACKNOWLEDGEMENTS

I would first like to thank my parents, sisters, brother-in-law, and nephew for their overwhelming support. I thank Christopher, my best friend and confidant, who has always been there for me, no matter the distance between us. Although experimental demands have required me to put a hold on life outside of the lab more often than not, they have all stood by me with great understanding and love.

I'd also like to thank my advisor, Dr. Yi Zhang for all his support during my Ph.D. training. Due to his unfaltering belief and confidence in me as a scientist, I was given the rare opportunity to independently design and pursue my own project. I will carry with me the invaluable experience and lessons I learned along the way throughout my scientific career.

To the Zhang lab, both past and present members, I thank you for your friendship, advice, wonderful discussions, and company on those late nights and weekends. I especially thank former post-doc associate Dr. Yuki Okada, who was the best mentor a student could ask for. Her incredible knowledge and scientific drive amazes me and has helped shape me into the scientist I am today.

I thank my committee members, Drs. Brian Strahl, Da-zhi Wang, Henrik Dohlman, and Leslie Parise, for their advice, encouragement, and willingness to meet with me whenever I

needed someone to talk to. I'd especially like to thank Dr. Da-zhi Wang. Even though his lab moved to Children's Hospital Boston, he's been fully supportive and continued to serve on my committee, traveling back to Chapel Hill when needed.

Finally, I would like thank my fellow graduate students. They have lent me their ears during my many trials and have celebrated with me during all the triumphs. Only they can truly understand life as a graduate student. I am indebted to them for their friendships over the years, which has made this journey all the more enjoyable.

TABLE OF CONTENTS

LIST OF TABLES

Table

LIST OF FIGURES

Figure

LIST OF ABBREVIATIONS

AEP	AF4 family/ENL family/P-TEFb complex
ALL	acute lymphoid leukemia
AML	acute myeloid leukemia
BMCs	bone marrow cells
BMT	bone marrow transplantation
CHF	congestive heart failure
ChIP	chromatin immunoprecipitation
CKO	cardiac conditional knockout
Cre-ERT2	Cre-recombinase-Oestrogen-Receptor-T2 allele
DCM	dilated cardiomyopathy
DGC	dystrophin-glycoprotein complex
Dmd	dystrophin
DNMT	DNA methyltransferase
DOT1	yeast disruptor of telomeric silencing
DOT1L	mammalian disruptor of telomeric silencing-like
DSBs	double strand breaks
EAP	elongation assisting proteins
ECHO	echocardiography
EKG	electrocardiography
FACS	fluorescence activated cell sorting
H3K79	histone H3 lysine 79
H3K79me	methylated histone H3 lysine 79

H3K79me2/3	di- and tri-methylated histone H3 lysine 79
H2B-K123ub	ubiquitinated histone H2B lysine 123
HMTase	histone methyltransferase
Hoxa	homeobox A cluster
HPCs	hematopoietic progenitor cells
KD	knockdown
KO	knockout
LCs	leukemic cells
LSCs	leukemic stem cells
Meis1	myeloid ecotropic viral integration site 1
MLL	mixed lineage leukemia
OM-LZ	octapeptide motif and leucine zipper
PAF complex	polymerase II-associated factor complex
Pol II	RNA polymerase II
rAAV-miniDmd	recombinant adeno-associated virus-CMV-DystrophinΔ3990
RT-qPCR	reverse transcriptase-quantitative polymerase chain reaction
SAM	S-adenosyl methionine
SET	Su(var)3-9, Enhancer-of-zeste, Trithorax
SIR	silent information regulator
SRF	serum response factor
TSS	transcription start site
Ttn	Titin
WT	wild type

wt/wt	DOT1L$^{wt/wt}$;Cre-ER^{T2}
2l/1l	DOT1L$^{2lox/1lox}$;Cre-ER^{T2}

Chapter 1

INTRODUCTION

Epigenetic contribution to cellular diversity

Every cell within an organism is derived from a single totipotent fertilized egg. Although each cell contains the same exact genetic information, very different cellular identities arise during development to ultimately form all the tissues and organs of the organism. How this remarkable phenomenon occurs in the developing embryo was commented on by Conrad Waddingtion in his book, *An Introduction to Modern Genetics*.

> It is, surely, obvious that the fertilized egg contains constituents which have definite properties which allow only a certain limited number of reactions to occur; in so far as this is true, one may say that development proceeds on a basis of the "preformed" qualities of the fertilized egg. But equally it is clear that the interaction of these constituents gives rise to new types of tissue and organ which were not present originally, and in so far development must be considered as "epigenetic". (Waddington 1939)

As such, the term "epigenetics" is credited to Conrad Waddington who later defined it as "the branch of biology which studies the causal interactions between genes and their products, which bring the phenotype into being" (Waddington 1942). Epigenetics has now evolved to refer to the heritable changes in gene expression that occur without changes in the underlying DNA sequence. Today we understand that the dynamic nature of chromatin is a major contributor to the establishment, maintenance, and variances in differential gene expression within any given cell type.

Two meters of eukaryotic DNA must be tightly condensed into chromatin to fit within the cell nucleus. Nucleosomes, containing 147 bp of DNA wrapped around a histone octamer (H3/H4 heterotetramer and two H2A/H2B dimers) serve as the basic building block for compaction into chromatin (Van Holde, Allen et al. 1980; Luger, Mader et al. 1997; Kornberg and Lorch 1999; Zhang and Dent 2005). In this highly compressed state, all DNA-

dependent processes, including replication and transcription, are hindered.

The four core histones, H3, H4, H2A, and H2B, are comprised of a globular domain and unstructured NH_3-, COOH- tails that protrude from the nucleosome center (Luger, Mader et al. 1997; Martin and Zhang 2005; Zhang and Dent 2005). These tails may influence histone-DNA interactions as well as histone-histone interactions to dynamically control the accessibility state of DNA for transcription. Histones undergo post-translational modifications such as acetylation, methylation, phosphorylation, ubiquitination, sumoylation, and ribosylation. These modifications influence chromatin structure and function directly or indirectly through the recruitment of effector proteins at heterochromatic (silenced genes) and euchromatic (active genes) regions (Strahl and Allis 2000; Martin and Zhang 2005; Kouzarides 2007).

The epigenetic factors responsible for these histone modifications are key regulators of gene expression, cell lineage commitment, and oncogenesis. In particular, methylation of histones has been shown to be critical in development (Cavalli 2006; Minard, Jain et al. 2009). Altered methylation by disruption of histone methyltransferase (HMTase) activity affects the expression level of both tumor suppressors and oncogenes, and has been implicated in hematologic, breast, prostate, and lung cancers (Feinberg, Oshimura et al. 2002; Handel, Ebers et al. 2009). Specifically, H3 methylation is important for X-inactivation, cell fate, terminal differentiation, and the spatio-temporal patterning of *Hox* genes during embryogenesis (Cavalli 2006; Minard, Jain et al. 2009).

Histone lysine methylation

In mammals, lysine methylation exists in the mono-, di-, and tri- states, occurring on histone H3 at residues K4, K9, K27, K36, and K79 and on histone H4 at residue K20 (Zhang and Reinberg 2001; Martin and Zhang 2005). These marks serve as a platform for the recruitment of effector proteins to regulate transcription. For example, H3K4me recruits activating proteins such as remodeling factors Chd1 and NURF and histone acetyltransferase complexes SAGA and NuA3 as well as the repressive deacetylase complex Sin3-Ndac1 (Berger 2007). Additionally, H3K36me is thought to recruit a histone deacetylase complex (Carrozza, Li et al. 2005; Joshi and Struhl 2005; Keogh, Kurdistani et al. 2005), while H3K9me recruits HP1 for the formation of pericentromeric heterochromatin (Bannister, Zegerman et al. 2001; Lachner, O'Carroll et al. 2001; Nakayama, Rice et al. 2001). The multitude of effector or "reader" proteins and their associated binding modules has been extensively reviewed by Taverna *et al.* (Taverna, Li et al. 2007).

Histone methylation results from the transfer of a methyl group from S-adenosylmethionine (SAM) to nitrogen atoms of lysine and arginine residues. Two classes of lysine methyltransferases exist. The first class of proteins contain an evolutionarily conserved SET (Su(var)3-9, Enhancer of Zeste (E(Z)), Trithorax (trx)) domain, first identified in *D. melanogastor* (Zhang and Reinberg 2001; Zhang and Dent 2005). The second class does not possess a SET domain, but rather, a catalytic methylase fold resembling that of class I methyltransferases (Ng, Feng et al. 2002; Min, Feng et al. 2003; Schubert, Blumenthal et al. 2003). Methylation at H3K9, H3K27, and H4K20 demarcate transcriptionally inactive genes, while H3K4, H3K36, and H3K79 methylation are indicative of actively transcribed genes

(Kouzarides 2002; Peterson and Laniel 2004; Martin and Zhang 2005).

Dot1-mediated H3K79 methylation marks active transcription

Dot1 (disruptor of telomeric silencing) is the only member of the second class of lysine methyltransferases. The *DOT1* gene contains four sequence motifs – I, post I, II, and III – that form an open α/β structure composed of a seven-stranded β-sheet, which is characteristic of the catalytic methylase fold found in arginine methylases (Cheng and Roberts 2001; Dlakic 2001; Min, Feng et al. 2003; Sawada, Yang et al. 2004). Despite its structure, yeast Dot1 and its mammalian homolog DOT1L, are histone H3 lysine 79 (H3K79) methyltransferases, whose substrate site is located within the globular domain of histone H3 instead of its N-terminal tail (Feng, Wang et al. 2002; Lacoste, Utley et al. 2002; van Leeuwen, Gafken et al. 2002; Zhang, Hayashizaki et al. 2004).

Dot1 was originally identified in *S. cerevisiae* as a regulator of telomeric silencing (Singer, Kahana et al. 1998). Conflicting data supports a requirement for both the presence and absence of H3K79 methylation to mediate association of SIR (silent information regulator) proteins, heterochromatic formation, and telomeric silencing in a mechanism reminiscent of position-effect-variegation observed in *D. melanogastor*. Surprisingly, over-expression and deletion of Dot1 and mutation of H3K79 results in a loss of telomeric silencing (Singer, Kahana et al. 1998; Ng, Feng et al. 2002; Ng, Ciccone et al. 2003). In all three cases, the level of SIR proteins bound at telomeres is reduced thus limiting their ability to silence genes. Since ~90% of the yeast genome is methylated at H3K79 and the remaining ~10% account for transcriptionally silenced genes, it is thought that H3K79 methylation by Dot1

affects the distribution of SIR proteins and serves as a euchromatic mark (Laurenson and Rine 1992; van Leeuwen, Gafken et al. 2002).

Data from several genome-wide profile analyses also support a role for H3K79 methylation in active transcription. Using chromatin immunoprecipitation (ChIP) coupled with gene expression microarray analysis, Schübeler *et al.* mapped the chromatin modification status of over 5000 *Drosophila* genes. They discovered that the presence of histone acetylation, H3K4me2, H3K4me3, and H3K79me2 positively correlate with active gene transcription (Schubeler, MacAlpine et al. 2004). Another study used ChIP-Chip with mouse 3T3 cells to show that H3K79 methylation marks are localized within the body of transcribed genes and that the amount of enrichment correlated with expression level (Steger, Lefterova et al. 2008). Furthermore, Zhao and colleagues used human CD4+ T cells to show that all levels of H3K79 methylation coincide with active transcription (Wang, Zang et al. 2008). Collectively, analyses of yeast, fly, mouse, and human genomes all reveal that H3K79 methylation is marker of euchromatin.

Trans-histone crosstalk regulates Dot1 enzymatic activity

During characterization of DOT1L enzymatic activity, it was observed that DOT1L preferentially methylates H3K79 in the context of nucleosomes rather than core histones or recombinant H3 (Feng, Wang et al. 2002). Based on the nucleosome structure, K79 lies within loop 1 that connects the first and second α-helices of the histone H3 globular domain and is in close proximity to histone H2B lysine 123 (H2B-K123) (Luger, Mader et al. 1997).

The unique position of H3K79 suggested that a trans-histone crosstalk may play a role in regulating DOT1L enzymatic activity.

In yeast, histone H2B is monoubiquitinated at lysine 123 (H2B-K123ub). This modification is catalyzed by the ubiquitin-conjugating enzyme Rad6 and its E3 ubiquitin ligase Bre1 (Robzyk, Recht et al. 2000; Wood, Krogan et al. 2003). Shortly after the characterization of Dot1 enzymatic activity, it was discovered that Rad6-mediated H2B-K123 ubiquitination is required for H3K79 methylation (Briggs, Xiao et al. 2002; Ng, Xu et al. 2002). This trans-histone regulation did not appear to play a general role in histone methylation as H3K36 methylation is unaffected by Rad6 deletion (Briggs, Xiao et al. 2002; Ng, Xu et al. 2002). The role of H2B ubiquitination in trans-histone crosstalk is evolutionarily conserved as human Bre1 was found to regulate ubiquitination of H2B-K120, corresponding to K123 in yeast, and, subsequently, methylation of and H3K79 (Ng, Robert et al. 2003). The PAF complex, composed of the proteins Rtf1, Paf1, Cdc73, Leo1, and Ctr9, associates with the elongating form of RNA Pol II (Costa and Arndt 2000; Mueller and Jaehning 2002; Pokholok, Hannett et al. 2002; Squazzo, Costa et al. 2002) and also regulates Dot1-mediated H3K79 methylation (Krogan, Dover et al. 2003). Mechanistically, Rtf1 and Paf1 are required for Rad6-Bre1 ubiquitination of H2B-K123, which, in turn, modulates H3K79 methylation (Krogan, Dover et al. 2003; Ng, Dole et al. 2003; Wood, Schneider et al. 2003).

In addition to H2B-K123 ubiquitination, interaction with histone H4 also regulates Dot1 enzymatic activity. Mutational analysis identified a basic patch within histone H4 tail ($R_{17}H_{18}R_{19}$) that is required for Dot1 interaction with histone H4 and for H3K79 methylation

but not H3K4 or H3K36 methylation (Fingerman, Li et al. 2007). Interestingly, post-translational modifications of histone H4, including acetylation and phosphorylation, have no effect on H3K79 methylation (Altaf, Utley et al. 2007).

Although Dot1 retains the ability to bind nucleosomes in the absence of histone H4 tail or its basic patch, loss of these two regions still affect H3K79 methylation (Altaf, Utley et al. 2007; Fingerman, Li et al. 2007), suggesting allosteric regulation of Dot1 enzymatic activity through $R_{17}H_{18}R_{19}$ binding. Since the positive charge of $R_{17}H_{18}R_{19}$ was most critical in regulating H3K79 methylation, it was reasoned that a negatively charged, acidic patch may exist in Dot1. Correspondingly, an acidic patch, EDVDE, within an exposed loop structure of the C-terminus of yeast Dot1 (aa 557-561) was shown to be required for Dot1 interaction with histone H4 tail and for di- and tri-methylation of H3K79 (Fingerman, Li et al. 2007). Collectively, these data exemplify intra-nucleosome cross-talk to regulate HMTase activity for tight control of gene expression.

Dot1 and the cell cycle response to DNA damage

Prior to cell division, the entire genome of a proliferating cell must be replicated in a highly efficient and accurate manner to preserve genetic integrity and genome stability. Therefore, progression through the cell cycle is tightly regulated by a number of checkpoints that become activated in response to DNA damage induced by both intrinsic and extrinsic factors. Several studies have linked Dot1 and its associated H3K79 methylation marks to DNA damage checkpoint function and repair in response to numerous extrinsic-induced injuries.

Human 53BP1 protein contains a tandem tudor domain that binds to methylated H3K79 and is recruited to DNA double strand breaks (DSBs). Strikingly, mutation of the tudor domain and Lys 79 of H3 or suppression of DOT1L all inhibit recruitment of 53BP1 to DSBs. Since H3K79 methylation levels do not accumulate upon DNA damage, it is believed that DSBs induce changes in chromatin structure to expose methylated H3K79, which are then recognized by 53BP1 (Huyen, Zgheib et al. 2004). The interaction of 53BP1 to H3K79me is evolutionarily conserved as Rad9, the yeast ortholog of 53BP1, also binds to H3K79me via its Tudor domain. In addition, loss of Dot1-mediated H3K79 methylation disrupts the activation and recruitment of Rad9 and phosphorylation of Rad53 upon ionizing radiation (IR) damage (Wysocki, Javaheri et al. 2005). Budding yeast cells treated with IR at G1 typically undergo a G1 checkpoint delay. Interestingly, Dot1 mutants are defective in G1 and intra-S phase checkpoints and progress through the cell cycle at a normal rate even after IR induced DNA damage (Wysocki, Javaheri et al. 2005). In addition, mutations that affect Dot1 methyltransferase activity such as disruption of H2B-K123 ubiquitination or mutation of H3K79 display the same checkpoint delay defects in response to multiple genotoxic stresses (Giannattasio, Lazzaro et al. 2005; Game, Williamson et al. 2006; Chernikova, Dorth et al. 2010).

In response to IR damage, the DOT1/Rad6/Bre1 pathway mediates G1 homologous recombination repair (Game, Williamson et al. 2006). Although *dot1* deletion mutants do not display a G2 arrest phenotype (Game, Williamson et al. 2006), Dot1 is required for Rad9 recruitment to repair foci at G2 upon IR-induced damage (Toh, O'Shaughnessy et al. 2006). It is proposed that Dot1-mediated H3K79 methylation plays two distinct roles during Rad9

DNA damage response, the first being G1/S checkpoint activation and the second being late G2 DNA repair (Grenon, Costelloe et al. 2007).

Repair of DSBs can occur via homologous recombination (HR) or nonhomologous end joining (NHEJ). HR with the sister chromatid (SCR) in mitosis ensures faithful transmission of the genetic material. A number of proteins, including cohesin, are required to maintain chromosome structure and for efficient SCR. Interestingly, not only is Dot1 required for the proper recruitment of Rad9 to sites of DSBs, it also promotes recruitment of cohesin and is necessary for efficient SCR (Conde, Refolio et al. 2009). Resection of DSBs is an important step in DNA damage repair, producing 3' single-stranded DNA (ssDNA) tail intermediates. It was demonstrated that H3K79 methylation and Rad9 recruitment play an integral role in regulating resection to limit the amount of ssDNA that is produced (Lazzaro, Sapountzi et al. 2008).

Ultraviolet radiation (UV) causes formation of cis-syn cyclopyrimidine and 6-4 photoproduct dimers, which can be repaired by nucleotide excision repair (NER), recombination repair, and post-replication repair (PRR). Dot1 and its associated H3K79 methylation are required to elicit an appropriate response to UV damage (Giannattasio, Lazzaro et al. 2005) with loss of methylation affecting all three repair pathways, resulting in hypersensitivity (Bostelman, Keller et al. 2007; Lazzaro, Sapountzi et al. 2008). When DNA damage cannot be repaired, cell cycle progression and cell survival may be achieved by the translesion synthesis pathway (TLS) that utilizes error-prone polymerases to bypass DNA lesions. Evidence indicate that

Dot1 negatively regulates TLS, thereby maintaining genome integrity upon DNA damage (Conde and San-Segundo 2008; Conde, Ontoso et al. 2010; Levesque, Leung et al. 2010).

Diploid parental cells undergo meiotic cell division to generate haploid gametes. Proper segregation of chromosomes during meiosis is ensured by the pachytene checkpoint, which monitors completion of chromosome synapsis and recombination to prevent premature nuclear division. In the event of defective meiotic recombination, the pachytene checkpoint induces arrest at mid-meiotic prophase. In yeast, arrest at pachytene can be observed in *dmc1* and *zip1* mutants, which are required for proper synapsis formation and repair of DSBs. In a genetic screen for pachytene checkpoint components, it was observed that *dmc1* and *zip1* mutants failed to arrest in the absence of Dot1. The failure to arrest is in part due to mis-localization of the nucleolar proteins Pch2 and Sir2, both required for pachytene checkpoint function (San-Segundo and Roeder 2000).

Collectively, an overwhelming amount of data supports a vital role for DOT1 in regulating cell cycle progression in yeast upon DNA damage. Surprisingly, very little work has been performed to determine if Dot1's role in checkpoint function is evolutionarily conserved. With respect to mouse DOT1L, reports show that the depletion of DOT1L elicits cell cycle arrests at both G1 and G2 in the absence of extrinsic-induced DNA damage; however, the molecular mechanisms governing these phenotypes have not been addressed (Jones, Su et al. 2008; Barry, Krueger et al. 2009; Feng, Yang et al. 2010) .

DOT1L regulatory role in cardiovascular development

The majority of research dedicated to understanding the function of Dot1-mediated H3K79 methylation were performed in yeast. When I first began my Ph.D. training in Dr. Zhang's lab, the only biological function known about mammalian DOT1L was its mis-targeting in leukemia. DOT1L and its associated methylation marks are evolutionarily conserved from yeast to humans, suggesting that it may have critical biological roles in mammals. Therefore, I sought to elucidate DOT1L biological functions using the mouse as a model system with a focus on the cardiovascular system.

The first indication of a DOT1L regulatory function in cardiac development arose from *ex vivo* studies investigating epigenetics in cardiac development. Mouse ES cells exposed to laminar shear stress undergo myocardiogenesis. During this process there is a correlation between increased H3K79 methylation and induced expression of cardiovascular marker genes, such as vascular endothelial growth factor (VEGF) receptor 2, smooth muscle actin (SM-actin), smooth muscle protein 22-alpha (SM22-α), platelet-endothelial cell adhesion molecule-1 (PECAM-1), myocyte enhancer factor-2C (MEF2C), and α-sarcomeric actin (Illi, Scopece et al. 2005). In addition, analysis of differentiated/lineage specific cells revealed that the transcription activator SRF (serum *r*esponse *f*actor) binds to a distinct histone modification signature at smooth muscle specific promoters (H3K4me2, H3K79me2, H3K9ac, H4ac) (McDonald, Wamhoff et al. 2006).

In collaboration with the Epigenetics Program at Novartis, we generated a DOT1L conditional knockout mouse. Germ-line deletion of DOT1L resulted in embryonic lethality

after the onset of organogenesis at E9.5-E10.5. Knockout embryos displayed defects in the cardiovascular system such as heart enlargement, decreased vasculature, and reduced red blood cells (Jones, Su et al. 2008). Collectively, these phenotypes suggested a DOT1L regulatory function in cardiovascular and hematopoiesis development. Subsequently, Fields and colleagues demonstrated that primitive erythropoiesis requires DOT1L. In the absence of DOT1L, erythroid progenitor cells undergo a G1 cell cycle arrest and fail to differentiate (Feng, Yang et al. 2010).

The heart enlargement phenotype observed in knockout embryos may be a primary abnormality due to DOT1L loss of function or a secondary defect in response to insufficient blood supply from a reduced vasculature network or defective erythropoiesis. To elucidate the role of DOT1L in cardiac development and/or function, we generated a cardiac-specific knockout mouse model, which is the focus of my first project. A further understanding of DOT1L's regulatory role in cardiac function may provide insight into the genetic causes of congenital heart diseases and lead to the development of novel gene therapies.

Mis-targeting of DOT1L in MLL-related leukemias

Chromosomal translocation of the *MLL* (mixed lineage leukemia) gene results in the expression of oncogenic fusion proteins and is a common cause of acute leukemia (Ayton and Cleary 2001; Hess 2004). MLL rearrangements account for 7-10% of acute lymphoid leukemias (ALL) and 5-6% of acute myeloid leukemias (AML). In addition, ~10% of these MLL-related leukemias are caused by chemotherapy (Daser and Rabbitts 2004). Importantly, MLL rearrangements account for ~80% of ALL and ~60% of AML infant leukemias (Ayton

and Cleary 2001; Hess 2004; Krivtsov and Armstrong 2007). Due to the high incidence of MLL-mediated acute leukemias, a better understanding of the molecular mechanisms utilized by MLL-fusion proteins is vital for the development of effective treatments.

MLL, an H3K4 methyltransferase, aids in maintaining the "on" state of *Hox* gene expression during embryonic development and hematopoiesis (Hsieh, Cheng et al. 2003; Guenther, Jenner et al. 2005). In acute myeloid leukemia, genes of the *Hoxa* cluster are frequently up-regulated and have been shown to be required for leukemogenesis (Argiropoulos and Humphries 2007; Guenther, Lawton et al. 2008). While the catalytic domain of MLL is removed upon translocation, its N-terminus, containing two DNA-binding domains (AT-hooks and DNMT homology region) and subnuclear localization motifs is retained in fusion proteins. Thus, MLL-fusion proteins are likely directed to genes targeted by MLL. Meanwhile, aberrant regulation of gene expression for leukemogenesis is mediated by activity of wild type MLL expressed from the non-mutant allele and by the fusion partner (Li, Liu et al. 2005; Krivtsov and Armstrong 2007).

Among the over 50 MLL fusion partners, AF4, AF9, AF10, ENL, and ELL account for 2/3 of all MLL-associated leukemias. With the exception of ELL, the other four proteins have been reported to associate with each other through direct and indirect protein-protein interactions, suggesting that a common mechanism may be exploited during leukemia development (Slany 2005; Krivtsov and Armstrong 2007). Interestingly, DOT1L has also been shown to associate with a number of MLL-fusion partners and participates in the activation of a leukemic transcriptional program (Okada, Feng et al. 2005; Zhang, Xia et al.

2006; Bitoun, Oliver et al. 2007; Mueller, Bach et al. 2007; Krivtsov, Feng et al. 2008; Mueller, Garcia-Cuellar et al. 2009).

For example, the Zhang lab previously demonstrated that DOT1L specifically associates with the OM-LZ region of AF10 and is required for leukemic transformation by MLL-AF10. Importantly, it was shown that mis-targeting of DOT1L to the *Hoxa9* gene and subsequent activation of *Hoxa9* by H3K79 hypermethylation contributes to the transformation capability of MLL-AF10 (Okada, Feng et al. 2005). AF17, another fusion partner of MLL, has an OM-LZ domain similar to that of AF10, making it a potential DOT1L interacting protein (Prasad, Leshkowitz et al. 1994). Through mutating ENL, Mueller *et al.* were able to demonstrate that DOT1L interaction is required for MLL-ENL transformation and increased expression of *Hoxa7* and *Hoxa9* (Mueller, Bach et al. 2007). Furthermore, knockdown of DOT1L in MLL-AF4 transformed cells impaired proliferation and caused down-regulation of *Hoxa* genes (Krivtsov, Feng et al. 2008).

Collectively, these data support a universal mechanism by which DOT1L is mis-targeted to gene loci for aberrant H3K79 methylation and transcriptional activation to promote MLL-mediated leukemogenesis. To further support this common pathway, my second project focuses on the role of DOT1L in MLL-AF9 leukemia development. I will utilize our DOT1L knockout mouse model in combination with bone marrow transplantation to investigate whether DOT1L is essential for *in vivo* acute leukemia development and progression, which has not been demonstrated before. The findings from this project may lead to the development of novel target-based drugs for the treatment of MLL-related leukemias.

References

Altaf, M., R. T. Utley, et al. (2007). "Interplay of chromatin modifiers on a short basic patch of histone H4 tail defines the boundary of telomeric heterochromatin." Mol Cell **28**(6): 1002-1014.

Argiropoulos, B. and R. K. Humphries (2007). "Hox genes in hematopoiesis and leukemogenesis." Oncogene **26**(47): 6766-6776.

Ayton, P. M. and M. L. Cleary (2001). "Molecular mechanisms of leukemogenesis mediated by MLL fusion proteins." Oncogene **20**(40): 5695-5707.

Bannister, A. J., P. Zegerman, et al. (2001). "Selective recognition of methylated lysine 9 on histone H3 by the HP1 chromo domain." Nature **410**(6824): 120-124.

Barry, E. R., W. Krueger, et al. (2009). "ES cell cycle progression and differentiation require the action of the histone methyltransferase Dot1L." Stem Cells **27**(7): 1538-1547.

Berger, S. L. (2007). "The complex language of chromatin regulation during transcription." Nature **447**(7143): 407-412.

Bitoun, E., P. L. Oliver, et al. (2007). "The mixed-lineage leukemia fusion partner AF4 stimulates RNA polymerase II transcriptional elongation and mediates coordinated chromatin remodeling." Hum Mol Genet **16**(1): 92-106.

Bostelman, L. J., A. M. Keller, et al. (2007). "Methylation of histone H3 lysine-79 by Dot1p plays multiple roles in the response to UV damage in Saccharomyces cerevisiae." DNA Repair (Amst) **6**(3): 383-395.

Briggs, S. D., T. Xiao, et al. (2002). "Gene silencing: trans-histone regulatory pathway in chromatin." Nature **418**(6897): 498.

Carrozza, M. J., B. Li, et al. (2005). "Histone H3 methylation by Set2 directs deacetylation of coding regions by Rpd3S to suppress spurious intragenic transcription." Cell **123**(4): 581-592.

Cavalli, G. (2006). "Chromatin and epigenetics in development: blending cellular memory with cell fate plasticity." Development **133**(11): 2089-2094.

Cheng, X. and R. J. Roberts (2001). "AdoMet-dependent methylation, DNA methyltransferases and base flipping." Nucleic Acids Res **29**(18): 3784-3795.

Chernikova, S. B., J. A. Dorth, et al. (2010). "Deficiency in Bre1 impairs homologous recombination repair and cell cycle checkpoint response to radiation damage in mammalian cells." Radiat Res **174**(5): 558-565.

Conde, F., D. Ontoso, et al. (2010). "Regulation of tolerance to DNA alkylating damage by Dot1 and Rad53 in Saccharomyces cerevisiae." DNA Repair (Amst) **9**(10): 1038-1049.

Conde, F., E. Refolio, et al. (2009). "The Dot1 histone methyltransferase and the Rad9 checkpoint adaptor contribute to cohesin-dependent double-strand break repair by sister chromatid recombination in Saccharomyces cerevisiae." Genetics **182**(2): 437-446.

Conde, F. and P. A. San-Segundo (2008). "Role of Dot1 in the response to alkylating DNA damage in Saccharomyces cerevisiae: regulation of DNA damage tolerance by the error-prone polymerases Polzeta/Rev1." Genetics **179**(3): 1197-1210.

Costa, P. J. and K. M. Arndt (2000). "Synthetic lethal interactions suggest a role for the Saccharomyces cerevisiae Rtf1 protein in transcription elongation." Genetics **156**(2): 535-547.

Daser, A. and T. H. Rabbitts (2004). "Extending the repertoire of the mixed-lineage leukemia gene MLL in leukemogenesis." Genes Dev **18**(9): 965-974.

Dlakic, M. (2001). "Chromatin silencing protein and pachytene checkpoint regulator Dot1p has a methyltransferase fold." Trends Biochem Sci **26**(7): 405-407.

Feinberg, A. P., M. Oshimura, et al. (2002). "Epigenetic mechanisms in human disease." Cancer Res **62**(22): 6784-6787.

Feng, Q., H. Wang, et al. (2002). "Methylation of H3-lysine 79 is mediated by a new family of HMTases without a SET domain." Curr Biol **12**(12): 1052-1058.

Feng, Y., Y. Yang, et al. (2010). "Early mammalian erythropoiesis requires the Dot1L methyltransferase." Blood.

Fingerman, I. M., H. C. Li, et al. (2007). "A charge-based interaction between histone H4 and Dot1 is required for H3K79 methylation and telomere silencing: identification of a new trans-histone pathway." Genes Dev **21**(16): 2018-2029.

Game, J. C., M. S. Williamson, et al. (2006). "The RAD6/BRE1 histone modification pathway in Saccharomyces confers radiation resistance through a RAD51-dependent process that is independent of RAD18." Genetics **173**(4): 1951-1968.

Giannattasio, M., F. Lazzaro, et al. (2005). "The DNA damage checkpoint response requires histone H2B ubiquitination by Rad6-Bre1 and H3 methylation by Dot1." J Biol Chem **280**(11): 9879-9886.

Grenon, M., T. Costelloe, et al. (2007). "Docking onto chromatin via the Saccharomyces cerevisiae Rad9 Tudor domain." Yeast **24**(2): 105-119.

Guenther, M. G., R. G. Jenner, et al. (2005). "Global and Hox-specific roles for the MLL1 methyltransferase." Proc Natl Acad Sci U S A **102**(24): 8603-8608.

Guenther, M. G., L. N. Lawton, et al. (2008). "Aberrant chromatin at genes encoding stem cell regulators in human mixed-lineage leukemia." Genes Dev **22**(24): 3403-3408.

Handel, A. E., G. C. Ebers, et al. (2009). "Epigenetics: molecular mechanisms and implications for disease." Trends Mol Med.

Hess, J. L. (2004). "MLL: a histone methyltransferase disrupted in leukemia." Trends Mol Med **10**(10): 500-507.

Hsieh, J. J., E. H. Cheng, et al. (2003). "Taspase1: a threonine aspartase required for cleavage of MLL and proper HOX gene expression." Cell **115**(3): 293-303.

Huyen, Y., O. Zgheib, et al. (2004). "Methylated lysine 79 of histone H3 targets 53BP1 to DNA double-strand breaks." Nature **432**(7015): 406-411.

Illi, B., A. Scopece, et al. (2005). "Epigenetic histone modification and cardiovascular lineage programming in mouse embryonic stem cells exposed to laminar shear stress." Circ Res **96**(5): 501-508.

Jones, B., H. Su, et al. (2008). "The histone H3K79 methyltransferase Dot1L is essential for mammalian development and heterochromatin structure." PLoS Genet **4**(9): e1000190.

Joshi, A. A. and K. Struhl (2005). "Eaf3 chromodomain interaction with methylated H3-K36 links histone deacetylation to Pol II elongation." Mol Cell **20**(6): 971-978.

Keogh, M. C., S. K. Kurdistani, et al. (2005). "Cotranscriptional set2 methylation of histone H3 lysine 36 recruits a repressive Rpd3 complex." Cell **123**(4): 593-605.

Kornberg, R. D. and Y. Lorch (1999). "Twenty-five years of the nucleosome, fundamental particle of the eukaryote chromosome." Cell **98**(3): 285-294.

Kouzarides, T. (2002). "Histone methylation in transcriptional control." Curr Opin Genet Dev **12**(2): 198-209.

Kouzarides, T. (2007). "Chromatin modifications and their function." Cell **128**(4): 693-705.

Krivtsov, A. V. and S. A. Armstrong (2007). "MLL translocations, histone modifications and leukaemia stem-cell development." Nat Rev Cancer **7**(11): 823-833.

Krivtsov, A. V., Z. Feng, et al. (2008). "H3K79 methylation profiles define murine and human MLL-AF4 leukemias." Cancer Cell **14**(5): 355-368.

Krogan, N. J., J. Dover, et al. (2003). "The Paf1 complex is required for histone H3 methylation by COMPASS and Dot1p: linking transcriptional elongation to histone methylation." Mol Cell **11**(3): 721-729.

Lachner, M., D. O'Carroll, et al. (2001). "Methylation of histone H3 lysine 9 creates a binding site for HP1 proteins." Nature **410**(6824): 116-120.

Lacoste, N., R. T. Utley, et al. (2002). "Disruptor of telomeric silencing-1 is a chromatin-specific histone H3 methyltransferase." J Biol Chem **277**(34): 30421-30424.

Laurenson, P. and J. Rine (1992). "Silencers, silencing, and heritable transcriptional states." Microbiol Rev **56**(4): 543-560.

Lazzaro, F., V. Sapountzi, et al. (2008). "Histone methyltransferase Dot1 and Rad9 inhibit single-stranded DNA accumulation at DSBs and uncapped telomeres." EMBO J **27**(10): 1502-1512.

Levesque, N., G. P. Leung, et al. (2010). "Loss of H3 K79 trimethylation leads to suppression of Rtt107-dependent DNA damage sensitivity through the translesion synthesis pathway." J Biol Chem **285**(45): 35113-35122.

Li, Z. Y., D. P. Liu, et al. (2005). "New insight into the molecular mechanisms of MLL-associated leukemia." Leukemia **19**(2): 183-190.

Luger, K., A. W. Mader, et al. (1997). "Crystal structure of the nucleosome core particle at 2.8 A resolution." Nature **389**(6648): 251-260.

Martin, C. and Y. Zhang (2005). "The diverse functions of histone lysine methylation." Nat Rev Mol Cell Biol **6**(11): 838-849.

McDonald, O. G., B. R. Wamhoff, et al. (2006). "Control of SRF binding to CArG box chromatin regulates smooth muscle gene expression in vivo." J Clin Invest **116**(1): 36-48.

Min, J., Q. Feng, et al. (2003). "Structure of the catalytic domain of human DOT1L, a non-SET domain nucleosomal histone methyltransferase." Cell **112**(5): 711-723.

Minard, M. E., A. K. Jain, et al. (2009). "Analysis of epigenetic alterations to chromatin during development." Genesis **47**(8): 559-572.

Mueller, C. L. and J. A. Jaehning (2002). "Ctr9, Rtf1, and Leo1 are components of the Paf1/RNA polymerase II complex." Mol Cell Biol **22**(7): 1971-1980.

Mueller, D., C. Bach, et al. (2007). "A role for the MLL fusion partner ENL in transcriptional elongation and chromatin modification." Blood **110**(13): 4445-4454.

Mueller, D., M. P. Garcia-Cuellar, et al. (2009). "Misguided transcriptional elongation causes mixed lineage leukemia." PLoS Biol **7**(11): e1000249.

Nakayama, J., J. C. Rice, et al. (2001). "Role of histone H3 lysine 9 methylation in epigenetic control of heterochromatin assembly." Science **292**(5514): 110-113.

Ng, H. H., D. N. Ciccone, et al. (2003). "Lysine-79 of histone H3 is hypomethylated at silenced loci in yeast and mammalian cells: a potential mechanism for position-effect variegation." Proc Natl Acad Sci U S A **100**(4): 1820-1825.

Ng, H. H., S. Dole, et al. (2003). "The Rtf1 component of the Paf1 transcriptional elongation complex is required for ubiquitination of histone H2B." J Biol Chem **278**(36): 33625-33628.

Ng, H. H., Q. Feng, et al. (2002). "Lysine methylation within the globular domain of histone H3 by Dot1 is important for telomeric silencing and Sir protein association." Genes Dev **16**(12): 1518-1527.

Ng, H. H., F. Robert, et al. (2003). "Targeted recruitment of Set1 histone methylase by elongating Pol II provides a localized mark and memory of recent transcriptional activity." Mol Cell **11**(3): 709-719.

Ng, H. H., R. M. Xu, et al. (2002). "Ubiquitination of histone H2B by Rad6 is required for efficient Dot1-mediated methylation of histone H3 lysine 79." J Biol Chem **277**(38): 34655-34657.

Okada, Y., Q. Feng, et al. (2005). "hDOT1L links histone methylation to leukemogenesis." Cell **121**(2): 167-178.

Peterson, C. L. and M. A. Laniel (2004). "Histones and histone modifications." Curr Biol **14**(14): R546-551.

Pokholok, D. K., N. M. Hannett, et al. (2002). "Exchange of RNA polymerase II initiation and elongation factors during gene expression in vivo." Mol Cell **9**(4): 799-809.

Prasad, R., D. Leshkowitz, et al. (1994). "Leucine-zipper dimerization motif encoded by the AF17 gene fused to ALL-1 (MLL) in acute leukemia." Proc Natl Acad Sci U S A **91**(17): 8107-8111.

Robzyk, K., J. Recht, et al. (2000). "Rad6-dependent ubiquitination of histone H2B in yeast." Science **287**(5452): 501-504.

San-Segundo, P. A. and G. S. Roeder (2000). "Role for the silencing protein Dot1 in meiotic checkpoint control." Mol Biol Cell **11**(10): 3601-3615.

Sawada, K., Z. Yang, et al. (2004). "Structure of the conserved core of the yeast Dot1p, a nucleosomal histone H3 lysine 79 methyltransferase." J Biol Chem **279**(41): 43296-43306.

Schubeler, D., D. M. MacAlpine, et al. (2004). "The histone modification pattern of active genes revealed through genome-wide chromatin analysis of a higher eukaryote." Genes Dev **18**(11): 1263-1271.

Schubert, H. L., R. M. Blumenthal, et al. (2003). "Many paths to methyltransfer: a chronicle of convergence." Trends Biochem Sci **28**(6): 329-335.

Singer, M. S., A. Kahana, et al. (1998). "Identification of high-copy disruptors of telomeric silencing in Saccharomyces cerevisiae." Genetics **150**(2): 613-632.

Slany, R. K. (2005). "When epigenetics kills: MLL fusion proteins in leukemia." Hematol Oncol **23**(1): 1-9.

Squazzo, S. L., P. J. Costa, et al. (2002). "The Paf1 complex physically and functionally associates with transcription elongation factors in vivo." EMBO J **21**(7): 1764-1774.

Steger, D. J., M. I. Lefterova, et al. (2008). "DOT1L/KMT4 recruitment and H3K79 methylation are ubiquitously coupled with gene transcription in mammalian cells." Mol Cell Biol **28**(8): 2825-2839.

Strahl, B. D. and C. D. Allis (2000). "The language of covalent histone modifications." Nature **403**(6765): 41-45.

Taverna, S. D., H. Li, et al. (2007). "How chromatin-binding modules interpret histone modifications: lessons from professional pocket pickers." Nat Struct Mol Biol **14**(11): 1025-1040.

Toh, G. W., A. M. O'Shaughnessy, et al. (2006). "Histone H2A phosphorylation and H3 methylation are required for a novel Rad9 DSB repair function following checkpoint activation." DNA Repair (Amst) **5**(6): 693-703.

Van Holde, K. E., J. R. Allen, et al. (1980). "DNA-histone interactions in nucleosomes." Biophys J **32**(1): 271-282.

van Leeuwen, F., P. R. Gafken, et al. (2002). "Dot1p modulates silencing in yeast by methylation of the nucleosome core." Cell **109**(6): 745-756.

Waddington, C. H. (1939). An introduction to modern genetics. New York,, The Macmillan company.

Waddington, C. H. (1942). "The epigenotype." Endeavour **1**: 18-20.

Wang, Z., C. Zang, et al. (2008). "Combinatorial patterns of histone acetylations and methylations in the human genome." Nat Genet **40**(7): 897-903.

Wood, A., N. J. Krogan, et al. (2003). "Bre1, an E3 ubiquitin ligase required for recruitment and substrate selection of Rad6 at a promoter." Mol Cell **11**(1): 267-274.

Wood, A., J. Schneider, et al. (2003). "The Paf1 complex is essential for histone monoubiquitination by the Rad6-Bre1 complex, which signals for histone methylation by COMPASS and Dot1p." J Biol Chem **278**(37): 34739-34742.

Wysocki, R., A. Javaheri, et al. (2005). "Role of Dot1-dependent histone H3 methylation in G1 and S phase DNA damage checkpoint functions of Rad9." Mol Cell Biol **25**(19): 8430-8443.

Zhang, K. and S. Y. Dent (2005). "Histone modifying enzymes and cancer: going beyond histones." J Cell Biochem **96**(6): 1137-1148.

Zhang, W., Y. Hayashizaki, et al. (2004). "Structure and regulation of the mDot1 gene, a mouse histone H3 methyltransferase." Biochem J **377**(Pt 3): 641-651.

Zhang, W., X. Xia, et al. (2006). "Dot1a-AF9 complex mediates histone H3 Lys-79 hypermethylation and repression of ENaCalpha in an aldosterone-sensitive manner." J Biol Chem **281**(26): 18059-18068.

Zhang, Y. and D. Reinberg (2001). "Transcription regulation by histone methylation: interplay between different covalent modifications of the core histone tails." Genes Dev **15**(18): 2343-2360.

Chapter 2

DOT1L REGULATES DYSTROPHIN EXPRESSION AND IS CRITICAL FOR CARDIAC FUNCTION

doi:10.1101/gad.2018511

Abstract

Histone methylation plays an important role in regulating gene expression. One such methylation occurs at lysine 79 of histone H3 (H3K79) and is catalyzed by the yeast Dot1 (disruptor of telomeric silencing) and its mammalian homolog DOT1L. Previous studies have demonstrated that germ line disruption of *Dot1L* in mouse resulted in embryonic lethality. Here we report that cardiac-specific knockout of *Dot1L* results in increased mortality rate with chamber dilation, increased cardiomyocyte cell death, systolic dysfunction, and conduction abnormalities. These phenotypes mimic those exhibited in patients with dilated cardiomyopathy (DCM). Mechanistic studies reveal that DOT1L performs its function in cardiomyocytes through regulating *Dystrophin* (*Dmd*) transcription and, consequently, stability of the Dystrophin-glycoprotein complex important for cardiomyocyte viability. Importantly, expression of a mini-Dmd can largely rescue the DCM phenotypes indicating that Dmd is a major target mediating DOT1L function in cardiomyocyte. Interestingly, analysis of available gene expression data sets indicates that DOT1L is down-regulated in idiopathic DCM patient samples compared to normal controls. Therefore, our study not only establishes a critical role for DOT1L-mediated H3K79 methylation in cardiomyocyte function, but also reveals the mechanism underlying the role of DOT1L in DCM. In addition, our study may open new avenues for the diagnosis and treatment of human heart disease.

Introduction

Chromatin is subject to reversible post-translational modifications that may directly alter chromatin structure and function or indirectly through the recruitment of effector proteins at heterochromatic (silenced) and euchromatic (active) DNA. Histone methylation plays an important role in regulating transcription at target loci and is important for X-inactivation, cell fate maintenance, and terminal differentiation (Peterson and Laniel 2004; Martin and Zhang 2005; Kouzarides 2007). One particular histone methylation event occurs at Lysine 79 within the globular domain of histone H3 (H3K79) and is catalyzed by yeast Dot1 (disruptor of telomeric silencing) and its mammalian homolog DOT1L (Feng et al. 2002; Lacoste et al. 2002; Ng et al. 2002a; van Leeuwen et al. 2002). Although Dot1 was originally identified as a regulator of telomeric silencing (Singer et al. 1998), more recent studies suggest that Dot1-mediated H3K79 methylation is linked to euchromatic gene transcription (Schubeler et al. 2004; Barski et al. 2007; Steger et al. 2008).

In yeast, Dot1 activity is positively regulated during transcription elongation through Rad6-Bre1 mono-ubiquitination of H2B (Ng et al. 2002b; Krogan et al. 2003; Wood et al. 2003). Additionally, Dot1 has been linked to the meiotic pachytene checkpoint control (San-Segundo and Roeder 2000) and DNA damage repair (Giannattasio et al. 2005; Wysocki et al. 2005; Conde et al. 2009). However, the biological function of mammalian DOT1L, particularly in the context of the animal, is less characterized. A recent study indicates that DOT1L exists in a large protein complex and regulates the expression of Wingless target genes (Mohan et al. 2010). We and others have previously demonstrated that mis-targeting of DOT1L and subsequent H3K79 hypermethylation plays an important role in leukemic

transformation (Okada et al. 2005; Okada et al. 2006; Mueller et al. 2007; Krivtsov et al. 2008). Most recently, DOT1L has been shown to regulate the erythroid and myeloid lineage switch during differentiation (Feng et al. 2010). In addition, loss of function studies revealed a critical role of DOT1L during mouse embryogenesis as germ-line *Dot1l* knockout (KO) causes lethality at embryonic day E10.5 with growth impairment, yolk sac angiogenesis defects, and cardiac dilation (Jones et al. 2008).

Congestive heart failure (CHF) is a common manifestation of cardiomyopathy, a disease caused by malfunction of the heart muscle (Seidman and Seidman 2001; Liew and Dzau 2004). Dilated cardiomyopathy (DCM) is characterized by dilation of the left or both ventricles and reduced contractile function (systolic dysfunction), and is the most prevalent form of cardiomyopathy (Seidman and Seidman 2001; Liew and Dzau 2004). Recent studies suggest that, in addition to genetic alterations, epigenetic factors also contribute to DCM. For example, several studies have linked histone acetylation to cardiac hypertrophy and DCM (Zhang et al. 2002; Kook et al. 2003; Montgomery et al. 2007; Ha et al. 2010; Hang et al. 2010). However, whether histone methylation contributes to DCM is not clear, although dysregulation of histone methylation has been linked to a number of human diseases (Feinberg et al. 2002; Handel et al. 2009).

To further characterize the function of DOT1L in the mouse heart, we generated a cardiomyocyte-specific knockout mouse model using the α-MHC-Cre line and demonstrate that DOT1L plays an important role in heart function. We provide evidence suggesting that

dysregulation of Dystrophin in cardiomyocytes is largely responsible for the phenotypes exhibited in the *Dot1L* cardiac conditional knockout mice.

Results

Dot1L deficiency in cardiomyocytes does not cause embryonic lethality

Previous studies demonstrate that germ-line *Dot1l* knockout (KO) causes lethality at embryonic day E10.5 with diverse impairments that include growth retardation, yolk sac angiogenesis defects, and cardiac dilation (Jones et al. 2008). To understand the molecular mechanism underlying the embryonic phenotypes, we take advantage that the *Dot1L* conditional allele contains a promoterless β-geo cassette (Jones et al. 2008) and analyzed *Dot1L* expression by X-gal staining. This study revealed that the heart is one of the highest *Dot1L*-expressing organs (Figure S2-1A). RT-qPCR analysis also indicates that cardiac expression of *Dot1L* peaks after birth (Figure S2-1B). This *Dot1L* expression pattern in combination with the timing of lethality suggests that heart defects might contribute to the embryonic lethality phenotype.

To explore a role for DOT1L in the heart, we generated a cardiac-specific conditional knockout mouse model by first crossing DOT1L$^{2lox/+}$ and DOT1L$^{1lox/+}$ with the (α-myosin heavy chain) α-MHC-Cre line (Abel et al. 1999) (Figure S2-2A). Cardiac conditional knockout (referred to as CKO for the remainder of the manuscript), DOT1L$^{2lox/1lox}$;α-MHC-Cre, mice were then obtained by crossing DOT1L$^{2lox/+}$;α-MHC-Cre mice with DOT1L$^{1lox/+}$;α-MHC-Cre mice. Cre-mediated deletion results in removal of 108 amino acids in the catalytic domain of DOT1L, rendering an enzymatically inactive DOT1L (Figure S2-2B). CKO mice were born at Mendelian ratio (Figure S2-2C) and recombination efficiency was verified by RT-qPCR using hearts derived from new-born, postnatal day 1 (P1) mice (Figure S2-2D). Consistent with loss function of DOT1L in the CKO hearts, Western blot

analysis and immunostaining using an antibody that recognizes both di- and tri-methylation of H3K79 (H3K79me2/3) demonstrate loss of H3K79me2/3 in the CKO hearts (Figure S2-2E, F). These results suggest that loss function of DOT1L in cardiomyocytes alone is not sufficient to cause embryonic lethality.

DOT1L deficiency in cardiomyocytes causes heart dilation and postnatal lethality

Although CKO mice are born in Mendelian ratio, sudden death was observed in 50% of the CKO mice within two weeks after birth, and the remaining 50% CKO mice die by six months of age (Figure 2-1A), indicating DOT1L has an important function in postnatal and adult cardiomyocytes. Analysis of the CKO mice revealed severely enlarged hearts (Figure 2-1B) and dilation of both chambers (Figure 2-1C). Consistently, heart to body weight ratios were also increased in CKO mice compared with that of their littermate controls (Figure 2-1D). The increased heart to body weight ratio is mainly caused by increased heart weight (Figure 2-1E) as the body weight is not significantly altered between WT and CKO mice (Figure S2-3A).

To determine whether concentric hypertrophy contributes to the increase in CKO heart mass, tissue sections were stained with Laminin antibody followed by measuring cardiomyocyte circumference. Quantification using ImageJ software indicates that the average cell circumference is not altered in CKO mice (Figure S2-3B, C), suggesting that the increase in CKO heart mass is in part due to eccentric hypertrophy. These data collectively indicate that loss of DOT1L function, particularly its H3K79 methyltransferase activity, in

cardiomyocytes results in congestive heart failure (CHF) that is likely due to dilated cardiomyopathy (DCM).

CKO hearts exhibit similar cardiac remodeling observed in DCM patients

In addition to chamber dilation, gross changes in heart morphology, such as deviation from an elliptical shape to a more spherical one and increased heart mass, was also observed (Figure 2-1C, E) indicating loss function of DOT1L in cardiomyocytes caused cardiac remodeling. Since DCM is often accompanied with pathologic remodeling (Cohn et al. 2000), we analyzed the histopathology of CKO hearts at P10. TUNEL staining revealed a dramatic increase in apoptotic cell death in CKO hearts compared to the WT control (Figure 2-2A). In addition, transmission electron microscopic (TEM) analysis revealed a significant increase of vacuoles in CKO myocytes (Figure 2-2B, ii, arrows), suggesting an increase in autophagic cell death, consistent with previous studies linking autophagy to DCM (Knaapen et al. 2001). In addition, TEM also revealed interstitial fibroblast cells in CKO heart tissue (Figure 2-2B, compare i. and iii.) indicating reactive fibrosis, a common feature of cardiac remodeling found in DCM (de Leeuw et al. 2001; Luk et al. 2009), took place in CKO hearts. Additionally, immunostaining with anti-HSPG2 (also known as Perlecan) shows increased interstitial HSPG2 staining (Figure 2-2C, arrowheads) as well as increased HSPG2 and myofibroblasts lining the inner left ventricular chamber (Figure 2-2C, yellow outlined) in CKO hearts supporting the presence of reactive fibrosis, which is further confirmed by Masson's Trichrome staining (Figure 2-2D, blue staining).

Previous studies have established that reactivation of a fetal gene expression program and increase in cellular proliferation is concomitant with the degeneration of cardiomyocytes in DCM (Kajstura et al. 1998; Cohn et al. 2000; Houweling et al. 2005). Consistent with the notion that DOT1L deficiency resulted in DCM, RT-qPCR demonstrated that expression of the fetal genes *Myh7, Acta1, Nppa,* and *Nppb* are up-regulated in CKO hearts (Figure 2-2E). In contrast, adult gene *Myh6* is down-regulated. Mouse cardiomyocytes retain a small capacity to proliferate after birth (Ahuja et al. 2007; Banerjee et al. 2007). To determine whether DOT1L deficiency results in an increased cell proliferation, as exhibited in DCM, heart tissue sections were immunostained for Ki-67 at P1 and P5. Results shown in Figure 2-2F demonstrate that the percentage of proliferating cells (ratio of Ki-67 positive nuclei to total nuclei, multiplied by 100) is significantly increased in the CKO hearts compared to the control, which may contribute to the observed increase in the CKO heart mass. We note that this increased cell proliferation in the DOT1L-deficient heart is in contrast to previous studies showing a requirement for DOT1L in ES cell cycle progression (Jones et al. 2008; Barry et al. 2009), suggesting cell type specificity. Taken together, the above data support that CKO hearts exhibit multiple phenotypes similar to those observed in DCM.

CKO hearts exhibit similar functional defects observed in DCM patients

To gain further support that DOT1L deficiency in cardiomyocytes results in DCM, we asked whether the morphological changes and cardiac remodeling observed in CKO hearts affect their function. To this end, we performed echocardiography (ECHO) analysis at different mouse age groups. Conscious ECHOs performed on P10 pups during the first stage of lethality (n=5 per genotype) demonstrate that CKO mice have increased left ventricular

internal dimensions and volume. Analysis of cardiac output by measuring ejection fraction (EF) and fractional shortening (FS) revealed that both EF and FS is reduced by almost half in CKO mice when compared with that of WT mice (Table 2-1). These results are indicative of left ventricular systolic dysfunction and are consistent with clinical DCM outcome (Karkkainen and Peuhkurinen 2007; Luk et al. 2009). Similar results were obtained at 2 and 5 months of age (Table 2-1). Interestingly, the smaller difference between WT and CKO mice at 2 months may reflect a compensation that allowed these mice to bypass the first stage of lethality.

Cardiac conduction abnormalities are frequently observed in DCM heart failure patients with left ventricular systolic dysfunction (Olson 2004). During heart contraction, an electrical impulse transmits from atria (P-wave) to ventricles (QRS-wave) at the atrioventricular node (AVN). The time delay for electrical propagation can be directly measured by electrocardiography (EKG) (Hatcher and Basson 2009). To determine whether the conduction system is perturbed in CKO mice, EKG was performed at 5 months of age (n=8 per genotype). All CKO mice displayed minimally a first degree heart block at the AVN, with an 80% penetration of either non-sustained ventricular tachycardia (n=1/8) (Figure 2-3A, CKOa), periodic third degree heart block (n=3/8), or second degree Type II heart block (n=3/8) (Figure 2-3A, CKOb). Overall, CKO mice have a significant increase in RR interval (Figure 2-3B), PR interval (Figure 2-3C), P-wave duration (Figure 2-3D), and QRS interval (Figure 2-3E). These EKG data from CKO mice are consistent with EKG findings in human DCM patients (Seidman and Seidman 2001; Towbin and Bowles 2006; Luk et al. 2009). The

physiological studies further support that DOT1L deficiency in cardiomyocytes confers phenotypes similar to those observed in patients with DCM.

Dot1L deficiency in cardiomyocytes down-regulates dystrophin expression

Having established that DOT1L deficiency in cardiomyocytes causes phenotypes similar to those observed in DCM, we next attempted to understand the molecular mechanism. To date, mutations in over 30 genes have been linked to human DCM (Table S2-1) (Towbin and Bowles 2006; Karkkainen and Peuhkurinen 2007; Kimura 2008; Luk et al. 2009). Given that DOT1L-mediated H3K79 methylation is associated with actively transcribed genes (Martin and Zhang 2005; Wang et al. 2008b), we anticipated that one or more of the DCM-associated genes might be down-regulated due to loss of H3K79 methylation in the CKO heart. To this end, we performed four independent gene expression microarrays using the dual-color Agilent 4X44K Whole Mouse Genome Array system. Data analysis revealed 751 down-regulated probes representing 471 genes that are statistically significant with a false positive rate of 0.06%. Comparison of the microarray data with known DCM-associated genes identified two common genes, *Titin* (*Ttn*) and *Dystrophin* (*Dmd*).

Ttn is a giant myofilament protein important for maintaining sarcomere structure and elasticity (Kostin et al. 2000). Mutations in *Ttn* have been reported in autosomal dominant forms of familial DCM (Gerull et al. 2002). Mouse models expressing M-line deficient Ttn exhibit widened M-lines and gradual disassembly of sarcomeres, which lead to cardiac failure (Gotthardt et al. 2003; Weinert et al. 2006). If *Ttn* down-regulation is responsible for the DCM in CKO mice, we anticipate abnormal sarcomere structure in DOT1L CKO hearts.

However, TEM analysis revealed that sarcomere integrity is maintained in DOT1L CKO hearts (Figure S2-4), suggesting that down-regulation of *Ttn* is not a major contributing factor for the DCM in DOT1L CKO mice.

Dmd was the first discovered DCM-associated gene that can cause both DCM and muscular dystrophy. Dmd is a membrane-associated protein that forms a dystrophin-glycoprotein complex (DGC), which connects contractile sarcomeres to the sarcolemma and extracellular matrix (ECM). This connection is vital for lateral force transduction between cardiomyocytes as well as for relieving mechanical stress on sarcolemma during contraction (Kostin et al. 2000; Kimura 2008). Since a loss of *Dmd* expression may be the cause of cell death and cardiac remodeling observed in CKO hearts, we first confirmed the microarray results by RT-qPCR. Data presented in Figure 2-4A demonstrate that the *Dmd* mRNA levels are down-regulated to ~25% of the WT level in the CKO hearts. In contrast, expression of other randomly selected DCM-relevant genes (*Actn2*, *Ldb3*, *Des*, and *Taz*) was not significantly altered by DOT1L deficiency (Figure 2-4A). Consistent with a reduction at the RNA level, immunostaining revealed that Dmd protein level is also greatly diminished in CKO hearts (Figure 2-4B,C). Previous studies have demonstrated that mutations affecting expression of *Dmd* or any *sarcoglycan* (*Sgc*) gene lead to DGC instability and reduced levels of all complex proteins (Deconinck et al. 1997; Grady et al. 1997). Consistently, immunostaining revealed great loss of β-dystroglycan (βDG) and α-sarcoglycan (SGCA) proteins in CKO mice (Figure 2-4B, C) although none of the DGC components is altered at the RNA level by DOT1L deficiency (Figure 2-4A). These results suggest that loss of Dmd caused degradation of the DGC components, which in turn affects cardiomyocyte viability.

We next sought to determine whether DOT1L directly regulates *Dmd* expression in mouse heart by chromatin immunoprecipitation (ChIP). Despite extensive efforts, none of the home-made or commercial DOT1L antibodies (Abgent: AP1198a, AP1198b; Cell Signaling: D8891, D8890; Abcam: ab7295) were able to detect endogenous DOT1L protein (*data not shown*); thus, unsuitable for ChIP. Therefore, we performed ChIP assays across the *Dmd* locus using an anti-H3K79me2/3 antibody. Results shown in Figure 2-4D demonstrate that relatively less H3K79me2/3 is observed upstream of *Dmd* transcription start site (TSS) but greatly increases downstream, continues to rise at 20kb downstream of TSS, and is still present as far as 59kb downstream of TSS. This H3K79me2/3 distribution pattern is consistent with published ChIP-seq results using various cell lines (Barski et al. 2007; Wang et al. 2008b). Importantly, the H3K79me2/3 enrichment on the *Dmd* gene depends on functional DOT1L as the enrichment is abolished when samples derived from *Dot1L* CKO hearts are used. In addition, the detected signals are specific as enrichment was not observed when IgG was used in a parallel ChIP assay. Previous studies have demonstrated that DOT1L-deficiency leads to a complete loss of H3K79 methylation (Jones et al. 2008), indicating DOT1L is the only H3K79 methyltransferase. The demonstration that H3K79 methylation of the *Dmd* gene is dependent on functional DOT1L supports the notion that *Dmd* is a direct DOT1L target.

It has been previously reported that Dmd expression is positively regulated by the binding of the transcription activator SRF (serum response factor) to a CArG box consensus sequence within the muscle-specific *Dmd* promoter (Galvagni et al. 1997). To examine whether transcription activation by SRF is affected in CKO hearts, we analyzed SRF RNA levels by

RT-qPCR. Results shown in Figure 2-4A demonstrate that SRF expression is not significantly altered in CKO hearts. In addition, ChIP analysis using an anti-SRF antibody indicates that SRF binding to the TSS or CArG box consensus region of *Dmd* is not affected by Dot1L knockout (Figure 2-4E). These results support that DOT1L and SRF function independently of each other and that transcriptional regulation of Dmd by DOT1L-mediated H3K79 methylation functions downstream of SRF.

DOT1L directly regulates dystrophin expression in C2C12 cells

To further demonstrate that DOT1L directly regulates *Dmd* expression we performed lentiviral shRNA knockdown (KD) and retroviral rescue experiments in C2C12 myoblast cells. KD of *mDot1L* effectively reduced both *mDot1L* and *Dmd* expression compared to control shRNA, whereas *Srf* is not significantly affected (Figure 2-4F). Despite similar expression levels of the WT and a catalytic mutant Flag-hDOT1L (Figure S2-5), *Dmd* expression is rescued only by WT Flag-hDOT1L, but not the catalytic mutant, indicating that DOT1L-mediated H3K79 methylation is critical for *Dmd* expression (Figure 2-4F). ChIP analysis demonstrates that the effect of DOT1L on *Dmd* expression is direct as both WT and catalytic mutant Flag-hDOT1L bind to the *Dmd* locus (Figure 2-4G). Consistent with transcriptional regulation of *Dmd* by DOT1L histone methyltransferase activity, H3K79 methylation is also enriched at the Dmd locus in control shRNA and WT Flag-hDOT1L rescued samples, while enrichment is reduced in mDOT1L KD and catalytic mutant rescued cells (Figure 2-4H). Thus, these data establish that H3K79 methylation by DOT1L directly regulates *Dmd* transcription.

Postnatal dystrophin gene delivery and expression in cardiomyocytes rescues cardiac function in CKO mice

Gene expression and ChIP analyses suggest that DOT1L's role in cardiomyocytes may be mediated through its regulation of Dmd expression. To determine if Dmd is a key target contributing to the DCM phenotype, we performed *in vivo* rescue experiments using an adeno-associated virus serotype 9 (AAV9) vector expressing a *minidystrophin* gene under the control of CMV promoter. AAV-mediated gene therapy with *minidystrophin* has been previously shown to effectively treat dystrophic pathology (Wang et al. 2000). The vector used to rescue *Dot1L* CKO mice, rAAV9-CMV-DysΔ3990 (rAAV9-miniDmd), provides high expression of *minidystrophin* in all muscle tissues including the heart (Wang et al. 2008a). To rescue CKO mice, rAAV9-miniDmd was administered at two different age groups, either at P3 via intraperitoneal injection or at 2 months via tail vein injection and analyzed by ECHO. As shown in Table 2-2, cardiac function, EF and FS, are restored in CKO rescued mice injected at P3 (compare Tables 2-1 and 2-2). Additionally, increases in LVID, LV Vol and LV mass are significantly reduced by expression of *minidystrophin* (compare Tables 2-1 and 2-2). Similar improvements were also observed in adult mice rescued at 2 months of age (compare Tables 2-1 and 2-2). Most significantly, adult rescued mice are able to survive past the second stage of lethality with no impairments in cardiac function (Table 2-2, 8 months).

In addition to ECHO analysis, EKG of rescued CKO mice was also analyzed. At 5 months during the second stage of lethality, EKG was obtained from mice rescued at P3. Results demonstrate that RR interval (Figure 2-5A), PR interval (Fig. 2-5B), P duration (Figure 2-

5C), and QRS interval (Figure 2-5D) were restored in the CKO mice. For mice rescued as adults, EKG was analyzed at 5 months and 8 months of age. The RR interval (Figure 2-5E), P duration (Figure 2-5G), and QRS interval (Figure 2-5H) were restored in these mice, while PR intervals improved partially (Figure 2-5B, compare p-values with Figure 2-3C). In addition, heart blocks observed prior to injection were no longer present in rescued CKO mice as indicated by the EKG images and echocardiograms of the same mice before and after treatment (Figure S2-6A, B). Collectively, the above studies demonstrate that the functional defects caused by DOT1L deficiency in cardiomyocytes can be largely rescued by postnatal expression of Dmd, supporting that Dmd is a key DOT1L target in cardiomyocytes.

Discussion

DOT1L is the only known H3K79 methyltransferase and is conserved from yeast to humans. It is highly expressed in the heart, blood cells, and testis although its expression in mammals is ubiquitously. Germ-line knockout of *Dot1L* has been shown to be embryonic lethal with cardiovascular and hematopoietic defects. In this study, we demonstrate that DOT1L H3K79 methyltransferase activity is vital for cardiac function in the mouse using a cardiac-specific knockout model. DOT1L loss of function results in postnatal and adult lethality from dilated cardiomyopathy and congestive heart failure due to down-regulation of *dystrophin* (model in Figure 2-6).

Dot1L CKO mouse is a useful model for understanding DCM

Cardiac-specific loss of DOT1L H3K79 methyltransferase activity caused gross changes in cardiac growth and shape that are reminiscent of dilated cardiomyopathy. DCM is a disease of the heart muscle characterized by enlargement of one or both heart chambers, eccentric hypertrophy, interstitial fibrosis, systolic dysfunction, and conduction defects. In this study, we show that *Dot1L* CKO mice hearts are spherical in shape with enlarged chamber volumes and increased mass. Through immunostaining, we demonstrate that eccentric hypertrophy, increased proliferation, and reactive fibrosis may contribute to the increase in heart mass. In addition, a significant increase in cellular apoptosis was observed in CKO hearts. Finally, EKG and ECHO analysis revealed severe defects in cardiac force transmission and output. Collectively, these data support that loss function of DOT1L in cardiomyocytes results in phenotypes similar to those observed in DCM patients making our mouse a valuable model for understanding DCM.

Dystrophin is a key target mediating DOT1L function in the heart

As the only known H3K79 methyltransferase, DOT1L is thought to play a genome-wide role in transcriptional regulation. Therefore, it may be inferred that loss of DOT1L enzymatic activity would silence a large number of genes vital for cardiac function. Microarray analysis revealed 751 down-regulated probes corresponding to 471 genes in CKO hearts. However, only two of these genes have been directly linked to DCM in mouse and humans, *Ttn* and *Dmd*. Our histopathology data, including myocyte loss and remodeling, is consistent with a Dmd-deficiency (Heydemann and McNally 2007) and not loss of Ttn since sarcomeres remain normal.

We demonstrate that cardiac Dmd expression correlates with DOT1L-mediated H3K79 methylation. In addition, we show that DOT1L methyltransferase activity regulates *Dmd* transcription in C2C12 myoblast cells and that exogenous Flag-DOT1L is localized to the *Dmd* locus. Collectively, these data conclusively demonstrates that DOT1L is a transcriptional regulator directly involved in *Dmd* expression. While other genes regulated by DOT1L may contribute to the DCM phenotype observed in CKO mice, the fact that the cardiac functional defects can be rescued by expression of a *minidystrophin* supports that Dmd is a critical target mediating DOT1L function in the heart.

In the *mdx* mouse, a nonsense mutation results in the loss of *Dmd* expression in all muscle cells. Surprisingly, these mice do not develop severe DCM phenotypes (Hoffman et al. 1987; Grady et al. 1997), while DOT1L deficiency caused *Dmd* down-regulation does. Since

the DOT1L deficiency in CKO mice occurs only in cardiomyocytes, *Dmd* expression is retained in CKO skeletal muscle, allowing for normal levels of exercise. The increased exercise in CKO mice compared to *mdx* mice causes additional workload and stress on the heart, which would escalate the severity of DCM. Indeed, it has been reported that targeted repair in *mdx* mice using a skeletal-muscle restricted *minidystrophin* transgene significantly enhanced cardiac injury and DCM (Townsend et al. 2008).

The apparent inconsistency between CKO and *mdx* mice can also be explained by the lack of a similar compensation mechanism. Previous studies have demonstrated that loss of *Dmd* expression in the *mdx* mouse is compensated by up-regulation of *Utrophin* (*Utrn*), an autosomal *Dmd* homolog (Deconinck et al. 1997; Grady et al. 1997). However, this compensation mechanism does not seem to exist in CKO mice as DOT1L deficiency did not cause up-regulation of *Utrn* (Figure S2-7). Thus, the *Dot1L* CKO mouse may serve as a useful model for comparative analysis of the molecular mechanisms underlying the regulation of Utrn.

A potential link between DOT1L and DCM/DMD

Congestive heart failure is a common manifestation of cardiomyopathy, a disease caused by malfunction of the heart muscle (Seidman and Seidman 2001; Liew and Dzau 2004). DCM is the most common form of cardiomyopathy affecting 36.5 per 100,000 people (Seidman and Seidman 2001; Liew and Dzau 2004; Luk et al. 2009). Although extensive work has been performed to identify signature DCM genes through global expression profiling (Barrans et al. 2002; Barth et al. 2006; Camargo and Azuaje 2008), little effort has been focused on the

epigenetic contribution with the exception of histone acetylation (Zhang et al. 2002; Kook et al. 2003; Montgomery et al. 2007; Ha et al. 2010; Hang et al. 2010). With regard to histone methylation, only two studies have investigated changes in methylation patterns in heart failure (Movassagh et al. ; Kaneda et al. 2009). However, whether it directly contributes to the development of DCM is not known.

The demonstration that loss of DOT1L enzymatic activity results in DCM not only establishes a connection between dysregulation of histone methylation to DCM, but also raises the possibility that malfunction of DOT1L might account for some DCM patients. To explore this possibility, we analyzed hDOT1L expression level in idiopathic DCM (n=27) and normal (n=11) myocardial samples from publically available microarray data (http://cardiogenomics.med.harvard.edu/project-detail?project_id=229). This analysis indicates that DOT1L is down-regulated in idiopathic DCM patients with all Affymetrix probe sets (*n*=11 probes per set) (Figure S2-8), supporting the notion that dysfunction of DOT1L may be a contributing factor to human idiopathic DCM. Mutations in *Dmd* is also the cause of both Duchenne and Becker Muscular Dystrophy (DMD and BMD, respectively), affecting 1 out of 3,500 males (Hoffman et al. 1987). Up to 90% of those patients manifest cardiomyopathies and many die of heart failure (Connuck et al. 2008). In this study, we established that DOT1L regulates *Dmd* expression in both cardiac and C2C12 cells, suggesting that a DOT1L-deficiency may contribute to DCM and human muscular dystrophy. Future studies should reveal whether DOT1L is genetically linked to DCM, DMD, and BMD in human patients.

Materials and Methods

Generation of cardiac-specific Dot1L CKO mice. The targeting vector and generation of DOT1L chimeric mice has been described previously (Jones et al. 2008). DOT1L$^{2lox/+}$ and DOT1L$^{1lox/+}$ mice were mated with α-MHC-Cre$^{+/+}$ transgenic mice to obtain DOT1L$^{2lox/+}$;α-MHC-Cre$^{+/+}$ and DOT1L$^{1lox/+}$;α-MHC-Cre$^{+/+}$ mating pairs. Mice are kept on a 129SvJ, C57BL/6J mixed background. DOT1L$^{2lox/1lox}$;α-MHC-Cre$^{+/+}$ mice and DOT1L$^{2lox/2lox}$; α-MHC-Cre$^{+/+}$ mice were used as CKO mice. Upon Cre recombination, exons 5 and 6 are excised from the *DOT1L* locus. After splicing of the DOT1L transcript from the CKO allele, exons 4 and 7 of the mature mRNA are translated in-frame generating a mutant DOT1L protein lacking a portion of the SAM-binding motif. All mice procedures were performed following the guidelines set by the Institutional Animal Care and Use Committee.

Echocardiography and electrocardiography. Experiments were performed at the Mouse Cardiovascular Models Core Facility at UNC-CH or in the lab of Dr. Xiao Xiao, UNC-CH. To restrain postnatal pups, paws are taped to a plastic board. For adult mice, soft cotton thread loops are placed around each leg, just proximal to the paw and gently snugged with a plastic slider. The distal ends of the threads are placed in notches cut into a plastic board and gently tightened to hold the animal in a supine position to prevent self-mutilation of the forelimbs. Warmed Aquasonic™ gel is applied over the thorax and a 30MHz probe is positioned over the chest in a parasternal position. Long and short axis B-mode and M-mode images are recorded. Upon completion of the procedure, the gel is wiped off and the animal is returned to its cage housed in a warm chamber. Time of restraint is 5 minutes or less. For electrocardiography, mice are anesthetized with inhaled isoflurane. Mice are taped to a warmed mouse board and their body temperature is monitored with a rectal probe and

maintained at 37+/-1 ^{0}C throughout the procedure. Thin (29 ga.) sharpened needle electrodes are passed subcutaneously into the area at the ventral base of each limb. After three leads are recorded, the needles are removed and the animals are allowed to recover.

Histology and Immunofluorescence staining. For all tissue sectioning, beating hearts were harvested from euthanized mice and immediately transferred to ice cold PBS containing 1M KCl until the hearts stopped beating at diastole state. For H&E staining, hearts were fixed in 4% paraformaldehyde overnight and paraffin embedded. Serial sections at 5 μm thickness were used for staining. Hearts used for all immunofluorescence staining were fixed in 4% PFA and subjected to sequential incubation with 10%, 20%, and 30% sucrose in PBS at 4ºC. Hearts were then flash frozen in OCT medium using liquid nitrogen and frozen serial sections of 5 μm thickness were prepared using a Leica Cryostat. Primary antibodies used for staining include anti-Dystrophin (Abcam; ab15277-500), anti-HSPG2 (Neomarkers; RT-794), anti-a-Laminin (Chemicon; AB2034), anti-H3K79me2/3 (Abcam; ab2621-100), anti-Ki-67 (Abcam; ab15580). Secondary antibodies used are Alexa Fluor 594 goat anti-rat IgG (Invitrogen; A21212), Alexa Fluor 594 donkey anti-rabbit IgG (Invitrogen; A21207), Alexa Fluor 488 donkey anti-rabbit IgG (Invitrogen; A21206). Sections were counterstained with DAPI.

TUNEL assay. TUNEL staining was performed on frozen sections using the ApopTag Fluorescein In Situ Apoptosis Detection Kit (Millipore; S7110) and counterstained with DAPI.

Masson's Trichrome Staining. Paraffin sections, 5 μm thick, of hearts from 5 month old mice were used for staining. Masson's Trichrome Stain Kit was purchased from Dako

(AR173) and procedures were followed according to manufacturer's specifications manually, without an Artisan staining system.

Transmission Electron Microscopy. WT and CKO mice were injected with 25U heparin i.m. prior to euthanasia by isofluorane overdose. The hearts were quickly exposed, and perfused with 3 mg/ml 2,3-Butanedione monoxime in Hepes-buffered Krebs solution, followed by perfusion with 2% glutaraldehyde plus 6% sucrose in 75 mM Na-Cacodylate buffer (pH 7.4) supplemented with 3 mg/ml BDM and 0.1% tannic acid, followed by 2% osmium tetroxide. Samples were stained with uranyl acetate *en bloc*. Images were acquired on a Zeiss EM 910 transmission electron microscope utilizing a Gatan SC1000 digital camera.

Microarray and RT-qPCR analysis. Hearts were flash frozen in liquid nitrogen and ground to a fine powder. Total RNA was purified from tissue powder using Qiagen RNeasy Kit. RNA from three hearts, 1ug each, was pooled together. Four pairs of pooled RNA, representing a total of 12 WT and 12 CKO hearts, were used for gene expression analysis. Samples were submitted to the UNC Genomics and Bioinformatics Core Facility for RNA labeling, amplification, hybridization, and scanning. The dual-color Agilent 4X44K Whole Mouse Genome Array system was used. All reagents were purchased from Agilent and procedures were followed according to Agilent's protocols. Raw data was uploaded into the UNC Microarray Database (Agi-Scanner-Reg-MM-4X44K-D20060807-BARCODE14868; Slide Run US82800149). Data was analyzed using the SAM algorithm (Tail strength 51.4%, se 63.8%) to yield 1379 significant probes with a Median number of false positives = 0.81 and false discovery rate of 0.06%. For RT-qPCR analysis, RNA prepared above was treated with DNase I, and first-strand DNA synthesis was performed using Improm II (Promega).

SYBR GreenER qPCR SuperMix (Invitrogen) was used for qPCR. Relative expression was normalized to *gapdh*. Primers are shown in Table S2-2.

Micro-Chromatin Immunoprecipitation and Western blot. Micro ChIP from frozen heart biopsies was performed as described previously (Dahl and Collas 2008) with the following modifications. Frozen hearts from P10 pups were ground to a fine powder prior to formaldehyde cross-linking. DNA was fragmented into 300-500 bp by sonication at 15% power (2X15 sec, 0.5 sec on and 2 sec off). Immunoprecipitation was performed using anti-H3K79me2/3 (Abcam) and anti-Rabbit IgG (Santa Cruz; sc-2027). ChIP'ed samples were washed twice with low salt (140 mM NaCl) RIPA buffer, once with high salt (500 mM NaCl) RIPA buffer, and twice with TE buffer. DNA was purified using the Chelex-100 method and qPCR was performed using the ChIP primers listed in Table S2-2. For Western blot analysis, P1 frozen hearts were ground to a fine powder for histone extraction and Western blot as described previously (Fang et al. 2002).

C2C12 knockdown and rescue. C2C12 cells were maintained in Dulbecco's modified Eagle's medium supplemented with 10% FBS and 1% penicillin/streptomycin. To establish stable KD cell lines, the lentivirus pTY-EF1a system was used as described previously (Cao et al. 2008; He et al. 2008). To knockdown mDOT1L, a shRNA 19mer was designed targeting the coding region (5'- GGAGCCAGATCTCAGAGAA-3'). The control shRNA is targeted against a bacterial protein with no mouse or human homology (5'-GTTCAGATGTGCGGCGAGT-3'). KD cells were selected and maintained in media containing 2μg/mL puromycin. For rescue experiments, KD cells were infected with retrovirus expressing WT and catalytic mutant Flag-tagged human DOT1L (Flag-hDOT1L) as described previously (Okada et al. 2005). Retrovirus infected cells were selected and

maintained in media containing 2μg/mL blasticidin. RNA was isolated using RNeasy Kit from Qiagen. The same micro-ChIP procedure described above was followed for ChIP using 50,000 cells per sample. Dynabeads Protein A and M2 Flag antibody (Sigma; F3165) were also used.

Postnatal rescue of CKO mice with rAAV-miniDmd. The functional miniature version of human dystrophin gene Δ3990 (miniDmd) under the transcriptional control of CMV promoter has been described previously (Wang et al. 2000). The miniDmd gene expression cassette was packaged into adeno-associated virus (AAV) serotype 9 vector using the helper-free, triple plasmids transfection method and purified by double CsCl density ultracentrifugation (Xiao et al. 1998). The rAAV9-CMV-miniDmd titers were determined by DNA dot blot at approximately 1×10^{13} viral genome (v.g) particles per ml. For 3-day-old neonatal CKO mice, a single dose of 1×10^{11} v.g./mouse in 50 μl was injected intraperitoneally (i.p). For 2-month-old CKO mice, a single dose of 1×10^{12} v.g./mouse in 600 μl was injected via tail vein (i.v.).

Statistics. Indicated *p*-values were calculated using two-tailed t-test.

Acknowledgements

We thank Jackie Kylander, Kristine Porter, and Mauricio Rojas at the UNC-CH Mouse Cardiovascular Models Core Facility for performing ECHO on P10 pups and EKG on adult control mice; Kai Xia for help with the microarray data analysis; Jin He for help in EKG data analysis, and Kwon-Ho Hong for critical reading of the manuscript. The work is supported by an NIH grant (CA119133). A.T.N is a recipient of the Pre-doctoral Fellowship from the American Heart Association. Y.Z. is an Investigator of the Howard Hughes Medical Institute.

Author contributions

Anh Nguyen performed the majority of experiments. Anh Nguyen and Yi Zhang prepared the manuscript. Bin Xiao performed ECHO and EKG and assisted in data analysis. Ronald Neppl assisted in TEM analysis. Eric Kallin assisted in gene expression microarray analysis. Juan Li generated the rAAV9-miniDmd virus for *in vivo* rescue experiments.

Figure 2-1. Disruption of DOT1L function in mouse cardiomyocytes results in heart dilation and lethality. (**A**) *Dot1L* CKO in mouse heart causes postnatal and adult lethality. Survival curves of WT, HET, and CKO mice. Fifty percent of CKO mice die within the first 2 wks after birth and the remaining 50% die by 6 months of age. (**B**) CKO hearts are severely enlarged compared to WT. Shown are WT and CKO hearts harvested from P10 and 5 month adult mice, respectively. Scale bar=1mm. **(C)** H&E staining of paraffin tissue sections indicated that CKO hearts are enlarged due to ventricular chamber dilation. Scale bar=1mm. **(D)** CKO mice have increased heart to body weight ratios. Heart weight (mg) to body weight (g) ratios were calculated using an analytical balance. CKO mice have increased ratios compared to WT littermates; * $p<0.06$, ** $p<0.006$, *** $p<0.0006$. **(E)** CKO mice have increased heart weight. Heart weight (mg) was measured using an analytical balance. * $p<0.06$.

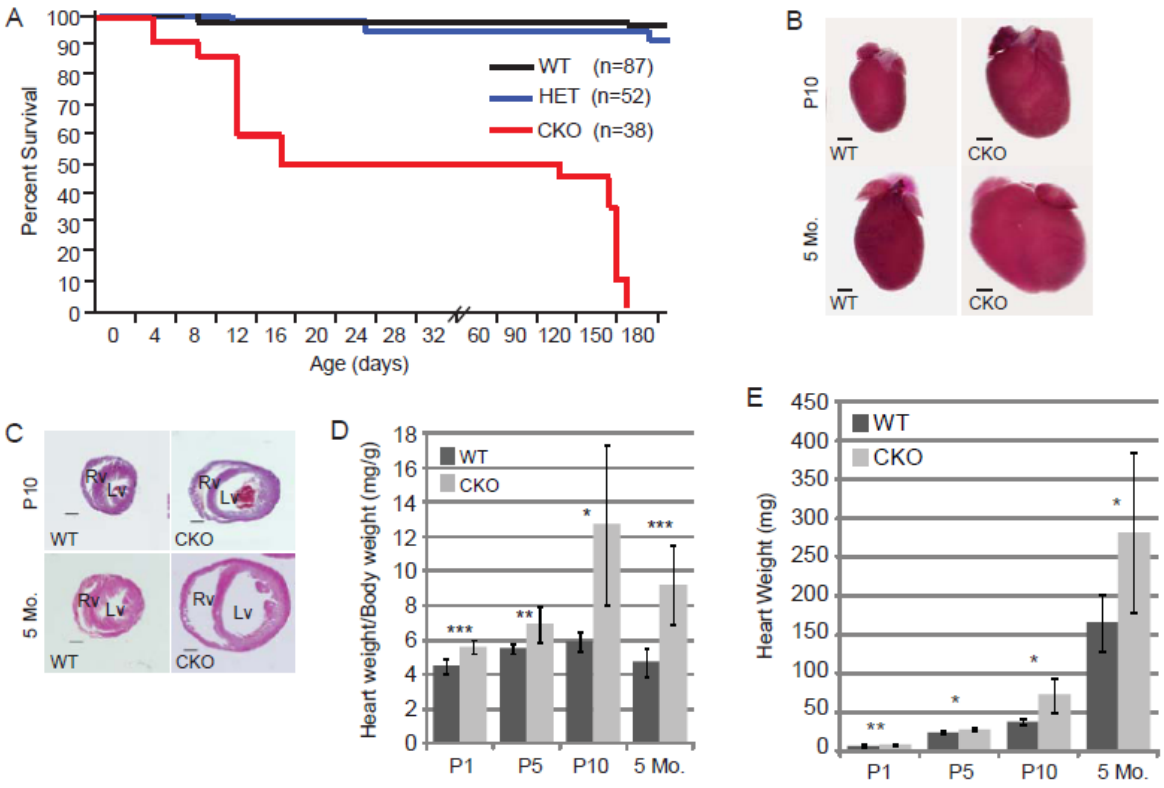
A
Percent Survival
Age (days)
WT (n=87)
HET (n=52)
CKO (n=38)
B
P10
5 Mo.
WT
CKO
C
P10
5 Mo.
Rv
Lv
WT
CKO
D
Heart weight/Body weight (mg/g)
WT
CKO
P1
P5
P10
5 Mo.
E
Heart Weight (mg)
WT
CKO
P1
P5
P10
5 Mo.

Figure 2-2. Disruption of DOT1L function in mouse cardiomyocytes results in pathologic cardiac remodeling. (**A**) Positive TUNEL staining (green) merged with DAPI (blue) demonstrates increased cell death in CKO hearts (P10, Scale bar=5 μm). (**B**) TEM analysis of P10 hearts demonstrates increased autophagic cell death (compare i. and ii.; yellow box is enlarged from ii.; vacuoles indicated by yellow arrows; scale bar=2 μm) and myofibroblast infiltration (indicated by * in iii) in CKO hearts. Note that myocytes in WT hearts show tight lateral association, whereas myocytes in CKO hearts have large gaps due to myofibroblasts infiltration. (**C**) Increased interstitial ECM, indicated by staining of the ECM component HSPG2 (red), is observed in the CKO hearts (arrowheads). Increased ECM and myofibroblasts lining the inner left ventricular chamber wall (between the two yellow lines) is also observed in CKO hearts. Scale bar=10 μm. (**D**) Masson's trichrome staining of paraffin tissue sections of mouse hearts (5 Mo. old). Two enlarged regions are shown (black and yellow boxes). Interstitial fibrosis is seen in CKO hearts but not in WT counterparts. Scale bar=5 mm. **(E)** RT-qPCR analysis demonstrates activation of fetal-specific genes (*Myh7*, *Acta1*, *Nppa*, and *Nppb*) in the CKO hearts. In contrast, down-regulation of adult *Myh6* is also observed. **(F)** Increased cell proliferation in CKO hearts (P1 and P5). Frozen tissue sections were stained with anti-Ki-67, a marker of cell proliferation, and counterstained with DAPI. The percentage of proliferating cells were calculated by dividing the number of Ki-67 positive nuclei by total nuclei and multiplying by 100.

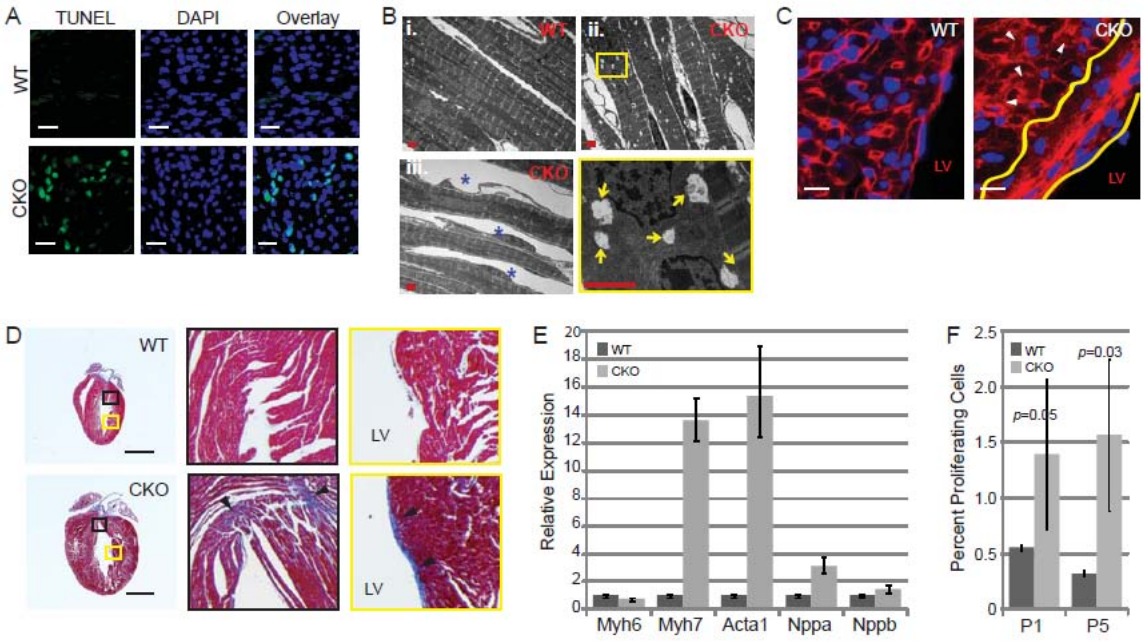
A
TUNEL
DAPI
Overlay
WT
CKO
B
i.
WT
ii.
CKO
iii.
CKO
C
WT
CKO
LV
LV
D
WT
CKO
LV
LV
E
WT
CKO
Relative Expression
20
18
16
14
12
10
8
6
4
2
0
Myh6
Myh7
Acta1
Nppa
Nppb
F
WT
CKO
p=0.03
p=0.05
Percent Proliferating Cells
2.5
2.0
1.5
1.0
0.5
0
P1
P5

Figure 2-3. Disruption of DOT1L function in mouse cardiomyocytes results in conduction abnormalities. (**A**) Representative electrocardiography for WT and CKO mice. The analysis was performed using 5 month old mice (*n*=8 per group). CKOa has complete AV dissociation as evidence by non-sustained ventricular tachycardia, while CKOb has a Type II second-degree heart block. Scale bar=200 ms. (**B-E**) Quantification of ECG data indicated an overall significant increase in RR interval (**B**), PR interval (**C**), P-wave duration (**D**), and QRS interval (**E**). p-values calculated by student t-test.

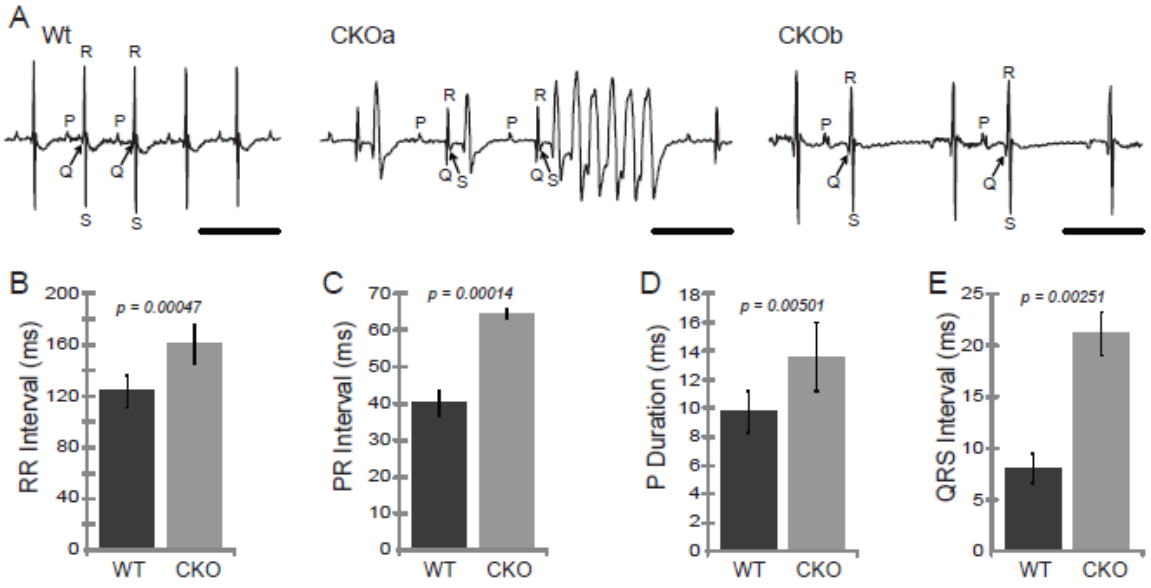

Figure 2-4. Dystrophin is a direct target of DOT1L. (**A**) RT-qPCR analysis using RNAs isolated from P10 WT and CKO hearts (*n*=12). *Dmd* and *Ttn* expression is down-regulated in *Dot1L* CKO hearts. Other members of the dystrophin-glycoprotein complex (*Dag1*, *Sgca*, *Sgcb*, *Sgcd*, and *Sgcg*) as well as selected DCM causal genes (*Actn2*, *Ldb3*, *Des*, and *Taz*) remain unchanged. (**B-C**) Immunostaining of frozen heart sections demonstrated loss of Dmd protein in CKO hearts (green). Consistent with a Dmd-deficiency and complex instability, reduction of βDG (**B**) and SGCA (**C**) is observed. **(D)** Micro-ChIP using heart tissues from P10 pups demonstrates that H3K79me2/3 is enriched in the gene body of *Dmd*, and the enrichment is dependent on functional DOT1L. Amplicon #1 located about 15 kb upstream of TSS serves as background for H3K79me2/3 enrichment. **(E)** ChIP using an anti-SRF antibody demonstrates that SRF binding to the CArG box consensus region of the Dmd muscle-specific promoter is not affected in *Dot1L* CKO hearts. Amplification at -15kb TSS serves as a background for SRF enrichment. (**F**) RT-qPCR analysis demonstrates that *Dot1L* knockdown in C2C12 cells results in *down-regulation* of *Dmd*. Error bars represent s.d. of three independent experiments. (**G,H**) ChIP analysis demonstrates binding of F-DOT1L to the *Dmd* locus and its methylation on H3K79 is dependent on DOT1L enzymatic activity.

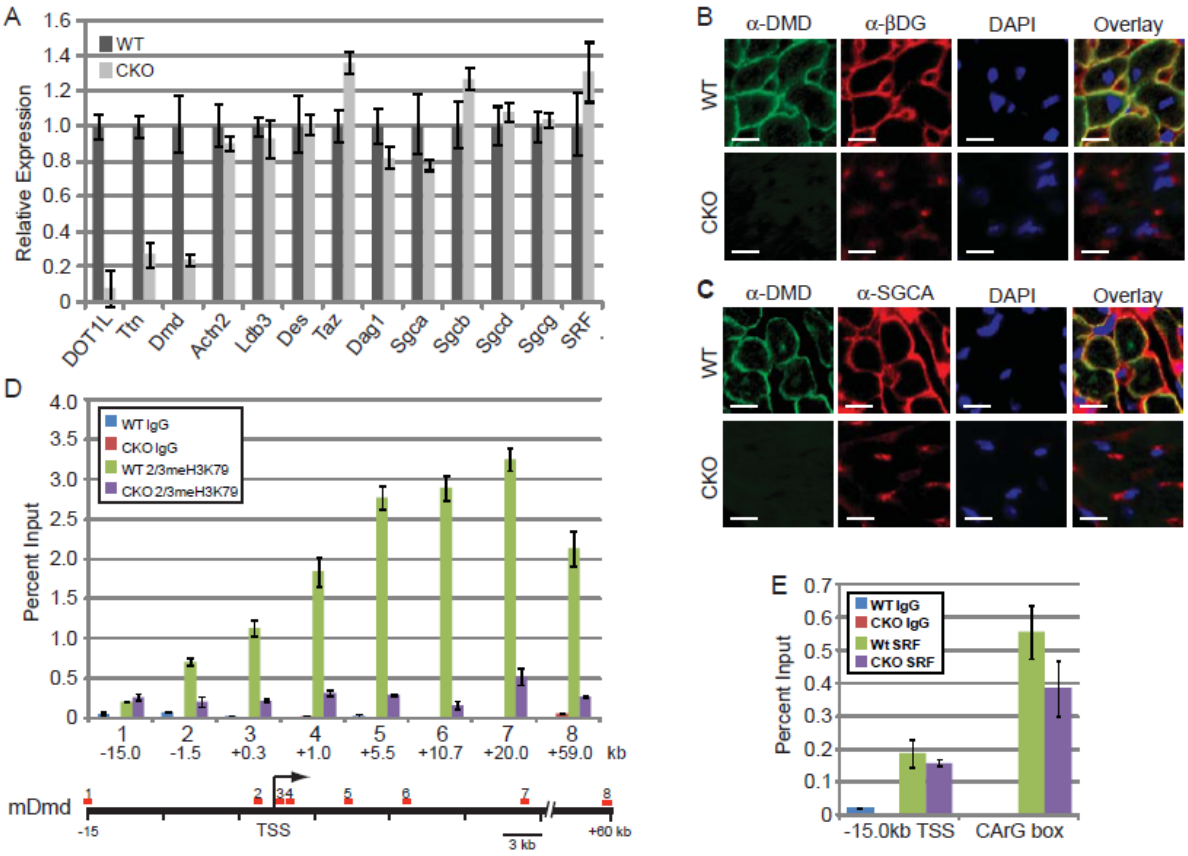
A
Relative Expression
WT
CKO
DOT1L
Ttn
Dmd
Actn2
Ldb3
Des
Taz
Dag1
Sgca
Sgcb
Sgcd
Sgcg
SRF
B
α-DMD
α-βDG
DAPI
Overlay
WT
CKO
C
α-DMD
α-SGCA
DAPI
Overlay
WT
CKO
D
Percent Input
WT IgG
CKO IgG
WT 2/3meH3K79
CKO 2/3meH3K79
-15.0
-1.5
+0.3
+1.0
+5.5
+10.7
+20.0
+59.0
kb
mDmd
TSS
3 kb
+60 kb
E
Percent Input
WT IgG
CKO IgG
Wt SRF
CKO SRF
-15.0kb TSS
CArG box
F
Relative Expression
Control shRNA
mDOT1L shRNA
mDOT1L shRNA + F-hDOT1L (WT)
mDOT1L shRNA + F-hDOT1L (Mut)
mDOT1L
mDmd
mSRF
G
ChIP: anti-Flag
Percent Input
H
ChIP: anti-H3K79me2/3
Percent Input

Figure 2-5. Rescue of electrical conduction in CKO mice by expression of *minidystrophin* gene. (**A-D**) The defective function of CKO heart can be rescued by expression of a mini-dystrophin gene when injected at P3 and analyzed at 5 months of age as indicated by the lack of significant difference between WT and CKO rescued mice. (**E-H**) Additionally, minidystrophin can rescue adult CKO mice injected at 2 months in terms of RR interval (**E**), P-wave duration (**G**), and QRS interval (**H**). In addition, PR interval (**F**) was partially rescued as the difference observed is less than without miniDmd. (p=0.02 in rescue vs *** p<0.0006 in without rescue at 5 months). At 8 months of age, past the second stage of lethality, CKO+miniDmd mice still maintain similar rescued levels of electrical conduction performance **(E-F).**

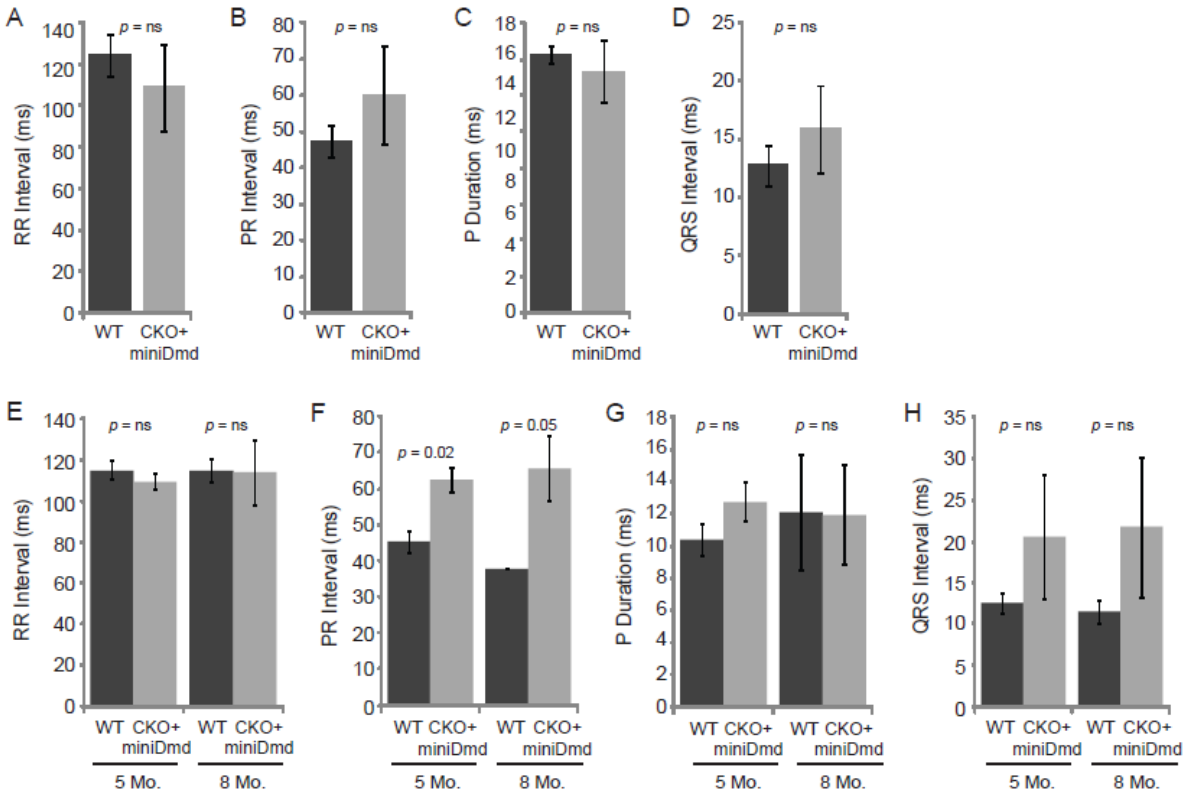

Figure 2-6. Model for role of DOT1L in regulating *dystrophin* transcription and cardiac function. DOT1L-mediated H3K79 methylation is required for active transcription of the dystrophin locus. In the absence of DOT1L enzymatic activity, *dystrophin* is silenced, resulting in reduced protein levels and destabilization of the DGC complex. Without DGC, sarcolemma damage, cell death, and reduced myocardial performance occur. Compensatory remodeling and chamber dilation is observed in an attempt to repair cardiac performance. However, this becomes maladaptive and is manifested by dilated cardiomyopathy and heart failure.

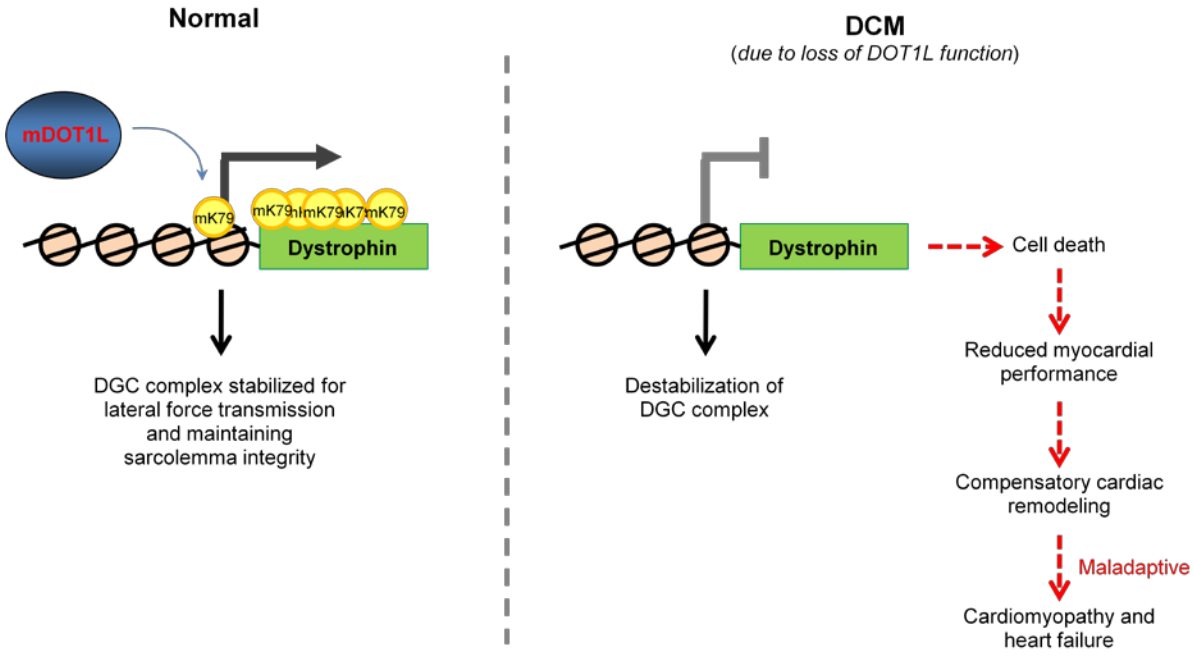

Table 2-1. Heart function of WT and CKO mice as measured by Echocardiography.

		%EF	%FS	LVID;d (mm)	LVID;s (mm)	LV Vol;d (μl)	LV Vol;s (μl)	LV mass	*n*
P10	WT	89.20±1.86	56.50±2.69	1.59±0.13	0.70±0.08	7.23±1.58	0.79±0.28	18.70±3.01	5
	CKO	55.80±3.83	27.30±2.15	2.16±0.25	1.57±0.23	15.79±4.82	7.15±2.87	21.41±3.47	5
	p-value	***	***	*	***	*	**	ns	
2 Months	WT	85.15±4.63	53.47±6.03	2.73±0.19	1.27±0.18	27.97±4.66	4.11±1.46	76.61±11.88	6
	CKO	72.56±5.77	40.81±4.73	3.12±0.13	1.85±0.20	38.83±4.12	10.87±2.91	98.51±18.0	4
	p-value	*	*	*	**	*	**	ns	
5 Months	WT	84.73±3.60	52.74±4.43	2.98±0.28	1.41±0.19	35.01±7.72	5.36±1.81	87.16±13.89	10
	CKO	47.02±18.48	24.44±10.84	4.91±1.43	3.85±1.60	127.58±83.67	80.83±70.08	205.86±101.11	7
	p-value	***	***	**	***	**	**	**	

EF = ejection fraction; FS = fractional shortening; LVID = left ventricular internal diameter;
LV Vol = left ventricular volume; LV mass = left ventricular mass (AW) corrected; d = end diastolic; s = end systolic

*** < 0.0006
** < 0.006
* < 0.06
ns ≥ 0.06

Table 2-2. Heart function of rAAV-miniDmd rescued CKO mice as measured by Echocardiography.

		%EF	%FS	LVID;d (mm)	LVID;s (mm)	LV Vol;d (μl)	LV Vol;s (μl)	LV mass	*n*
rAAV-Dmd at P3									
2 Months	WT	85.85±2.79	53.43±3.32	2.57±0.23	1.20±0.18	24.25±5.29	3.54±1.31	75.83±8.52	5
	CKO	79.53±6.76	46.97±6.59	2.77±0.35	1.48±0.36	29.59±9.75	6.51±4.12	82.19±14.13	4
	p-value	ns	ns	ns	ns	ns	ns	ns	
5 Months	WT	83.00±0.92	50.40±0.66	2.90±0.33	1.44±0.17	32.70±9.43	5.64±1.82	78.30±15.62	5
	CKO	78.47±11.52	47.81±12.36	3.10±0.46	1.66±0.60	39.38±14.11	9.51±7.08	103.62±29.65	4
	p-value	ns	ns	ns	ns	ns	ns	ns	
rAAV-Dmd at 2 Mo.									
5 Months	WT	73.47±17.81	42.62±14.20	2.79±0.22	1.62±0.54	29.57±6.05	8.61±7.53	78.83±6.95	3
	CKO	82.87±3.53	50.39±4.07	2.81±0.12	1.40±0.16	30.04±3.14	5.27±1.54	104.25±9.60	3
	p-value	ns	ns	ns	ns	ns	ns	ns	
8 Months	WT	88.29±1.03	57.14±1.21	3.12±0.25	1.34±0.14	38.69±7.38	4.57±1.24	84.01±18.93	3
	CKO	83.32±2.13	50.97±2.22	3.15±0.25	1.55±0.20	40.30±8.67	6.87±2.44	120.48±19.58	3
	p-value	ns	ns	ns	ns	ns	ns	ns	

To perform postnatal rescue, pups at P3 were administered rAAV-Dmd via intraperitoneal injection.
To perform adult rescue, mice at 2 Mo. of age were administered rAAV-Dmd via tail vein injection.

EF = ejection fraction; FS = fractional shortening; LVID = left ventricular internal diameter; LV Vol = left ventricular volume; LV mass = left ventricular mass (AW) corrected; d = end diastolic; s = end systolic

*** < 0.0006
** < 0.006
* < 0.06
ns ≥ 0.06

Figure S2-1. DOT1L expression in mouse heart tissue. (**A**) The Dot1L conditional allele contains a promoterless b-geo cassette. LacZ staining was performed to analyze Dot1L expression in mouse tissues. As shown, Dot1L is highly expressed in the heart. (**B**) RT-qPCR analysis of heart RNA extracts during embryonic development indicates that Dot1L expression peaks after birth. Relative expression normalized to Gapdh and expression at E10.5 set to 1.

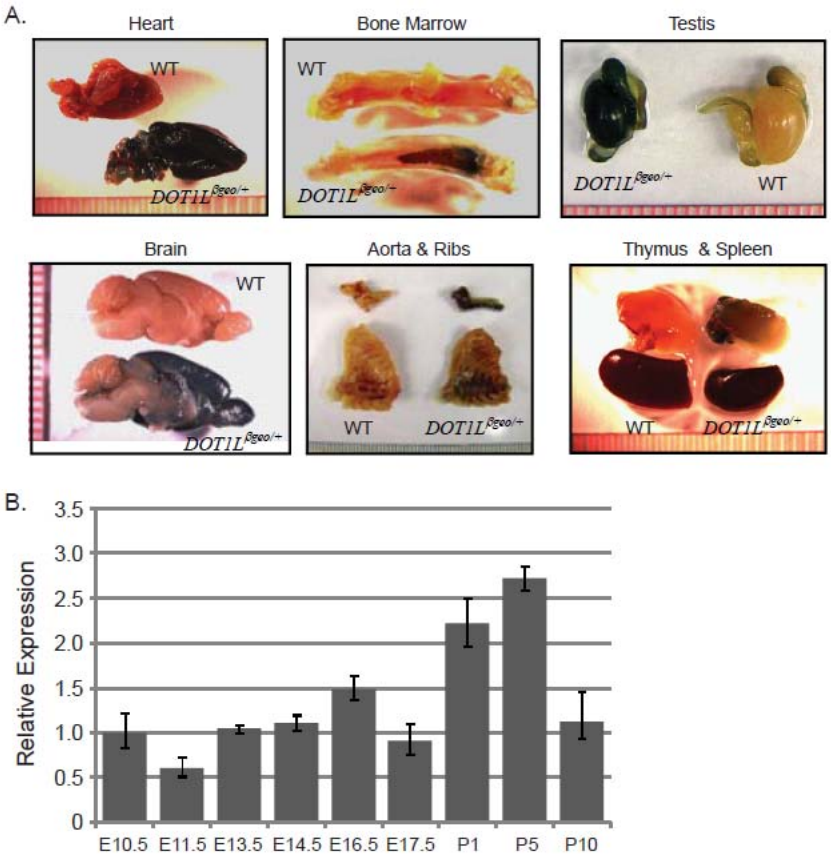

Figure S2-2. Generation of cardiac-specific DOT1L CKO mice. (**A**) Schematic diagram of Dot1L locus to generate cardiac conditional knockout (CKO) by crossing DOT1L$^{2lox/+}$ and DOT1L$^{1lox/+}$ mice with α-MHC-Cre mice. The DOT1L$^{2lox/+}$ conditional allele contains loxP sites (triangles) flanking Exons 5 and 6. Primer pairs DF1 and DR1 were used for genotyping, RTa and RTb were used for RT-qPCR analysis. (**B**) Diagram of DOT1L WT and CKO protein that harbors a deletion of 108 aa in the SAM binding motif (+, positive-charged region; NES, nuclear export signals; LZ, leucine zipper motif). (**C**) Dot1L CKO mice are born at Mendelian ratio from intercrosses of heterozygote mice (DOT1L$^{2lox/+;}$α-MHC-Cre with DOT1L1$^{lox/+;}$α-MHC-Cre). (**D**) RT-qPCR analysis confirms efficient recombination at Dot1L locus in P1 CKO hearts. (**E**) Western blot analysis demonstrates loss of H3K79me2/3 in CKO P1 heart histone extracts. (**F**) Immunostaining of frozen mouse heart sections (5 μm thick) with anti-H3K79me2/3 (red) demonstrates loss of H3K79me2/3 in CKO hearts. The sections were counterstained with DAPI (blue).

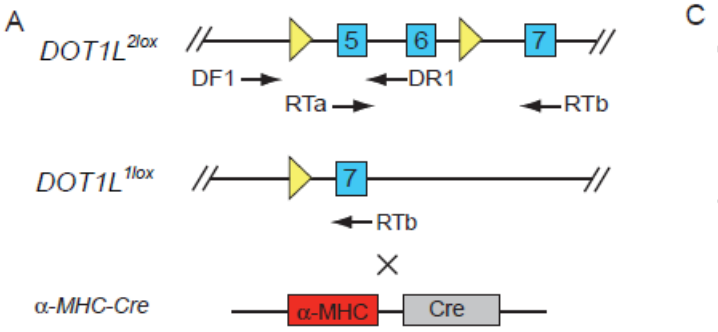

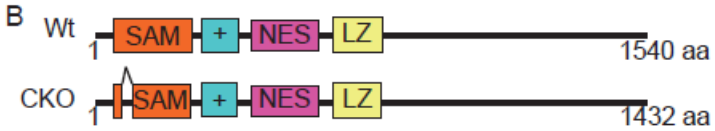

C

Genotype	#Pups	Percentage
2lox/wt	32	23.4(25)
1lox/wt	30	21.9(25)
2lox/1lox	35	25.5(25)
wt/wt	40	29.2(25)

*Expected Mendelian ratio in parentheses

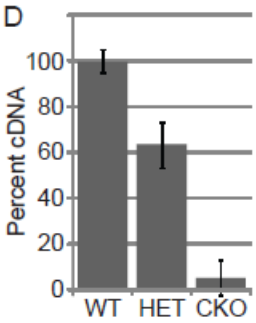

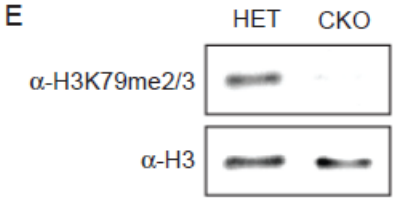

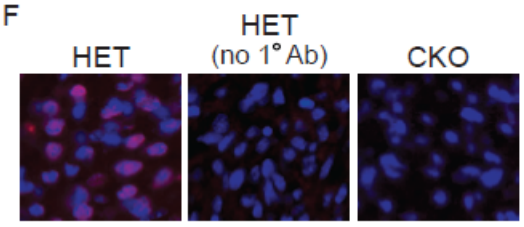

Figure S2-3. Concentric hypertrophy does not contribute to increased CKO heart mass. (**A**) Body weights of WT and CKO mice were measured (g) using an analytical balance. No significant difference in body weights was observed between WT and CKO littermates. (**B**) No significant difference in the size of WT and CKO cardiomyocytes is observed. Frozen tissue sections were stained with anti-Laminin and cardiomyocyte circumference measured (pixels) using ImageJ software. The average circumference with s.d. are shown with the number of cells measured per sample indicated. (**C**) Representative images of cardiomyocyte cross-sections visualized by anti-Laminin staining.

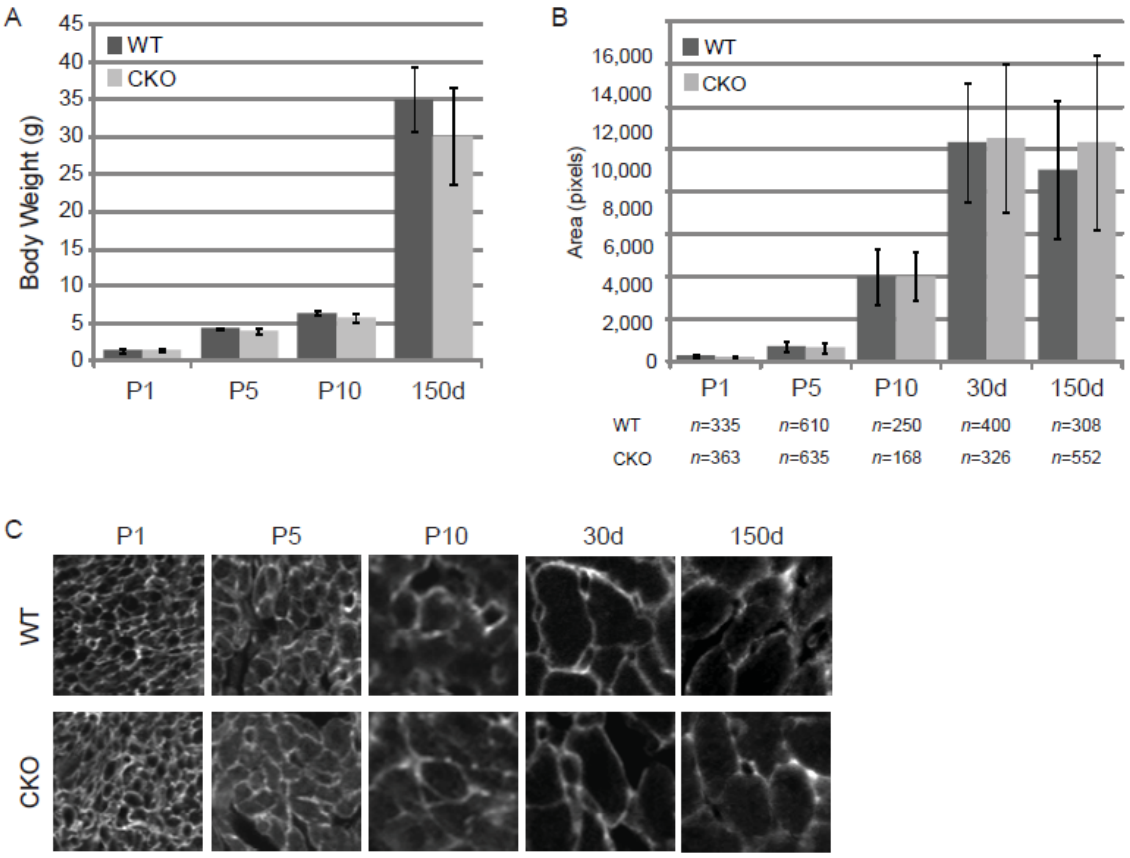

Figure S2-4. Sarcomere integrity remains intact in CKO hearts. Sections from P10 perfused hearts were analyzed by TEM. The overall sarcomere length and structure appears normal in CKO mice and do not exhibit the defects observed in Ttn-deficient hearts. Representative image of each genotype is shown.

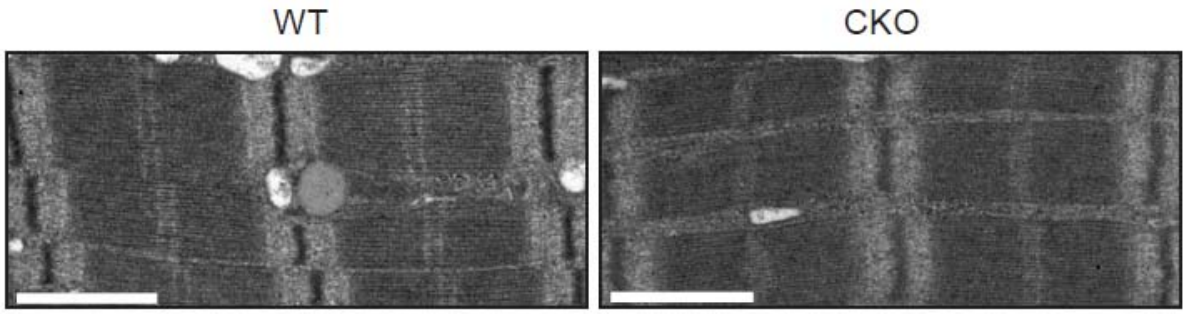

Figure S2-5. Expression level of human DOT1L rescue constructs. WT and catalytic mutant, Mut, retrovirus constructs are expressed at similar levels in shRNA KD cells. Relative expression was normalized to mouse Gapdh and background level of hDOT1L primers in shRNA sample was set to one.

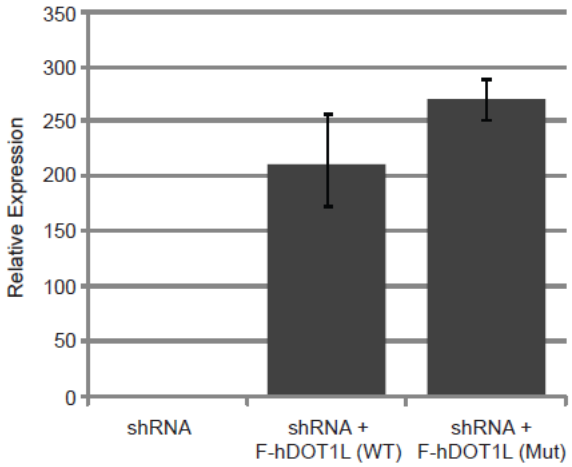

Figure S2-6. Heart blocks absent in adult rescued CKO mice. Representative EKG (**A**) and echocardiogram (**B**) images of the same mice taken from an ECHO machine before and after tail vein injection with rAAV9-miniDmd. The data indicates that a heart block observed before the injection is alleviated by 5 months of age.

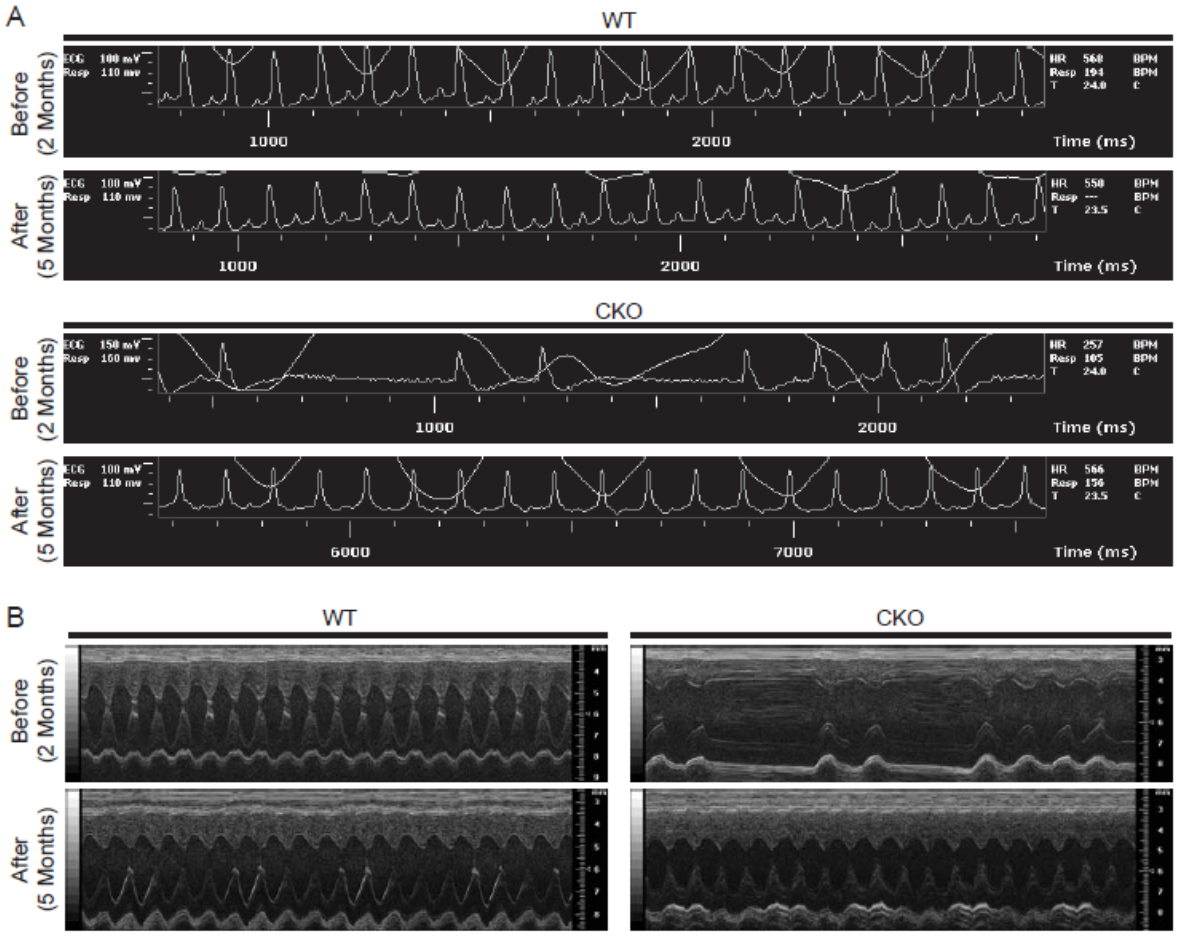

Figure S2-7. Utrophin expression is not up-regulated in CKO hearts. RT-qPCR was performed to compare Utrn RNA levels in WT and CKO hearts (n=12 per genotype). Relative expression is shown, normalized to Gapdh.

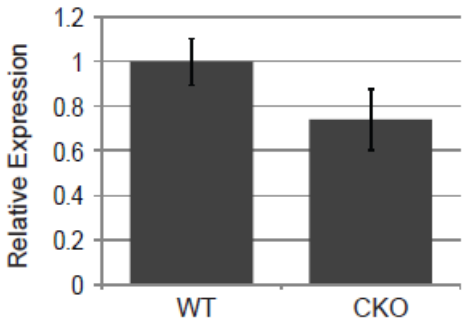

Figure S2-8. hDOT1L is down-regulated in human idiopathic DCM myocardia.

hDOT1L expression level was analyzed from a publically available microarray database (CardioGenomics). The database represents myocardial samples from patients undergoing heart transplantation with different etiologies as well as "normal" organ donors whose hearts could not be used for transplants. Gene expression microarray was performed using Affymetrix Human Genome U133 Plus 2.0 Array. Data from three different probe sets for hDOT1L is shown. Each probe set consists of 11 different probes. p-Values were calculated using two-tailed t-test.

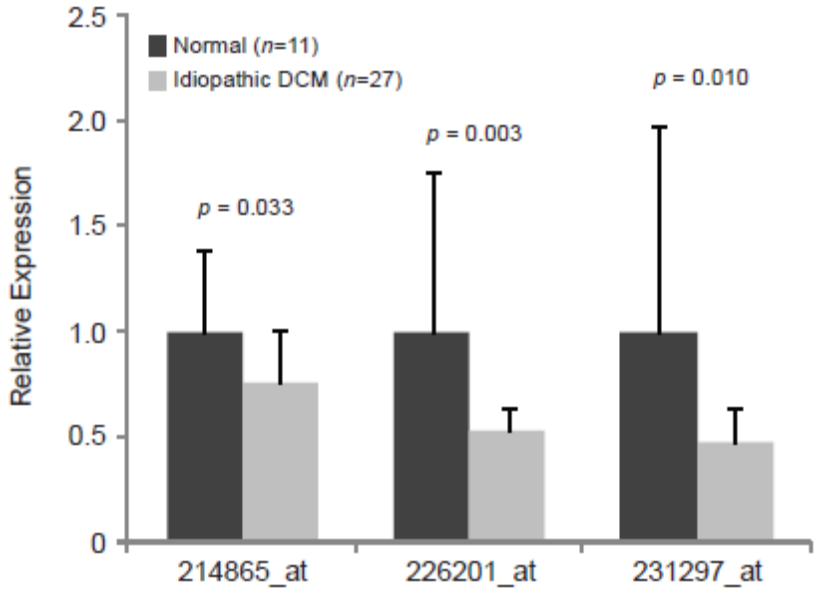

Table S2-1. Genes with DCM-associated mutations.

Gene	Coding Protein	Gene	Coding Protein
ABCC9	K-ATP channel	*MYBPC3*	Cardiac myosin binding protein-C
ACTC1	Cardiac α-actin	*MYPN*	Myopalladin
ACTN2	α-actinin-2	*PLN*	Phospholamban
CRYAB	αB crystalline	*JUP*	Plakoglobin
LDB3	Cypher	*RYR2*	Cardiac ryanodine receptor 2
DES	Desmin	*SGCD*	Sarcoglycan
DSP	Desmoplakin	*SCN5A*	Cardiac Na Channel
DMD	Dystrophin	*TAZ*	Tafazzin
EMD	Emerin	*TCAP*	Telethonin
FHL2	Four-and-a-half LIM protein-2	*TMPO*	Thymopoietin
FKTN	Fukutin	*TNNC1*	Cardiac troponin C
LMNA	Lamin a/c	*TNNI3*	Cardiac troponin I
LMNA4	Laminin α4	*TNNT2*	Cardiac troponin T
VCL	Metavinculin	*TPM1*	α-Tropomyosin
CSRP3	Muscle LIM protein, MLP	*TTN*	Titin
MYH7	Cardiac β-myosin heavy chain		

Table S2-2. RT-qPCR and ChIP-qPCR primer sequences.

RT-qPCR		Forward Primer (5'-3')	Reverse Primer (5'-3')	
mDot1L		CAGAGGATGACCTGTTTGTCG	CATCCACTTCCTGAACTCTCG	
mDmd		AAAACATGCCCAAGAGGAACT	CTGCTTTTTCTCGTGCTATGG	
mSrf		GGCCCTGTCTCCTCTGGGGG	GATGGTGGCGGGCAACGTCA	
mSgcg		TGGAAGGAGAGTCGGAATTTT	ACTGTCACGTTCTGGGTTGA	
mSgcd		CAGAAGCTGGCAATATGGAAG	GGTAGTTTGATTTTCGCAGCA	
mSgca		ACACAGCGCAGTCCCTATAAC	CCAGGAACTCAGCTTGGTATG	
mSgcb		CTGGCCGTCATCAATCTACTTC	GACACTTGCTTGAACCTCAGC	
mDag1		CTCATTTCGAGTGAGCATTCC	ACTGTGTGGGTCCCAGTGTAG	
mTaz		CACTCCCATTTCTTCAGCTTG	CAGGATGATGGGATTCAGATG	
mDes		AGGAGGAGATCCGACACCTAA	CTCGGAAGTTGAGAGCAGAGA	
mLdb3		TTCAACATGCCCCTCACTATC	CTGTCGTGGAGATGGGAATAG	
mActn2		GACCTGCAGGACATGTTCATT	TGCTGTAGCTCTGGATCACCT	
mMyh7		GCATTCTCCTGCTGTTTCCTT	TGGATTCTCAAACGTGTCTAGTGA	
mMyh6		CCGTAGCAAGAAGGAAAATCC	CTCCAAAGTGGATCCTGATGA	
mActa1		GATCTGGCACCACACCTTCTA	TCATCTTCTCCCGGTTAGCTT	
mNppa		GAGTGGACTAGGCTGCAACAG	CGTGATAGATGAAGGCAGGAA	
mNppb		CCTCAAAATTCCAAGGTGACA	GCCAGGAGGTCTTCCTACAAC	
mGapdh		CATGGCCTTCCGTGTTCCTA	GCCTGCTTCACCACCTTCTT	
hDot1L		CTCAGCACCGTGCAGCCCAA	GGGCCAGGGCAAGGCTTCTG	
ChIP Primer	**Position Relative to TSS**	**Forward Primer (5'-3')**	**Reverse Primer (5'-3')**	**Amplicon Length**
Dmd_c1	-15kb	GGCATAGCTCCTTTCCTTTTT	TGCACACAAAAGCATGCAATA	93bp
Dmd_c6	-1.5kb	AACATGACTGGGGAGGGTAAG	TCATGATGCAGCACTATTCCA	87bp
Dmd_c9	+0.3kb	AATGCTTTGGTGGGAAGAAGT	AGCTGAAAGTCATGCCACAGT	82bp
Dmd_c12	+1.0kb	GAAGGGTTGTCATCCCATTTT	AAACAAGTGGGAGGCATTTT	114bp
Dmd_c15	+5.5kb	TTCACAAAACCCTGGTATGGA	TTGACCCTCTGGCTGCTATTA	83bp
Dmd_c17	+10.7kb	TCCAGAGCTGCATTTCTCTACA	CTTTCTGCCAAACACCTTGAG	93bp
Dmd_c20	+20.0kb	TGCCCCCTAAGAGGGTAAGTA	CCCCTAGTCAACCTGCAAAAT	99bp
Dmd_c21	+58.5kb	GGTGAGCAATCACCCAAAATA	CCTGGCCACATGAAAACTTTA	92bp
SRF_2 (CArG consensus)	-0.2kb	CCTGTGCTATTCTGGTTTGGA	TAAGGCTGTGCTTCCAGAATG	89bp

References

Abel ED, Kaulbach HC, Tian R, Hopkins JC, Duffy J, Doetschman T, Minnemann T, Boers ME, Hadro E, Oberste-Berghaus C et al. 1999. Cardiac hypertrophy with preserved contractile function after selective deletion of GLUT4 from the heart. *J Clin Invest* **104**: 1703-1714.

Ahuja P, Sdek P, MacLellan WR. 2007. Cardiac myocyte cell cycle control in development, disease, and regeneration. *Physiol Rev* **87**: 521-544.

Banerjee I, Fuseler JW, Price RL, Borg TK, Baudino TA. 2007. Determination of cell types and numbers during cardiac development in the neonatal and adult rat and mouse. *Am J Physiol Heart Circ Physiol* **293**: H1883-1891.

Barrans JD, Allen PD, Stamatiou D, Dzau VJ, Liew CC. 2002. Global gene expression profiling of end-stage dilated cardiomyopathy using a human cardiovascular-based cDNA microarray. *Am J Pathol* **160**: 2035-2043.

Barry ER, Krueger W, Jakuba CM, Veilleux E, Ambrosi DJ, Nelson CE, Rasmussen TP. 2009. ES cell cycle progression and differentiation require the action of the histone methyltransferase Dot1L. *Stem Cells* **27**: 1538-1547.

Barski A, Cuddapah S, Cui K, Roh TY, Schones DE, Wang Z, Wei G, Chepelev I, Zhao K. 2007. High-resolution profiling of histone methylations in the human genome. *Cell* **129**: 823-837.

Barth AS, Kuner R, Buness A, Ruschhaupt M, Merk S, Zwermann L, Kaab S, Kreuzer E, Steinbeck G, Mansmann U et al. 2006. Identification of a common gene expression signature in dilated cardiomyopathy across independent microarray studies. *J Am Coll Cardiol* **48**: 1610-1617.

Camargo A, Azuaje F. 2008. Identification of dilated cardiomyopathy signature genes through gene expression and network data integration. *Genomics* **92**: 404-413.

Cao R, Wang H, He J, Erdjument-Bromage H, Tempst P, Zhang Y. 2008. Role of hPHF1 in H3K27 methylation and Hox gene silencing. *Mol Cell Biol* **28**: 1862-1872.

Cohn JN, Ferrari R, Sharpe N. 2000. Cardiac remodeling--concepts and clinical implications: a consensus paper from an international forum on cardiac remodeling. Behalf of an International Forum on Cardiac Remodeling. *J Am Coll Cardiol* **35**: 569-582.

Conde F, Refolio E, Cordon-Preciado V, Cortes-Ledesma F, Aragon L, Aguilera A, San-Segundo PA. 2009. The Dot1 histone methyltransferase and the Rad9 checkpoint adaptor contribute to cohesin-dependent double-strand break repair by sister chromatid recombination in Saccharomyces cerevisiae. *Genetics* **182**: 437-446.

Connuck DM, Sleeper LA, Colan SD, Cox GF, Towbin JA, Lowe AM, Wilkinson JD, Orav EJ, Cuniberti L, Salbert BA et al. 2008. Characteristics and outcomes of cardiomyopathy in children with Duchenne or Becker muscular dystrophy: a comparative study from the Pediatric Cardiomyopathy Registry. *Am Heart J* **155**: 998-1005.

Dahl JA, Collas P. 2008. A rapid micro chromatin immunoprecipitation assay (microChIP). *Nat Protoc* **3**: 1032-1045.

de Leeuw N, Ruiter DJ, Balk AH, de Jonge N, Melchers WJ, Galama JM. 2001. Histopathologic findings in explanted heart tissue from patients with end-stage idiopathic dilated cardiomyopathy. *Transpl Int* **14**: 299-306.

Deconinck AE, Rafael JA, Skinner JA, Brown SC, Potter AC, Metzinger L, Watt DJ, Dickson JG, Tinsley JM, Davies KE. 1997. Utrophin-dystrophin-deficient mice as a model for Duchenne muscular dystrophy. *Cell* **90**: 717-727.

Fang J, Feng Q, Ketel CS, Wang H, Cao R, Xia L, Erdjument-Bromage H, Tempst P, Simon JA, Zhang Y. 2002. Purification and functional characterization of SET8, a nucleosomal histone H4-lysine 20-specific methyltransferase. *Curr Biol* **12**: 1086-1099.

Feinberg AP, Oshimura M, Barrett JC. 2002. Epigenetic mechanisms in human disease. *Cancer Res* **62**: 6784-6787.

Feng Q, Wang H, Ng HH, Erdjument-Bromage H, Tempst P, Struhl K, Zhang Y. 2002. Methylation of H3-lysine 79 is mediated by a new family of HMTases without a SET domain. *Curr Biol* **12**: 1052-1058.

Feng Y, Yang Y, Ortega MM, Copeland JN, Zhang M, Jacob JB, Fields TA, Vivian JL, Fields PE. 2010. Early mammalian erythropoiesis requires the Dot1L methyltransferase. *Blood*.

Galvagni F, Lestingi M, Cartocci E, Oliviero S. 1997. Serum response factor and protein-mediated DNA bending contribute to transcription of the dystrophin muscle-specific promoter. *Mol Cell Biol* **17**: 1731-1743.

Gerull B, Gramlich M, Atherton J, McNabb M, Trombitas K, Sasse-Klaassen S, Seidman JG, Seidman C, Granzier H, Labeit S et al. 2002. Mutations of TTN, encoding the giant muscle filament titin, cause familial dilated cardiomyopathy. *Nat Genet* **30**: 201-204.

Giannattasio M, Lazzaro F, Plevani P, Muzi-Falconi M. 2005. The DNA damage checkpoint response requires histone H2B ubiquitination by Rad6-Bre1 and H3 methylation by Dot1. *J Biol Chem* **280**: 9879-9886.

Gotthardt M, Hammer RE, Hubner N, Monti J, Witt CC, McNabb M, Richardson JA, Granzier H, Labeit S, Herz J. 2003. Conditional expression of mutant M-line titins results in cardiomyopathy with altered sarcomere structure. *J Biol Chem* **278**: 6059-6065.

Grady RM, Teng H, Nichol MC, Cunningham JC, Wilkinson RS, Sanes JR. 1997. Skeletal and cardiac myopathies in mice lacking utrophin and dystrophin: a model for Duchenne muscular dystrophy. *Cell* **90**: 729-738.

Ha CH, Kim JY, Zhao J, Wang W, Jhun BS, Wong C, Jin ZG. 2010. PKA phosphorylates histone deacetylase 5 and prevents its nuclear export, leading to the inhibition of gene transcription and cardiomyocyte hypertrophy. *Proc Natl Acad Sci U S A* **107**: 15467-15472.

Handel AE, Ebers GC, Ramagopalan SV. 2009. Epigenetics: molecular mechanisms and implications for disease. *Trends Mol Med.*

Hang CT, Yang J, Han P, Cheng HL, Shang C, Ashley E, Zhou B, Chang CP. 2010. Chromatin regulation by Brg1 underlies heart muscle development and disease. *Nature* **466**: 62-67.

Hatcher CJ, Basson CT. 2009. Specification of the cardiac conduction system by transcription factors. *Circ Res* **105**: 620-630.

He J, Kallin EM, Tsukada Y, Zhang Y. 2008. The H3K36 demethylase Jhdm1b/Kdm2b regulates cell proliferation and senescence through p15(Ink4b). *Nat Struct Mol Biol* **15**: 1169-1175.

Heydemann A, McNally EM. 2007. Consequences of disrupting the dystrophin-sarcoglycan complex in cardiac and skeletal myopathy. *Trends Cardiovasc Med* **17**: 55-59.

Hoffman EP, Brown RH, Jr., Kunkel LM. 1987. Dystrophin: the protein product of the Duchenne muscular dystrophy locus. *Cell* **51**: 919-928.

Houweling AC, van Borren MM, Moorman AF, Christoffels VM. 2005. Expression and regulation of the atrial natriuretic factor encoding gene Nppa during development and disease. *Cardiovasc Res* **67**: 583-593.

Jones B, Su H, Bhat A, Lei H, Bajko J, Hevi S, Baltus GA, Kadam S, Zhai H, Valdez R et al. 2008. The histone H3K79 methyltransferase Dot1L is essential for mammalian development and heterochromatin structure. *PLoS Genet* **4**: e1000190.

Kajstura J, Leri A, Finato N, Di Loreto C, Beltrami CA, Anversa P. 1998. Myocyte proliferation in end-stage cardiac failure in humans. *Proc Natl Acad Sci U S A* **95**: 8801-8805.

Kaneda R, Takada S, Yamashita Y, Choi YL, Nonaka-Sarukawa M, Soda M, Misawa Y, Isomura T, Shimada K, Mano H. 2009. Genome-wide histone methylation profile for heart failure. *Genes Cells* **14**: 69-77.

Karkkainen S, Peuhkurinen K. 2007. Genetics of dilated cardiomyopathy. *Ann Med* **39**: 91-107.

Kimura A. 2008. Molecular etiology and pathogenesis of hereditary cardiomyopathy. *Circ J* **72 Suppl A**: A38-48.

Knaapen MW, Davies MJ, De Bie M, Haven AJ, Martinet W, Kockx MM. 2001. Apoptotic versus autophagic cell death in heart failure. *Cardiovasc Res* **51**: 304-312.

Kook H, Lepore JJ, Gitler AD, Lu MM, Wing-Man Yung W, Mackay J, Zhou R, Ferrari V, Gruber P, Epstein JA. 2003. Cardiac hypertrophy and histone deacetylase-dependent transcriptional repression mediated by the atypical homeodomain protein Hop. *J Clin Invest* **112**: 863-871.

Kostin S, Hein S, Arnon E, Scholz D, Schaper J. 2000. The cytoskeleton and related proteins in the human failing heart. *Heart Fail Rev* **5**: 271-280.

Kouzarides T. 2007. Chromatin modifications and their function. *Cell* **128**: 693-705.

Krivtsov AV, Feng Z, Lemieux ME, Faber J, Vempati S, Sinha AU, Xia X, Jesneck J, Bracken AP, Silverman LB et al. 2008. H3K79 methylation profiles define murine and human MLL-AF4 leukemias. *Cancer Cell* **14**: 355-368.

Krogan NJ, Dover J, Wood A, Schneider J, Heidt J, Boateng MA, Dean K, Ryan OW, Golshani A, Johnston M et al. 2003. The Paf1 complex is required for histone H3 methylation by COMPASS and Dot1p: linking transcriptional elongation to histone methylation. *Mol Cell* **11**: 721-729.

Lacoste N, Utley RT, Hunter JM, Poirier GG, Cote J. 2002. Disruptor of telomeric silencing-1 is a chromatin-specific histone H3 methyltransferase. *J Biol Chem* **277**: 30421-30424.

Liew CC, Dzau VJ. 2004. Molecular genetics and genomics of heart failure. *Nat Rev Genet* **5**: 811-825.

Luk A, Ahn E, Soor GS, Butany J. 2009. Dilated cardiomyopathy: a review. *J Clin Pathol* **62**: 219-225.

Martin C, Zhang Y. 2005. The diverse functions of histone lysine methylation. *Nat Rev Mol Cell Biol* **6**: 838-849.

Mohan M, Herz HM, Takahashi YH, Lin C, Lai KC, Zhang Y, Washburn MP, Florens L, Shilatifard A. 2010. Linking H3K79 trimethylation to Wnt signaling through a novel Dot1-containing complex (DotCom). *Genes Dev* **24**: 574-589.

Montgomery RL, Davis CA, Potthoff MJ, Haberland M, Fielitz J, Qi X, Hill JA, Richardson JA, Olson EN. 2007. Histone deacetylases 1 and 2 redundantly regulate cardiac morphogenesis, growth, and contractility. *Genes Dev* **21**: 1790-1802.

Movassagh M, Choy MK, Goddard M, Bennett MR, Down TA, Foo RS. Differential DNA methylation correlates with differential expression of angiogenic factors in human heart failure. *PLoS One* **5**: e8564.

Mueller D, Bach C, Zeisig D, Garcia-Cuellar MP, Monroe S, Sreekumar A, Zhou R, Nesvizhskii A, Chinnaiyan A, Hess JL et al. 2007. A role for the MLL fusion partner ENL in transcriptional elongation and chromatin modification. *Blood* **110**: 4445-4454.

Ng HH, Feng Q, Wang H, Erdjument-Bromage H, Tempst P, Zhang Y, Struhl K. 2002a. Lysine methylation within the globular domain of histone H3 by Dot1 is important for telomeric silencing and Sir protein association. *Genes Dev* **16**: 1518-1527.

Ng HH, Xu RM, Zhang Y, Struhl K. 2002b. Ubiquitination of histone H2B by Rad6 is required for efficient Dot1-mediated methylation of histone H3 lysine 79. *J Biol Chem* **277**: 34655-34657.

Okada Y, Feng Q, Lin Y, Jiang Q, Li Y, Coffield VM, Su L, Xu G, Zhang Y. 2005. hDOT1L links histone methylation to leukemogenesis. *Cell* **121**: 167-178.

Okada Y, Jiang Q, Lemieux M, Jeannotte L, Su L, Zhang Y. 2006. Leukaemic transformation by CALM-AF10 involves upregulation of Hoxa5 by hDOT1L. *Nat Cell Biol* **8**: 1017-1024.

Olson EN. 2004. A decade of discoveries in cardiac biology. *Nat Med* **10**: 467-474.

Peterson CL, Laniel MA. 2004. Histones and histone modifications. *Curr Biol* **14**: R546-551.

San-Segundo PA, Roeder GS. 2000. Role for the silencing protein Dot1 in meiotic checkpoint control. *Mol Biol Cell* **11**: 3601-3615.

Schubeler D, MacAlpine DM, Scalzo D, Wirbelauer C, Kooperberg C, van Leeuwen F, Gottschling DE, O'Neill LP, Turner BM, Delrow J et al. 2004. The histone modification pattern of active genes revealed through genome-wide chromatin analysis of a higher eukaryote. *Genes Dev* **18**: 1263-1271.

Seidman JG, Seidman C. 2001. The genetic basis for cardiomyopathy: from mutation identification to mechanistic paradigms. *Cell* **104**: 557-567.

Singer MS, Kahana A, Wolf AJ, Meisinger LL, Peterson SE, Goggin C, Mahowald M, Gottschling DE. 1998. Identification of high-copy disruptors of telomeric silencing in Saccharomyces cerevisiae. *Genetics* **150**: 613-632.

Steger DJ, Lefterova MI, Ying L, Stonestrom AJ, Schupp M, Zhuo D, Vakoc AL, Kim JE, Chen J, Lazar MA et al. 2008. DOT1L/KMT4 recruitment and H3K79 methylation are ubiquitously coupled with gene transcription in mammalian cells. *Mol Cell Biol* **28**: 2825-2839.

Towbin JA, Bowles NE. 2006. Dilated cardiomyopathy: a tale of cytoskeletal proteins and beyond. *J Cardiovasc Electrophysiol* **17**: 919-926.

Townsend D, Yasuda S, Li S, Chamberlain JS, Metzger JM. 2008. Emergent dilated cardiomyopathy caused by targeted repair of dystrophic skeletal muscle. *Mol Ther* **16**: 832-835.

van Leeuwen F, Gafken PR, Gottschling DE. 2002. Dot1p modulates silencing in yeast by methylation of the nucleosome core. *Cell* **109**: 745-756.

Wang B, Li J, Fu FH, Chen C, Zhu X, Zhou L, Jiang X, Xiao X. 2008a. Construction and analysis of compact muscle-specific promoters for AAV vectors. *Gene Ther* **15**: 1489-1499.

Wang B, Li J, Xiao X. 2000. Adeno-associated virus vector carrying human minidystrophin genes effectively ameliorates muscular dystrophy in mdx mouse model. *Proc Natl Acad Sci U S A* **97**: 13714-13719.

Wang Z, Zang C, Rosenfeld JA, Schones DE, Barski A, Cuddapah S, Cui K, Roh TY, Peng W, Zhang MQ et al. 2008b. Combinatorial patterns of histone acetylations and methylations in the human genome. *Nat Genet* **40**: 897-903.

Weinert S, Bergmann N, Luo X, Erdmann B, Gotthardt M. 2006. M line-deficient titin causes cardiac lethality through impaired maturation of the sarcomere. *J Cell Biol* **173**: 559-570.

Wood A, Schneider J, Dover J, Johnston M, Shilatifard A. 2003. The Paf1 complex is essential for histone monoubiquitination by the Rad6-Bre1 complex, which signals for histone methylation by COMPASS and Dot1p. *J Biol Chem* **278**: 34739-34742.

Wysocki R, Javaheri A, Allard S, Sha F, Cote J, Kron SJ. 2005. Role of Dot1-dependent histone H3 methylation in G1 and S phase DNA damage checkpoint functions of Rad9. *Mol Cell Biol* **25**: 8430-8443.

Xiao X, Li J, Samulski RJ. 1998. Production of high-titer recombinant adeno-associated virus vectors in the absence of helper adenovirus. *J Virol* **72**: 2224-2232.

Zhang CL, McKinsey TA, Chang S, Antos CL, Hill JA, Olson EN. 2002. Class II histone deacetylases act as signal-responsive repressors of cardiac hypertrophy. *Cell* **110**: 479-488.

Chapter 3

DOT1L IS REQUIRED FOR MLL-AF9 LEUKEMOGENESIS

Abstract

Chromosomal translocations of the *MLL*, mixed lineage leukemia, gene are a common cause of acute leukemias. The oncogenic function of MLL fusion proteins is partly mediated through aberrant up-regulation of *Hoxa* and *Meis1* genes. Here we use a tamoxifen-inducible Cre mouse model to demonstrate that DOT1L, the H3K79 methyltransferase, is required for both initiation and maintenance of MLL-AF9 induced leukemogenesis *in vitro* and *in vivo*. Through gene expression and ChIP analysis we demonstrate that mis-targeting of DOT1L, subsequent H3K79 methylation, and up-regulation of *Hoxa* and *Meis1* genes underly the molecular mechanism of how DOT1L contributes to MLL-AF9 mediated leukemogenesis. Our provides the first *in vivo* evidence for the function of DOT1L in leukemia and reveals the molecular mechanism for DOT1L in MLL-AF9 mediated leukemia. Thus, DOT1L may serve as a potential therapeutic target for the treatment of leukemia caused by *MLL* translocations.

Introduction

MLL1 (mixed lineage leukemia 1) is a SET domain-containing protein, capable of methylating histone H3 lysine 4 (H3K4), which correlates with transcriptional activation (Martin and Zhang 2005; Kouzarides 2007). One important function of MLL is to maintain the "on" state of homeobox (*Hox*) gene expression during embryonic development and hematopoiesis (Guenther et al. 2005). The full-length MLL1 precursor protein is proteolytically cleaved by Taspase1 to generate N-terminal 300kDa (MLL1N) and C-terminal 180kDa (MLL1C) proteins that form a heterodimer as part of a multi-subunit protein complex (Hsieh et al. 2003a). Previous studies indicated that MLL dimerization is required for its stability as well as proper spatio-temporal activation of *Hox* gene expression (Hsieh et al. 2003a; Hsieh et al. 2003b).

The gene that encodes human MLL1 is located at 11q23 and harbors an 8.3kb breakpoint cluster region, which is known to be involved in chromosomal rearrangements with over 50 different genes (Ayton and Cleary 2001; Hess 2004). Translocation of *MLL* is a common cause of acute leukemias, accounting for 5-10% of adult acute myeloid leukemia (AML) and acute lymphoid leukemia (ALL). Of these MLL-related leukemias, 10% are secondary cancers caused by chemotherapy (Daser and Rabbitts 2004). Strikingly, MLL rearrangements also account for ~80% of ALL and ~60% of AML in infants (Ayton and Cleary 2001; Hess 2004). In MLL-related leukemias, genes of the *Hoxa* cluster are frequently up-regulated, and their sustained expression is required for leukemic stem cell (LSC) maintenance (Argiropoulos and Humphries 2007).

The MLL N-terminus retained in oncogenic fusion proteins lack the enzymatic SET domain, but maintain two DNA-binding domains (AT-hooks and DNMT homology region) and subnuclear localization motifs (Li et al. 2005). Thus, MLL-fusion proteins are likely directed to MLL gene targets, and heterodimerization with wild type MLL1C expressed from the non-rearranged allele confers *Hoxa* gene activation. Meanwhile, the translocation partner proteins also contribute to maintaining gene expression either through intrinsic transcriptional activation activity or recruitment of other effector molecules (Krivtsov and Armstrong 2007).

Among the ~50 different MLL fusion partners, AF4, AF9, AF10, and ENL account for over 2/3 of all MLL-related leukemias and have been reported to associate with each other through direct or indirect protein-protein interactions (Erfurth et al. 2004; Zeisig et al. 2005; Krivtsov and Armstrong 2007). AF4 and AF9 are serine/proline rich nuclear proteins with transcriptional activation domains and directly interact with one another. Not only does AF4 associate with AF9, it also binds directly to ENL. ENL belongs to a family of proteins which contain a YEATS domain responsible for H3 binding and association with histone-modifying complexes. In addition, ENL interacts with AF10, and AF10 co-localizes with AF4 (Slany 2005; Zeisig et al. 2005; Krivtsov and Armstrong 2007). Recently, AF4, AF9, and ENL were shown to be components of a large protein complex named AEP (Yokoyama et al. 2010) or EAP (Bitoun et al. 2007), which also contain the transcription elongation factor P-TEFb.

Yeast Dot1 (disruptor of telomeric silencing) and its mammalian homolog DOT1L methylate Lysine 79 within the globular domain of histone H3 (H3K79) (Feng et al. 2002; Lacoste et al. 2002; van Leeuwen et al. 2002). Although Dot1 was originally identified as a regulator of

telomeric silencing (Singer et al. 1998), data suggest that Dot1-mediated H3K79 methylation is linked to euchromatic gene transcription (Schubeler et al. 2004; Steger et al. 2008) and transcription elongation. A recent study indicates that DOT1L exists in a large protein complex that regulates expression of Wingless target genes (Mohan et al. 2010). Additionally, DOT1L has been shown to regulate erythroid differentiation during embryonic hematopoiesis (Feng et al. 2010).

Using *in vitro* methylcellulose re-plating assays, we have shown that mis-targeting of DOT1L and dysregulation of MLL-target genes contributes to leukemogenesis in MLL-AF10 and CALM-AF10 (Okada et al. 2005; Okada et al. 2006). Similar *in vitro* studies were also reported for leukemic transformation caused by MLL-ENL (Mueller et al. 2007) and MLL-AF4 (Krivtsov et al. 2008). Interestingly, DOT1L was previously shown to be part of the EAP complex (Bitoun et al. 2007; Mueller et al. 2009). These data raise the possibility that DOT1L interaction with MLL-fusion proteins and aberrant targeting to gene loci may be a universal mechanism mediating MLL leukemogenesis. To further substantiate the role of DOT1L in leukemia, we generated a conditional DOT1L knockout mouse model and evaluated the role of DOT1L in MLL-AF9-mediated leukemogenesis. Our studies not only establish a critical function of DOT1L in the initiation and maintenance of leukemia *in vivo*, but also demonstrate a role for DOT1L in the activation of leukemia genes such as *Meis1* and the *Hoxa* cluster.

Results

DOT1L is required for MLL-AF9-induced transformation *in vitro*

Previous studies had only analyzed the role of DOT1L in MLL-mediated leukemogenesis *in vitro* (Okada et al. 2005; Okada et al. 2006; Mueller et al. 2007; Krivtsov et al. 2008), and the pathophysiological relevance of those data need to be confirmed *in vivo*. To this end, we generated an inducible knockout system by crossing mice harboring a *Dot1L* conditional allele (DOT1l^{2lox}) (Jones et al. 2008) with mice harboring a Cre-recombinase-Oestrogen-Receptor-T2 allele (Cre-ER^{T2}) at the ubiquitous ROSA26 locus (Ventura et al. 2007). Upon tamoxifen (TAM) administration, the Cre-ER^{T2} system allows for translocation of Cre-recombinase into the nucleus, resulting in efficient recombination of genomic *loxP* sites (Ventura et al. 2007). Previous studies have confirmed that Cre-recombination of the *DotL* allele removes exons 5 and 6, which encode part of the SAM binding motif required for enzymatic activity, to generate the DOT1l^{1lox} null allele, abolishing all H3K79 mono-, di-, and tri-methylation (Jones et al. 2008).

Using this inducible system, we first investigated the role of DOT1L in the initial transformation of hematopoietic progenitor cells (HPCs) by expression of MLL-AF9. FACS sorted c-Kit^{+} HPCs from bone marrow of conditional DOT1L$^{2lox/1lox}$;Cre-ER^{T2} (*2l/1l*) and control DOT1L$^{wt/wt}$;Cre-ER^{T2} (*wt/wt*) mice (Figure 3-1B) were infected with retroviruses expressing MLL-AF9 or empty vector control. After infection, cells were treated with TAM for 7 days and efficient deletion of *Dot1l* was confirmed by RT-qPCR (Figure 3-1C). To evaluate the effect of DOT1L depletion on MLL-AF9 mediated transformation, infected *2l/1l* and *wt/wt* cells were subjected to serial methylcellulose re-plating, which selects for self-

renewing cells. As shown in Figure 3-1D, no colonies were observed by the second and third round in DOT1L depleted cells, suggesting that DOT1L is required for initial transformation by MLL-AF9.

DOT1L is required for MLL-AF9-mediated leukemogenesis *in vivo*

We next asked whether DOT1L is required for MLL-AF9 mediated leukemogenesis in the mouse via bone marrow transplantation (BMT). In our system, donor *2l/1l* and *wt/wt* mice are maintained on a 129Sv/Jae and C57/B6 Ly5.2 mixed background, while recipient mice are maintained on a C57/B6 Ly5.1 background. Thus, donor leukemic cells (LCs) can be distinguished from wild-type recipient and radio-protector cells, which do not contain the *Dot1L* conditional allele or Cre-ER^{T2} allele, by fluorescence activated cell sorting (FACS). Donor MLL-AF9 LCs, collected from the third round of methylcellulose re-plating, were mixed with radio-protector Ly5.1/Ly5.2 BMCs at a 1:5 ratio and transplanted into recipient mice. TAM administration was initiated three weeks post-BMT, prior to the detection of LCs in bone marrow (Figure 3-2E), to induce *Dot1L* recombination in donor LCs. RT-qPCR analysis confirmed efficient deletion of *Dot1L* by the TAM treatment (Figure S3-1). As expected, all mice transplanted with *wt/wt* MLL-AF9 LCs died by 14 weeks post-BMT (Figure 3-2B). However, TAM treatment increased survival of mice transplanted with *2l/1l* MLL-AF9 LCs (Figure 3-2B). The extended life span of the *2l/1l* MLL-AF9 TAM treated group (red dotted line) is not due to other effects of TAM as only a 1-2 weeks increase in survival was observed between treated and untreated *wt/wt* MLL-AF9 (Figure 3-2B, dotted and solid black lines). Consistent with increased survival, TAM treatment prevented splenomegaly (Figure 3-2C) and leukemia infiltration of liver (Figure 3-2D) in mice that

received *2l/1l* MLL-AF9 LC transplantation, but not to those receiving *wt/wt* MLL-AF9 LCs. Furthermore, FACS analysis demonstrates that donor *wt/wt* MLL-AF9 LCs constituted a third (or 58%) of the bone marrow population at 6 weeks (or 9 weeks) post-BMT, whereas no *2l/1l* MLL-AF9+TAM LC donor cells were detectable (Figure 3-2E-F), indicating that the ability of MLL-AF9 LCs to repopulate the recipient bone marrow requires functional DOT1L. Strikingly, by 24 weeks post-BMT no *2l/1l* MLL-AF9 LCs are detected in the peripheral blood of TAM treated mice (Figure 3-2G), demonstrating that MLL-AF9 LCs fail to establish AML in the absence of DOT1L. Collectively, these results demonstrate a critical function for DOT1L in the initiation of leukemia *in vivo*.

DOT1L is required for maintaining MLL-AF9 leukemic transformation *in vitro*

Having established the function for DOT1L in the initiation of leukemia, we next asked whether DOT1L is also required for maintaining the leukemic state induced by MLL-AF9. To this end, MLL-AF9 LCs were propagated in liquid culture in the presence or absence of TAM for a period of 7 days. After verification of efficient TAM-induced *Dot1l* recombination by genotyping (Figure 3-3B) and RT-qPCR (Figure 3-3C), an equal number of cells were plated onto methylcellulose. MLL-AFX LCs were used as a negative control since DOT1L was previously shown not to be required for maintaining transformation induced by MLL-AFX (Okada et al. 2005). Results shown in Figure 3-3D demonstrate that *2l/1l* MLL-AF9 transformed cells failed to produce colonies upon TAM-induced depletion of DOT1L. In contrast, similar treatment exhibited no effect on MLL-AFX transformed cells, indicating that depletion of DOT1L did not cause a general cytotoxic effect. Additionally, TAM treatment by itself had no effect on *wt/wt* LC colony formation potential (Figure 3-3D).

This study demonstrates that MLL-AF9 transformed cells require DOT1L for maintaining leukemic self-renewal *in vitro*.

DOT1L is required for MLL-AF9-induced acute leukemia progression *in vivo*

The *in vivo* results in Figure 3-2E-J suggest that DOT1L is required for MLL-AF9 leukemogenesis. In those experiments, TAM administration was initiated at 3 weeks post-BMT. At this stage, acute leukemia has yet to develop since donor LCs in the bone marrow were undetectable by FACS (Figure 3-2E). To investigate the importance of DOT1L in the maintenance of MLL-AF9-induced acute leukemia *in vivo*, we administrated TAM at 6 weeks post-BMT when the transplanted LCs account for ~30% of the bone marrow population (Figure 3-2F). At 9 weeks post-BMT, TAM-induced DOT1L depletion greatly reduced splenomegaly (Figure 3-4B) and liver infiltration (Figure 3-4C) in *2l/1l* MLL-AF9 mice. FACS analysis of recipient bone marrow revealed that *2l/1l* MLL-AF9 LCs represented a lower percentage of total BMCs in treated mice compared to untreated controls (Figure 3-4D; 44.2% vs 60.7% at 9 weeks; 27.9% vs 83.0% at 12 weeks). In TAM treated mice, we also observed a decrease in *2l/1l* MLL-AF9 donor LCs at 12 weeks compared to 9 weeks post-BMT (Figure 3-4D; 27.9% vs 44.2%). In contrast, the percentage of *wt/wt* donor LCs increased from 60.7% to 83.0% in the same period (Figure 3-4D). Moreover, FACS analysis indicated that the remaining DOT1L deficient donor LCs at 12 weeks expressed lower levels of stem cell/progenitor cell marker c-Kit (Figure 3-4D), indicating a depletion of clonogenic leukemic progenitor/stem cells in the absence of DOT1L.

To analyze the effect of *in vivo* DOT1L deficiency on the self-renewal capacity of LCs, we sorted donor LCs at 12 weeks post-BMT and plated equal numbers onto methylcellulose. Results shown in Figure 3-4E demonstrate that the colony formation capacity of *2l/1l* LCs from TAM treated mice is greatly reduced. Although colonies were observed after the first round of plating, those cells failed to give rise to additional colonies after the second round. In contrast, *wt/wt* LCs have increased colony formation capacity (Figure 3-4E). Thus, TAM-induced DOT1L depletion *in vivo* blocks AML progression by disrupting MLL-AF9 LC self-renewal capacity, which is consistent with the decreased c-Kit expression (Figure 3-4D).

Loss of DOT1L function causes cell cycle arrest in MLL-AF9-induced leukemic cells

Previous studies have shown that loss of DOT1L induces cell cycle arrest in ES cells (Jones et al. 2008; Barry et al. 2009) and erythroid cells (Feng et al. 2010). To analyze the effect of DOT1L on cell proliferation, we cultured LCs in liquid media in the presence or absence of TAM. Results shown in Figure 3-5A demonstrate that loss of DOT1L inhibits proliferation of cells transformed by MLL-AF9, but not cells transformed by MLL-AFX, indicating that depletion of DOT1L did not cause a general cytotoxic effect. FACS analysis of cells stained with propidium iodide demonstrates that MLL-AF9 LCs arrest at G0/G1 after DOT1L depletion, while no effect on cell cycle progression was observed for MLL-AFX LCs (Figure 3-5B). General cytotoxic effects from TAM treatment were not responsible for the cell cycle arrest as no effect was observed with *wt/wt* MLL-AF9 LCs (Figure 3-5A-B). Consistent with a G0/G1 arrest, substantial up-regulation of two regulators of G1 progression, pRb and the CDK inhibitor p16 (Lukas et al. 1995; Medema et al. 1995), was detected in *2l/1l* MLL-AF9 LCs upon loss of DOT1L (Figure 3-5C). Since H3K79 methylation is generally linked to

transcription activation, DOT1L loss of function is expected to down-regulate direct gene targets of DOT1L. Therefore, the observed up-regulation of *p16* and *pRb* expression is likely to be an indirect consequence.

DOT1L regulates expression of *Hoxa* cluster and *Meis1*

Previous studies have shown that the *Hoxa* gene cluster is up-regulated in MLL-AF9 LSCs (Krivtsov et al. 2006; Somervaille and Cleary 2006). To determine whether DOT1L is involved in *Hoxa* genes up-regulation, we analyzed their expression by RT-qPCR. We found that all analyzed *Hoxa* genes are up-regulated in MLL-AF9 transformed cells when compared to normal HPCs (Figure 3-6A). Importantly, DOT1L plays a crucial role in activation of the *Hoxa* cluster as TAM-induced DOT1L depletion resulted in their down-regulation (Figure 3-6A). In addition, two *Hoxa* co-factors, Meis1 and Pbx3, required for maintaining MLL-AF9 leukemic stem cell potential (Wong et al. 2007), are also down-regulated in response to TAM-induced DOT1L depletion (Figure 3-6A). Studies have shown that in addition to their role in maintaining LSC identity, continued *Hoxa* and *Meis1* expression also help block differentiation (Somervaille and Cleary 2006; Muntean et al. 2010). Accordingly, *Csf3r* and *Ltf*, genes associated with myeloid differentiation and down-regulated in MLL-AF9 LCs, are re-activated upon TAM-induced DOT1L deletion (Figure 3-6B). These data support the notion that DOT1L is required for maintaining a transcriptional program that supports LSC self-renewal and blocks differentiation.

Next, chromatin immunoprecipitation (ChIP) was performed to determine whether DOT1L is directly targeted to *Hoxa* and *Meis1* loci to regulate their expression in MLL-AF9 LCs.

Because no ChIP-grade DOT1L antibody is available, we used an antibody that recognizes H3K79 di- and tri-methylation (H3K79me2/3; Abcam), modifications deposited by DOT1L (Feng et al. 2002). *Hoxa5* and *Hoxa9* loci were analyzed because they were shown to be required for leukemogenesis of various MLL-fusion proteins (Okada et al. 2005; Okada et al. 2006; Faber et al. 2009). *Hoxa10* was also included because its over-expression has been reported to induce transplantable AML in mice (Thorsteinsdottir et al. 1997). ChIP analysis verified that all three loci, in addition to *Meis1*, are preferentially enriched for H3K79me2/3 in MLL-AF9 transformed cells when compared to control HPCs (Figure 3-6C,D). These data suggest that DOT1L-mediated H3K79 methylation contributes directly to *Hoxa* and *Meis1* gene activation in MLL-AF9 induced leukemogenesis.

Discussion

Leukemia caused by MLL-AF9 fusions represents ~1/3 of all infant acute leukemias and ~1/3 of adult AML (Krivtsov and Armstrong 2007). Recent studies demonstrating the interaction between MLL-AF9 and several functional partners such as Menin (Yokoyama et al. 2005; Chen et al. 2006; Caslini et al. 2007), wild-type MLL (Thiel et al. 2010), and the PAF complex (Milne et al. 2010; Muntean et al. 2010) have shed some light on the underlying mechanisms of MLL-AF9 leukemogenesis. DOT1L has been previously shown to directly interact with the C-terminus of AF9 (Zhang et al. 2006) and has been identified in AF9-associated protein complexes (Zeisig et al. 2005; Bitoun et al. 2007; Mueller et al. 2009). In addition, H2B ubiquitination mediated by the PAF complex is required for both DOT1L methyltransferase activity (Krogan et al. 2003; Wood et al. 2003) and for MLL-AF9 leukemic transformation (Milne et al. 2010; Muntean et al. 2010). These data suggest a possible link between DOT1L and MLL-AF9-mediated leukemogenesis.

In this study, we demonstrate that DOT1L is required for the initiation of leukemic transformation by MLL-AF9 both *in vitro* by methylcellulose colony formation assays and *in vivo* by bone marrow transplantation assays (Figure 3-1). Additionally, we demonstrate that DOT1L is required for maintaining the transformed state of MLL-AF9 leukemic cells *in vitro* and *in vivo* as loss of DOT1L abrogated colony formation in methylcellulose colony re-plating as well as AML progression in mice (Figure 3-2). Further analysis revealed that DOT1L is required for maintaining LSC identity, self-renewal capacity, and proliferation of MLL-AF9 transformed, but not MLL-AFX transformed, cells (Figures 3-2 and 3-3). Moreover, gene expression analysis demonstrates that activation of a group of LSC-

associated genes, including the *Hoxa* cluster, *Meis1*, and *Pbx3*, is compromised upon loss of DOT1L function (Figure 3-4). Finally, ChIP assay supports that DOT1L-mediated H3K79 methylation directly contributes to activation of these genes.

It is important to note that during completion of this study two papers were published confirming a requirement for DOT1L in MLL-AF9 transformation (Chang et al. 2010; Monroe et al. 2011). However, neither one evaluated the role of DOT1L *in vivo*, leaving open the question of pathobiological relevance of their studies. Through bone marrow transplantation, we demonstrate that DOT1L plays a critical role in the initiation and maintenance of MLL-AF9-mediated acute leukemia; thus, firmly establishing the function of DOT1L in leukemogenesis. In contrast to our data on MLL-AFX, Chang and colleagues (Chang et al. 2010) found that DOT1L is required for maintaining MLL-AFX transformation *in vitro*. One possible explanation is that the two studies used different mouse models. Upon Cre-recombination of the *Dot1L* conditional allele in our mouse, both exons 5 and 6 are excised. Given that exons 4 and 7 will still be transcribed and translated in-frame, a truncated DOT1L mutant missing 108 residues within the catalytic domain can still be generated. However, recombination of the conditional allele used in Chang *et al.* only removes exon 5, which results in a frame-shift and the expression of a truncated protein containing only the first 87 residues (Chang et al. 2010). Their deletion may have a more severe phenotype due to loss of other DOT1L functions aside from its methyltransferase activity.

We and others have previously shown that mis-targeting of DOT1L and subsequent methylation on H3K79 plays an important role in the leukemic process involving MLL-

AF10, MLL-ENL, MLL-AF4 transformation *in vitro* (Okada et al. 2005; Mueller et al. 2007; Krivtsov et al. 2008). Consistently, DOT1L has been shown to associate with all three of the aforementioned MLL fusion partners through direct or indirect interactions (Erfurth et al. 2004; Okada et al. 2005; Zeisig et al. 2005; Bitoun et al. 2007; Mueller et al. 2007; Mueller et al. 2009). Of noteworthy, two reports have failed to identify DOT1L in an AF4-associated complex (Lin et al. 2010; Yokoyama et al. 2010), putting into question the role of DOT1L in MLL-AF4 leukemia. However, direct interaction of AF4 with AF9 and AF9 with DOT1L is unquestionable; thus, DOT1L may be mis-targeted to genomic loci by MLL-AF4 indirectly through their mutual association with AF9. In support of this possibility, it has been demonstrated that disruption of the AF4-AF9 interaction by the synthetic peptide PFWT inhibits MLL-AF4 leukemic cell proliferation (Srinivasan et al. 2004), which is similar to the results we observe with MLL-AF9 in the absence of DOT1L.

This study, together with previous ones, strongly suggests a common mechanism by which DOT1L contributes to leukemogenesis of MLL-fusion proteins. We believe that mis-targeting of DOT1L to *Hoxa* and *Meis1* genes, subsequent H3K79 methylation, and up-regulation of these genes is a common mechanism underlying the involvement of DOT1L in leukemogenesis (Figure 3-7). Although a similar mechanism for MLL-AF10 and MLL-AF4 has been previously proposed (Okada et al. 2005; Guenther et al. 2008; Krivtsov et al. 2008), all previous studies were performed using an *in vitro* system with DOT1L knockdown. Here we not only extended the those studies by demonstrating the involvement of DOT1L in MLL-AF9 mediated leukemogenesis, but also provided the first evidence demonstrating an essential role for DOT1L in leukemogenesis *in vivo*. Our study thus solidifies DOT1L's role

in leukemias involving *MLL* rearrangements and makes DOT1L a prime candidate for targeted therapeutic intervention.

Materials and Methods

Mice and *in vivo* Tamoxifen Treatment. The DOT1L conditional mouse was previously described (Jones et al. 2008). The R26-Cre-ERT2 mice were generated by Tyler Jacks lab (Ventura et al. 2007) and were obtained from the NCI Mouse Models of Human Cancers Consortium (Strain 01XAB). DOT1L$^{2lox/+}$ and DOT1L$^{1lox/+}$ mice were intercrossed to generate DOT1L$^{2lox/1lox}$;Cre-ERT2 and DOT1L$^{+/+}$;Cre-ERT2 mice. Mice were kept on a 129Sv/Jae and C57/B6 Ly5.2 background. Wild type C57/B6 Ly5.1 and Ly5.2 mice were purchased from Jackson Laboratory and were intercrossed to generate Ly5.1/Ly5.2 mixed background BMCs. For *in vivo* Cre-recombination, tamoxifen (Sigma) was administered via intraperitoneal injection every 2 days (100 μl of 100 mg/ml in corn oil) for a period of 3 weeks. All animal protocols adhere to the National Institutes of Health Guide for the Care and Use of Laboratory Animals and were approved by the UNC Institutional Animal Care and Use Committee.

Retrovirus Production, Transduction, Methylcellulose Colony Re-plating Assay, and Cell Culture. The pMSCN-MLL-AF9 construct was a gift from Jay Hess . The pMSCN-MLL-AFX construct was a gift from Michael Cleary . Retroviral production was performed as described previously (Okada et al. 2005). Briefly, pMSCN-MLL-AF9 and pMSCN-MLL-AFX were co-transfected with pGag-pol and pVSVG into 293T cells using Superfect (Qiagen). At 48 hrs post-transfection, viral supernatant were collected for transduction of c-Kit positive HPCs purified as follows: Mice 4-10 weeks old were injected intravenously with 5-fluorouracil (150 mg/kg). Bone marrow was harvested from both femurs 5 days post-injection and stained with c-Kit-APC (BD Biosciences). Positive stained HPCs were FACS sorted using a BD FACSAria II Flow Cytometer. Viral supernatants were used to transduce

the FACS sorted cells via spinoculation, and cells plated onto methylcellulose 24hrs post-infection. For methylcellulose colony formation assays, 1x10^4 transduced cells were plated into 0.9% Methocult M3534 (StemCell Technologies) supplemented with 10 ng/ml GM-CSF and 1 mg/ml G418 (GIBCO) for selection. After 7 days of culture, G418-resistant colonies were collected and single-cell suspensions re-plated into M3534 with GM-CSF in the absence of G418. Re-plating was performed every 7-10 days. Liquid cultures of transformed HPCs and LSCs were maintained in mFTOC (20% FBS in RPMI1640, 1 mM MEM sodium pyruvate, 1% MEM non-essential amino acid, 10 mM HEPES at pH 7.3, 50 μm 2-mercaptoethanol with 5 ng/ml mIL-3 (Peprotech). For *in vitro* recombination, 4-OHT (Sigma) was resuspended in ethanol and added to cell culture media at final concentration of 250 μM. Media was changed daily during 7 day period of 4-OHT treatment.

Bone Marrow Transplantation. Recipient C57/B6 Ly5.1 mice (6-12 weeks old) began a prophylactic regimen to prevent gastro-intestinal infections through oral administration of sulfamethoxazole/trimethoprim (SMZ, TW Medical) at a concentration of 6 mg/1.2 mg per mL water one week prior to bone marrow transplantation (BMT) procedures and continued for 4 weeks post-transplantation. SMZ containing water was changed every other day. On the day of transplantation recipient mice received two doses, 4.8 Gy each, of total body irradiation (TBI) 4 hours apart using a cesium radiation source. Four hours after the second irradiation dose, recipient mice were anaesthetized through intraperitoneal injection of 300 ul per 10 g body weight of avertin (0.0125 g/ml 2,2,2, tribromoethanol and 1.25% tert-amyl alcohol in PBS). Once anaesthetized, 0.5x10^5 LCs plus 2.5x10^5 radio-protector Ly5.1/Ly5.2 cells resuspended in 100 μl PBS (1:5 ratio) were transplanted via retro-orbital injection.

Histology. Tissues were harvested from mice and fixed in 4% paraformaldehyde. Livers were paraffin embedded and tissue sections, 5 μm thick, were used for hematoxylin and eosin staining.

FACS Analysis and Cell Sorting. Bone marrow cells were flushed from both femurs of mice using 25G needle and syringe. Red blood cells were lysed using ammonium chloride (StemCell Technologies). Cells were resuspended in PBS + 2% FBS at a concentration of 10^6 cells per 100 μl. Cells were stained for 30min at 4^0C, washed three times with PBS, and resuspended in PBS + 2% FBS. Antibodies used for FACS analysis and sorting are: Rat anti-mouse c-Kit-APC, Ly5.1-PE-Cy7, and Ly5.2-PerCP-Cy5.5 plus corresponding Rat IgG2a Isotype controls (EBiosciences). All analysis and sorting was performed using BD FACSAria II Flow Cytometer.

PI Staining for DNA content. Cells grown in liquid culture were washed twice with ice cold PBS and resuspended in 500 μl of PBS. While vortexing gently, 4.5 ml of ice cold 70% ethanol was slowly added and then stored at 4^0C overnight. On the following day, fixed cells were pelleted by centrifugation at 4^0C for 5 minutes at 1500rpm. Cell pellet was washed with PBS, centrifuged, and resuspended in 250 μl of PBS. PI staining mix (RNase A 100 μg/ml, propidium iodide 40 μg/ml, and 0.1% Triton X-100 in PBS) was prepared fresh, and 750 μl added to cells. Cells were incubated for 15 minutes at 37^0C and then analyzed by FACS using a Beckman Coulter CyAn Flow Cytometer. Data was analyzed using ModFit LT software.

RT-qPCR and ChIP. For gene expression analysis, total RNA was isolated from cells using RNeasy Kit (Qiagen) and reverse transcribed using Improm II (Promega). SYBR GreenER qPCR SuperMix (Invitrogen) was used for qPCR. qPCR was performed using Applied

Biosystems 7300 Real-Time PCR System. Relative expression was normalized to *Gapdh*. Primer sequences are listed in Table S3-1. ChIP experiments were carried out as previously described (Okada et al. 2005) with the following modifications. DNA was fragmented into 300-500 bp in length by sonication. Immunoprecipitation was performed using anti-H3K79me2/3 (Abcam) and anti-Rabbit IgG (Santa Cruz; sc-2027) and DynaBeads (Invitrogen). ChIP'ed samples were washed twice with low salt (140mM NaCl) RIPA buffer, once with high salt (500 mM NaCl) RIPA buffer, and twice with TE buffer. DNA was purified using Chelex-100. Quantitative real-time PCR of ChIP'ed DNA was analyzed using SYBR GreenER qPCR SuperMix (Invitrogen) and Applied Biosystems 7300 Real-Time PCR System. Primer sequences are listed in Table S3-2.

Acknowledgements

We thank Jay Hess for providing the pMSCN-MLL-AF9 construct and Michael Cleary for providing the pMSCN-MLL-AFX construct. The work is supported by an NIH grant (CA119133). A.T.N is a recipient of the Pre-doctoral Fellowship from the American Heart Association. Y.Z. is an Investigator of the Howard Hughes Medical Institute.

Author contributions

Anh Nguyen and Yi Zhang designed research and wrote the manuscript; Anh Nguyen performed research; Olena Taranova generated tamoxifen-inducible mice; Jin He helped with bone marrow transplantation.

Figure 3-1. DOT1L is required for MLL-AF9-induced leukemic transformation *in vitro.* ***(*A**) Diagram of the procedure used for *in vitro* analysis. (**B**) Bone marrow cells were stained with rat IgG2a-APC isotype control to identify c-Kit negative population. Bone marrow cells were stained with rat anti-mouse c-Kit-APC. c-Kit+ cells were sorted using a BD FACSAria II instrument. (**C**)RT-qPCR analysis of DOT1L expression level, normalized to Gapdh, after 7 days of TAM treatment (250 nM final concentration) demonstrates efficient recombination. Mouse genotype is indicated. (**D**) Serial methylcellulose colony re-plating assay shows that MLL-AF9 fails to transform HPCs in the absence of DOT1L. An equal number of cells transduced with empty vector MSCN or MLL-AF9 were plated at each round and colony forming units (CFUs) counted after 7-10 days. Experiment was performed three times and presented as average number of CFUs with standard deviation (SD).

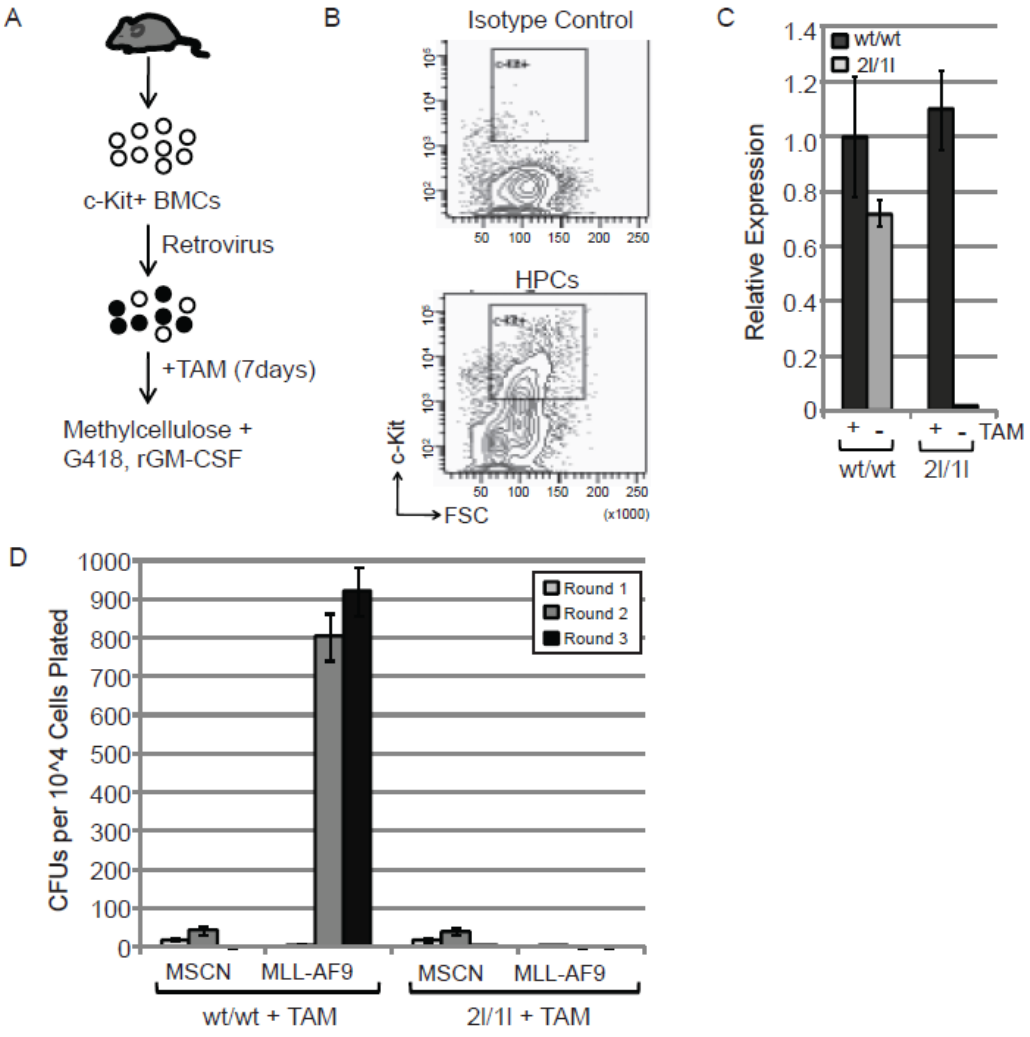
A
c-Kit+ BMCs
Retrovirus
+TAM (7days)
Methylcellulose +
G418, rGM-CSF
B
Isotype Control
HPCs
c-Kit
FSC
(x1000)
C
wt/wt
2l/1l
Relative Expression
TAM
wt/wt
2l/1l
D
CFUs per 10^4 Cells Plated
Round 1
Round 2
Round 3
MSCN
MLL-AF9
MSCN
MLL-AF9
wt/wt + TAM
2l/1l + TAM

Figure 3-2. DOT1L is required for MLL-AF9-mediated leukemogenesis *in vivo*. (**A**) Diagram of the bone marrow transplantation procedure to examine the effect of DOT1L depletion on the establishment of AML by MLL-AF9 LCs *in vivo*. TAM treatment began at 3 weeks post-transplantation. (**B-G**) *In vivo* deletion of DOT1L prevents MLL-AF9 mediated acute leukemia development. (**B**) Kaplan-Meier plot showing survival of transplanted mice treated and untreated with TAM. Median survival of *wt/wt* MLL-AF9 transplanted mice without TAM = 7 weeks (n=17) and *wt/wt* MLL-AF9 transplanted mice treated with TAM = 7 weeks (n=14). All *2lox/1lox* MLL-AF9 transplanted mice treated with TAM (n=18) survive at least 24 weeks post-transplantation. (**C**) Image of spleens harvested from transplanted mice at 6 weeks post-transplantation show splenomegaly in *wt/wt* MLL-AF9 transplanted mice. (**D**) H&E staining of liver tissue sections at 6 weeks post-transplantation show leukemic infiltration in *wt/wt* MLL-AF9 transplanted mice. (**E**) Donor leukemic cells depleted of DOT1L are absent in recipient bone marrow. Representative images showing FACS analysis of bone marrow cells isolated from transplanted mice. Donor MLL-AF9 LCs are Ly5.2+ (blue) while recipient/protector cells are Ly5.1+/Ly5.2+ (red). (**F**) Percentage of MLL-AF9 LCs present in recipient bone marrow at 6 and 9 weeks post-transplantation as determined by FACS analysis (n=3 per group). (**G**) No leukemic cells are detected by FACS analysis of peripheral blood obtained from *2lox/1lox* MLL-AF9+TAM mice at 24 weeks post-transplantation. Representative image from one of the 6 mice analyzed.

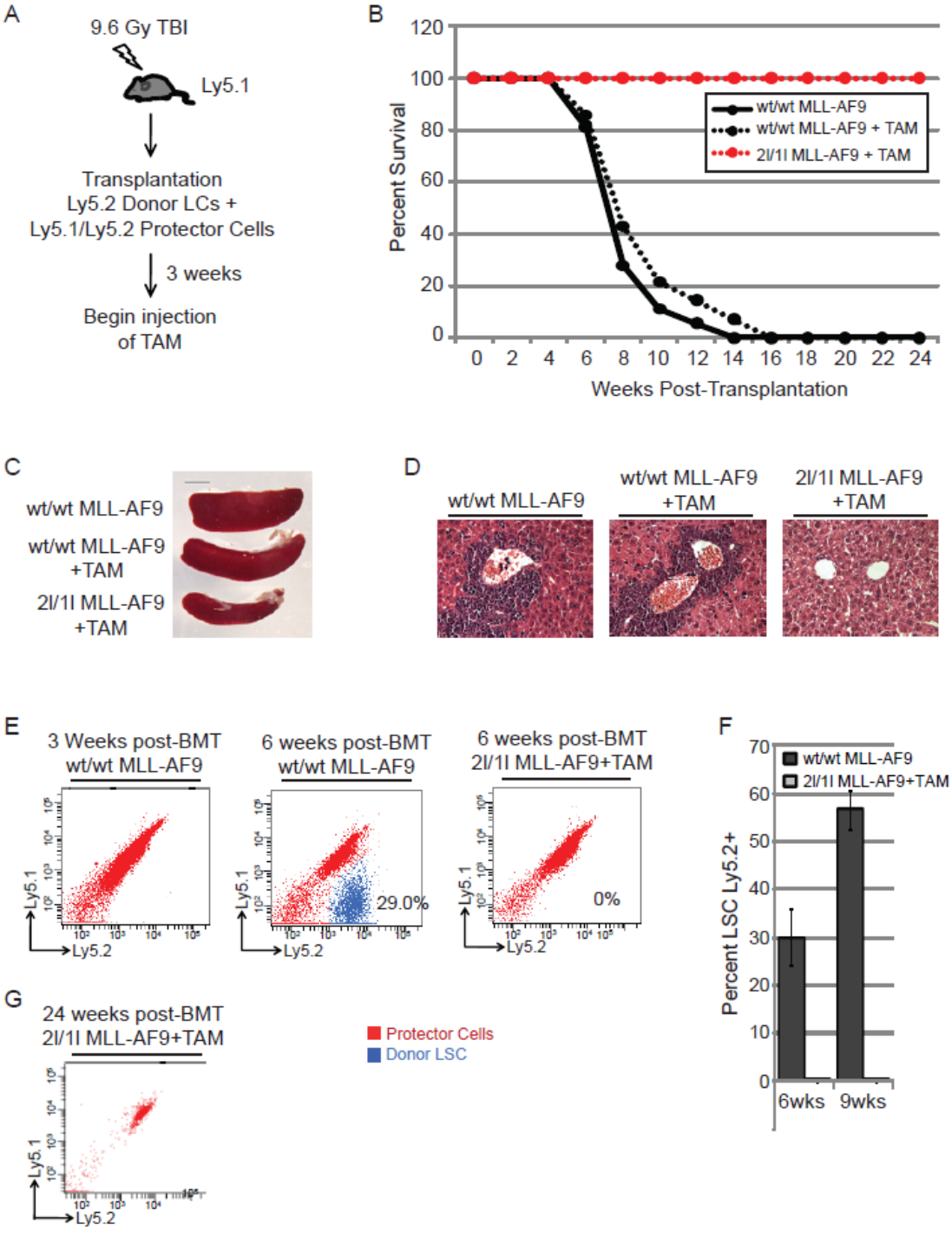
A
9.6 Gy TBI
Ly5.1
Transplantation
Ly5.2 Donor LCs +
Ly5.1/Ly5.2 Protector Cells
3 weeks
Begin injection
of TAM
B
Percent Survival
Weeks Post-Transplantation
wt/wt MLL-AF9
wt/wt MLL-AF9 + TAM
2l/1l MLL-AF9 + TAM
C
wt/wt MLL-AF9
wt/wt MLL-AF9
+TAM
2l/1l MLL-AF9
+TAM
D
wt/wt MLL-AF9
wt/wt MLL-AF9
+TAM
2l/1l MLL-AF9
+TAM
E
3 Weeks post-BMT
wt/wt MLL-AF9
6 weeks post-BMT
wt/wt MLL-AF9
6 weeks post-BMT
2l/1l MLL-AF9+TAM
Ly5.1
Ly5.2
29.0%
0%
F
wt/wt MLL-AF9
2l/1l MLL-AF9+TAM
Percent LSC Ly5.2+
6wks
9wks
G
24 weeks post-BMT
2l/1l MLL-AF9+TAM
Protector Cells
Donor LSC
Ly5.1
Ly5.2

Figure 3-3. MLL-AF9 leukemic cells require DOT1L to maintain transformation *in vitro*. (**A)** Diagram of the procedure analyzing role of DOT1L for LC maintenance *in vitro*. (**B**) Genotyping to verify efficient Cre-mediated recombination of DOT1L^{2lox} conditional allele. (**C**) RT-qPCR analysis of DOT1L expression level in *2lox/1lox* MLL-AF9 LCs, normalized to Gapdh, after 7 days of TAM treatment (250 nM final concentration) demonstrates efficient recombination. (**D**) DOT1L is required for maintaining MLL-AF9 leukemic transformation but not for MLL-AFX. Methylcellulose colony formation assay after TAM treatment of LCs. Equal number of cells were plated and average numbers of CFUs from 3 independent experiments are shown. Error bars represent SD.

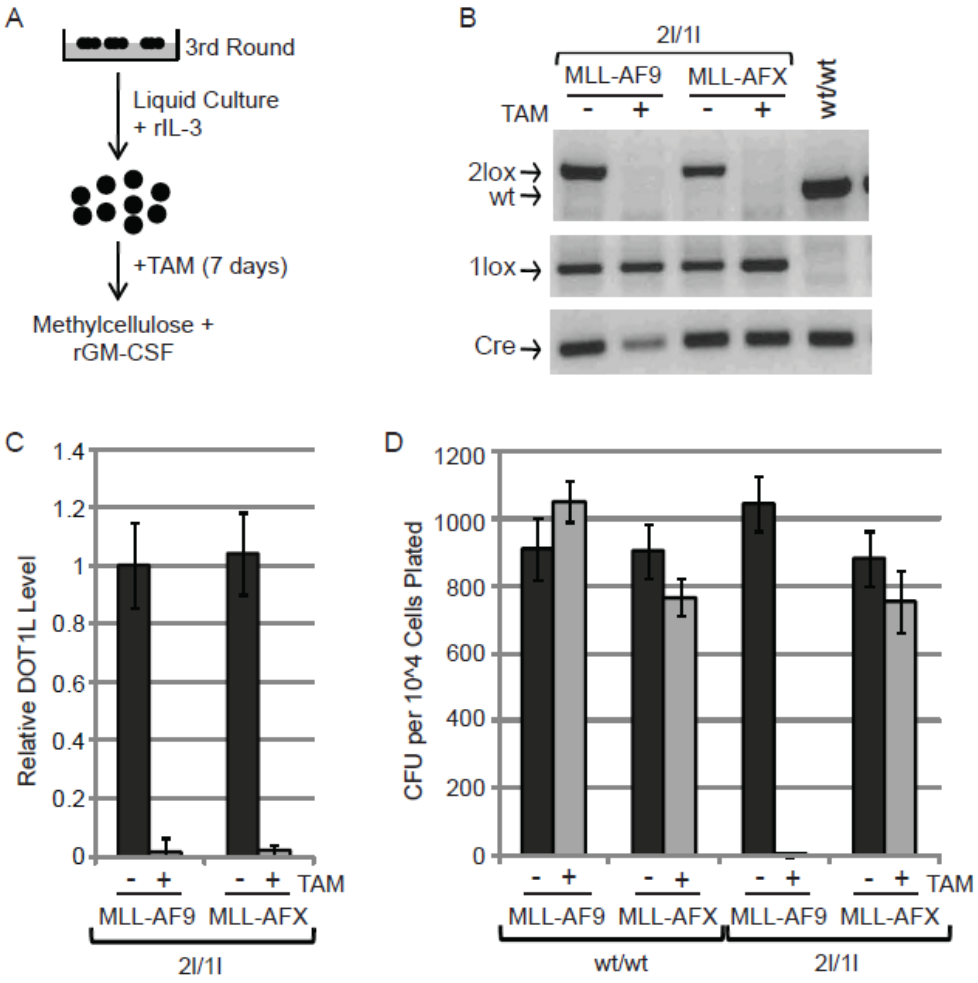
A
3rd Round
Liquid Culture
+ rIL-3
+TAM (7 days)
Methylcellulose +
rGM-CSF
B
2l/1l
MLL-AF9
MLL-AFX
wt/wt
TAM
- + - +
2lox
wt
1lox
Cre
C
Relative DOT1L Level
1.4
1.2
1
0.8
0.6
0.4
0.2
0
- + - + TAM
MLL-AF9 MLL-AFX
2l/1l
D
CFU per 10^4 Cells Plated
1200
1000
800
600
400
200
0
- + - + - + - + TAM
MLL-AF9 MLL-AFX MLL-AF9 MLL-AFX
wt/wt
2l/1l

Figure 3-4. DOT1L is required for MLL-AF9-induced acute leukemia progression *in vivo*. (**A**) Diagram of bone marrow transplantation procedure to examine the requirement of DOT1L in MLL-AF9 AML progression. TAM treatment began at 6 weeks post-transplantation after leukemia development. (**B-E**) *In vivo* deletion of DOT1L prevents MLL-AF9 acute myeloid leukemia progression. (**B**) Reduced spleen size in TAM-treated *2lox/1lox* MLL-AF9 recipient mice. Representative images of spleens harvested from transplanted mice at 9 weeks post-transplantation. (**C**) TAM-induced DOT1L deletion prevents leukemic infiltration of the liver. H&E staining of liver tissue sections at 9 weeks post-transplantation. (**D**) Upon DOT1L depletion, the percentage of leukemic cells in bone marrow diminishes over time. FACS analysis of bone marrow cells isolated from transplanted mice. Donor MLL-AF9 LCs are Ly5.2+ (blue) while recipient/protector cells are Ly5.1+/Ly5.2+ (red). Percentage of donor Ly5.2 cells in the total bone marrow cell population at 9 weeks and 12 weeks post-transplantation are indicated. At 12 weeks post-transplantation, cells were also stained with the stem cell/progenitor marker c-Kit. Leukemic donor Ly5.2 population is gated and percentage of c-Kit$^+$ cells indicated. Shown are representative images from three independent experiments. (**E**) Loss of *in vivo* clonogenic leukemic stem cells after DOT1L depletion. Methylcellulose colony formation assay of LC donor cells sorted from mice at 12 weeks post-transplantation. Average CFUs are shown for 3 different mice. Error bars represent SD.

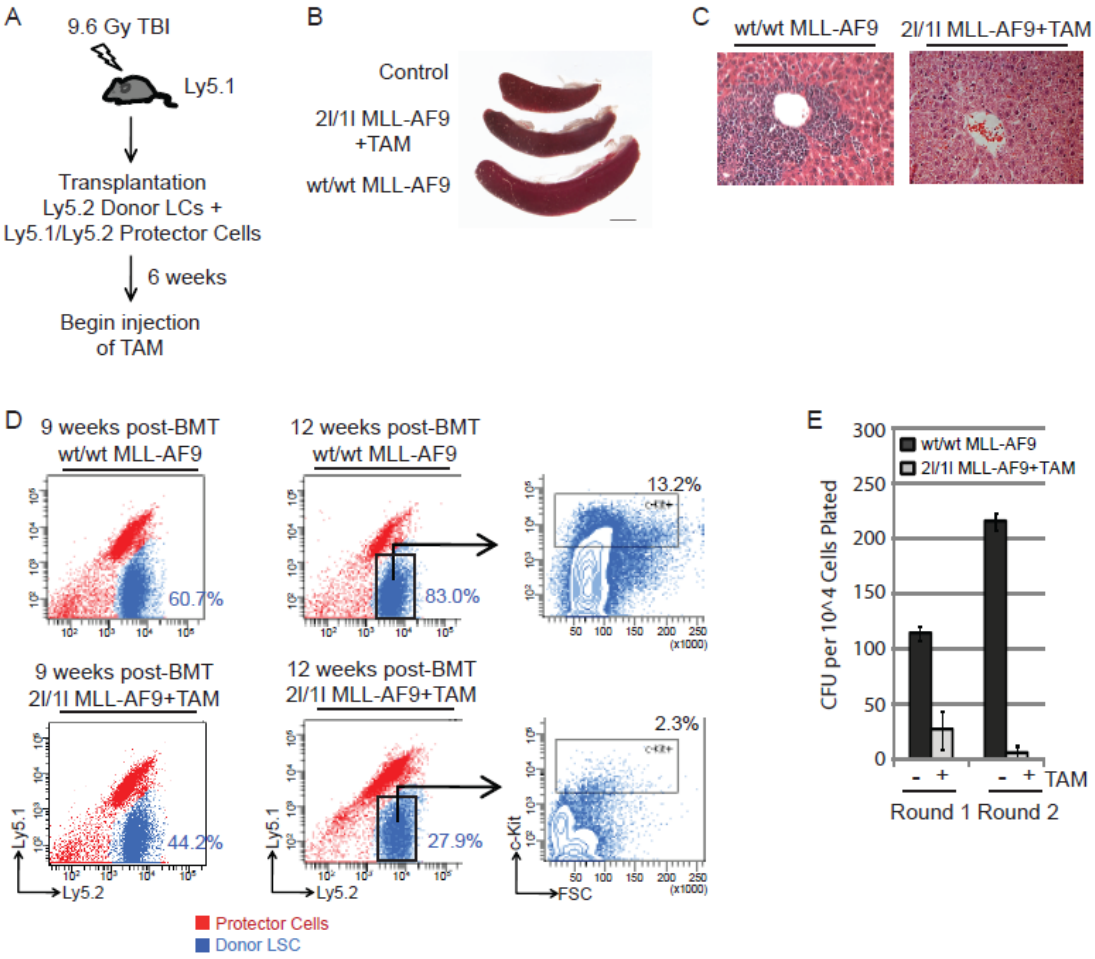
A
9.6 Gy TBI
Ly5.1
Transplantation
Ly5.2 Donor LCs +
Ly5.1/Ly5.2 Protector Cells
6 weeks
Begin injection
of TAM
B
Control
2l/1l MLL-AF9
+TAM
wt/wt MLL-AF9
C
wt/wt MLL-AF9
2l/1l MLL-AF9+TAM
D
9 weeks post-BMT
wt/wt MLL-AF9
60.7%
12 weeks post-BMT
wt/wt MLL-AF9
83.0%
13.2%
9 weeks post-BMT
2l/1l MLL-AF9+TAM
44.2%
12 weeks post-BMT
2l/1l MLL-AF9+TAM
27.9%
2.3%
Ly5.1
Ly5.2
c-Kit
FSC
Protector Cells
Donor LSC
E
wt/wt MLL-AF9
2l/1l MLL-AF9+TAM
CFU per 10^4 Cells Plated
300
250
200
150
100
50
0
- + - +
TAM
Round 1 Round 2

Figure 3-5. Loss of DOT1L inhibits cell proliferation due to a G0/G1 cell cycle arrest. (**A**) *In vitro* TAM-induced DOT1L deletion inhibits MLL-AF9 LC proliferation in liquid culture but not MLL-AFX. Total cell numbers were counted every 2 days. Shown is the average of three independent experiments with error bars. (**B**) *In vitro* TAM-induced DOT1L deletion causes cell cycle arrest at G0/G1 phase for MLL-AF9 transformed cells. Cell cycle analysis was performed by propidium iodide staining. Experiment was repeated twice. Data was analyzed using ModFit software. (**C**) Gene expression analysis by RT-qPCR shows up-regulation of CDK inhibitors after DOTL depletion, normalized to *Gapdh*.

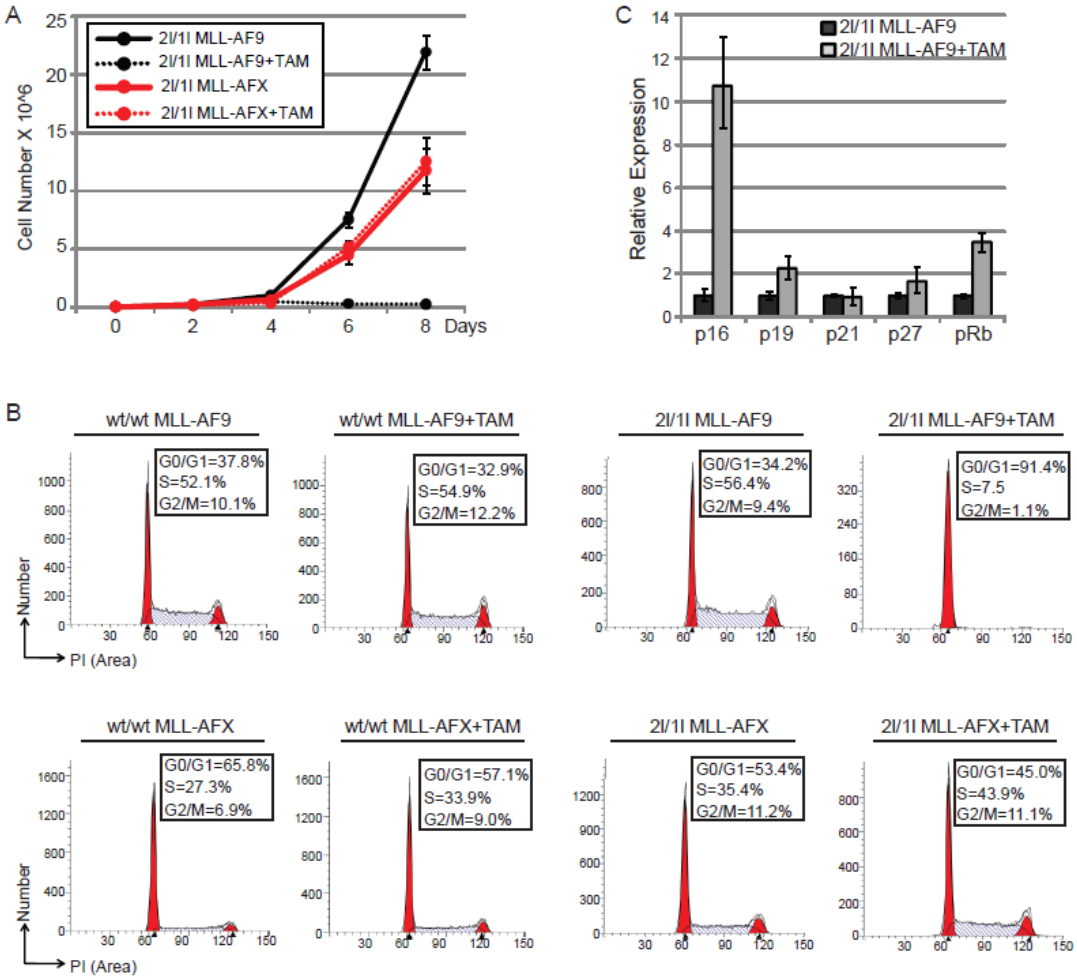

Figure 3-6. DOT1L directly regulates expression of *Hoxa* and *Meis1* genes in MLL-AF9 leukemic cells. (**A**) RT-qPCR analysis shows up-regulation of Hoxa cluster and their co-factors Meis1 and Pbx3, normalized to Gapdh, in MLL-AF9 LCs, which become down-regulated upon DOT1L deletion. (**B**) RT-qPCR analysis shows down-regulation of myeloid differentiation markers, normalized to Gapdh, in MLL-AF9 LCs, which become up-regulated upon DOT1L deletion. (**C**) ChIP analysis demonstrates that H3K79me2/3 is enriched in *Hoxa* loci in MLL-AF9 LCs compared with that in the control HPCs. IgG was used for control ChIP and amplicon positions are indicated. TSS indicates transcription start site. (**D**) ChIP analysis demonstrates that H3K79me2/3 is enriched in the *Meis1* gene in MLL-AF9 LCs compared with that in the control HPCs. IgG was used for control ChIP and amplicon positions are indicated. TSS indicates transcription start site.

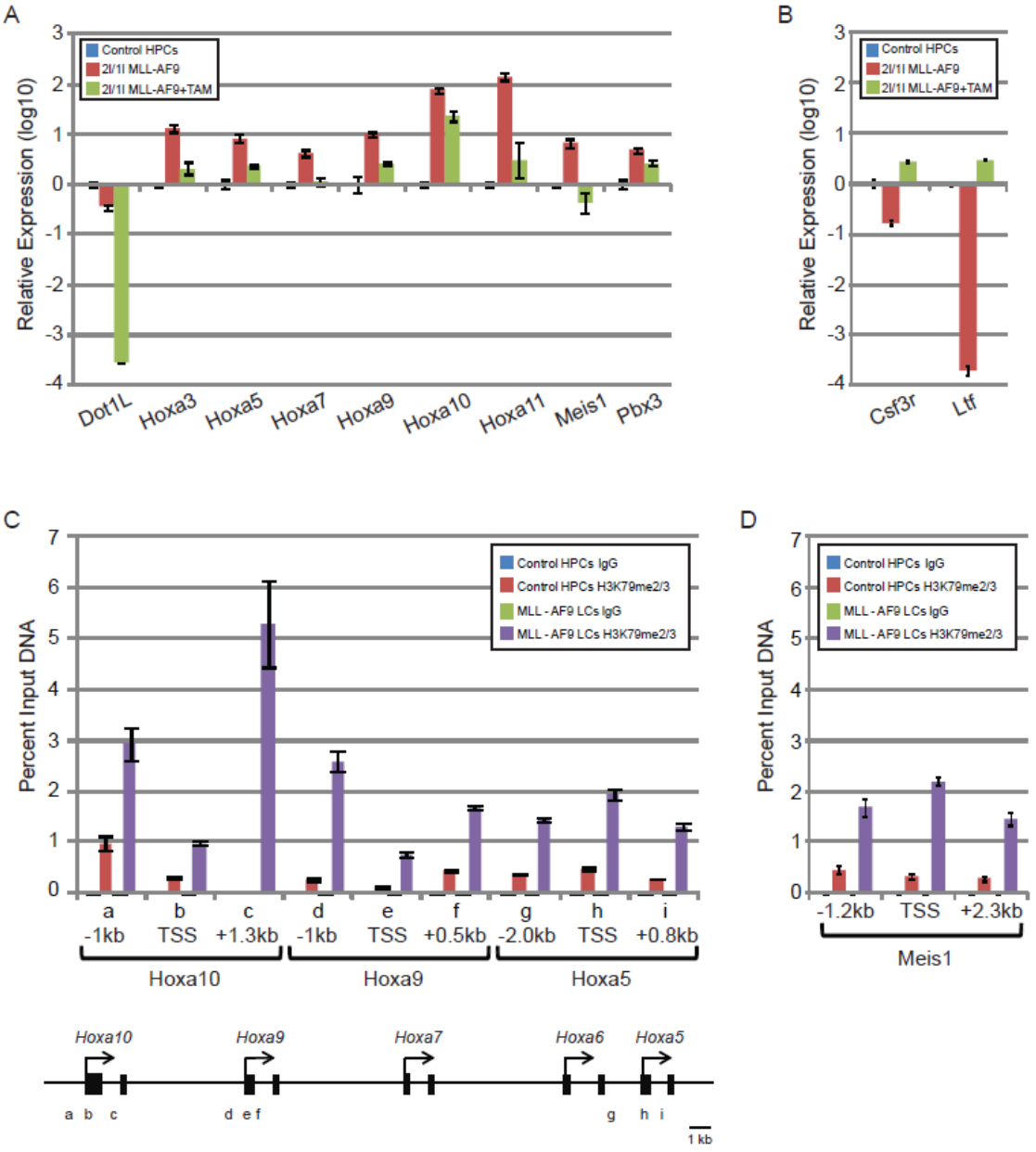
A
Control HPCs
2l/1l MLL-AF9
2l/1l MLL-AF9+TAM
Relative Expression (log10)
Dot1L
Hoxa3
Hoxa5
Hoxa7
Hoxa9
Hoxa10
Hoxa11
Meis1
Pbx3
B
Csf3r
Ltf
C
Control HPCs IgG
Control HPCs H3K79me2/3
MLL - AF9 LCs IgG
MLL - AF9 LCs H3K79me2/3
Percent Input DNA
a -1kb
b TSS
c +1.3kb
d -1kb
e TSS
f +0.5kb
g -2.0kb
h TSS
i +0.8kb
Hoxa10
Hoxa9
Hoxa5
Hoxa10
Hoxa9
Hoxa7
Hoxa6
Hoxa5
a b c
d e f
g h i
1 kb
D
-1.2kb
TSS
+2.3kb
Meis1

Figure 3-7. Model for mis-targeting of DOT1L by MLL-fusion proteins to up-regulate *Hoxa* gene expression.

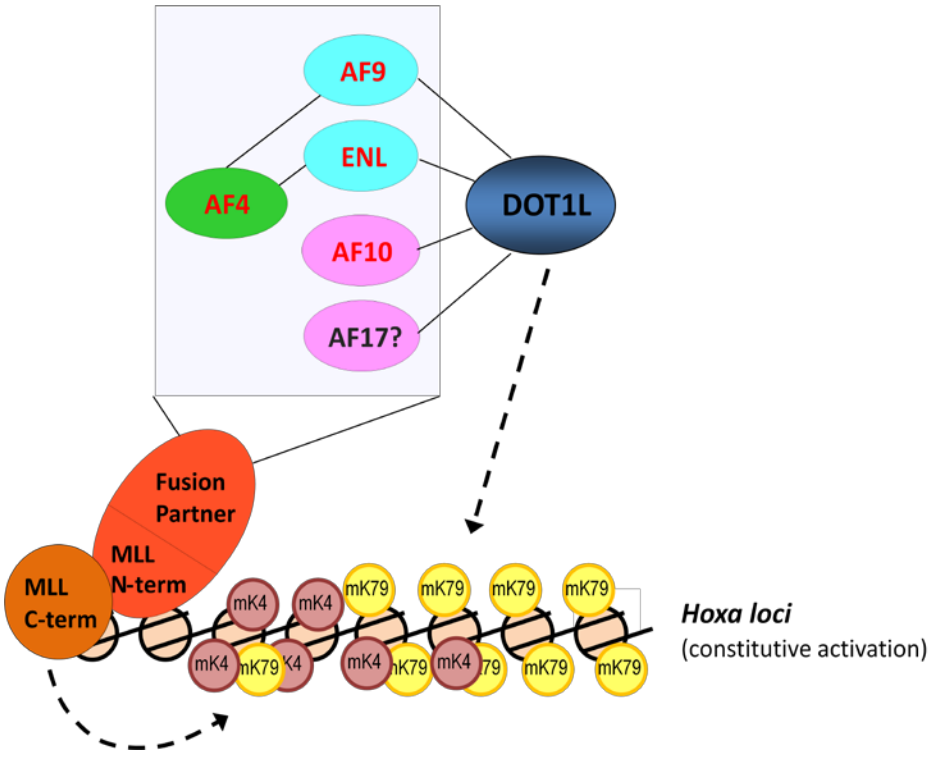

Figure S3-1. *In vivo* tamoxifen-induced recombination efficiency. DOT1L$^{2lox/1lox}$;Cre-ERT2 mice were administered TAM via intraperitoneal injection every 2 days for 3 weeks. Bone marrow cells were purified to evaluate recombination efficiency by RT-qPCR. DOT1L expression was normalized to Gapdh.

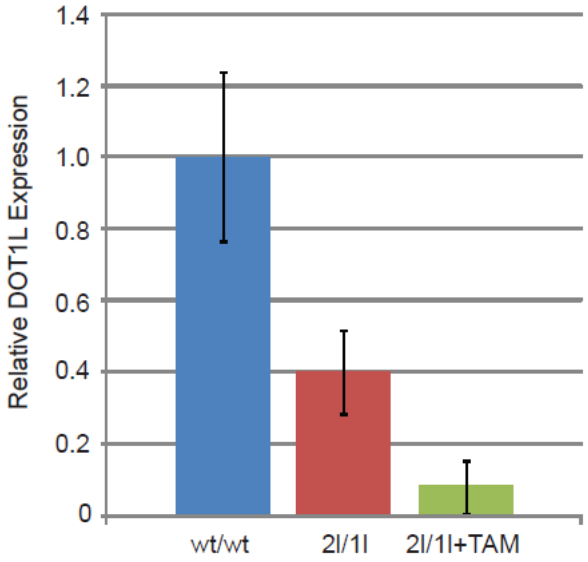

Table S3-1. Primers used for RT-qPCR gene expression analysis.

Gene	Forward Primer	Reverse Primer
DOT1L	CAGAGGATGACCTGTTTGTCG	CATCCACTTCCTGAACTCTCG
Hoxa3	CAGCACAGCCAAGAGCCCCC	GTCACCAGCGCAGCTCTCCC
Hoxa5	CCCCATTAGTGCACGAGTTTA	ACATGTACTCGGTTCCCTCCT
Hoxa7	AACCTGCCCTGCGCCTCCTA	CGCGTGTAGGTCTGGCGTCC
Hoxa9	GAGAGCGGCGGAGACAAGCC	TCGTACCTGCGGTCCCGTGT
Hoxa10	GGCACACGCGTCATCCTCGG	CCGGCCGCTCTTTGCTGTGA
Hoxa11	TGAGGACAAGGCCGGTGGCT	GCGGGACAGTTGCAGACGCT
Meis1	ACACAGTGGGGATAACAGCAG	TTTTTGTGACGCTTTTTGTCC
Pbx3	CAGCGTCTTGTGTGAGATCAA	TCTGCCAAAAGCATATTGTCC
Csf3r	ACCCAAGAGTCCCTCATCACT	CTCAGCTTGATCCAGGAGTTG
Ltf	ACCAGAGGAAGCACGGTATTT	TTGTATTCTGTCACCGGCTTC
p16	GAACTCTTTCGGTCGTACCC	CGAATCTGCACCGTAGTTGA
p19	GCTCTGGCTTTCGTGAACAT	GCAGAAGAGCTGCTACGTGA
p21	TTGCACTCTGGTGTCTGAGC	TGCGCTTGGAGTGATAGAAA
p27	AACTAACCCGGGACTTGGAG	CCAGGGGCTTATGATTCTGA
pRb	GTGAGCATCGAATCATGGAAT	TGCAGTATGGTTACCCTGGAG
Gapdh	CATGGCCTTCCGTGTTCCTA	GCCTGCTTCACCACCTTCTT

Table S3-2. Primers used for ChIP-qPCR analysis.

Primer Name	Distance from TSS	Forward Primer	Reverse Primer
Hoxa5_c4	-2.0kb	CTGCTCCCCAAGTTTTATTCC	GTTTGGACGCTTTTCCCTAAG
Hoxa5_c1	TSS	CCCCATTAGTGCACGAGTTTA	AATCACGTGCTTTTGTTGTCC
Hoxa5_c6	+0.8kb	GGTGGCCGAGTAAGTTTAAATG	CCTGACCCTGAAGAGAGTTCC
Hoxa9_c4	-1.0kb	AAGGATACCAGAGCGGTTCAT	AAATCGCCAGTCAACATCAAG
Hoxa9_c1	TSS	CTTCGTTGGCCACAATTAAAA	TGTTTTTATGCAAAGGGATCG
Hoxa9_c5	+0.5kb	CTTGTGGTTCTCCTCCAGTTG	CTCATTCTCGGCATTGTTTTC
Hoxa10_c2	-1.0kb	CCAAGGTTTTCCTTCCAGTTC	GCATACTCCCCATCCTCTACC
Hoxa10_c6	TSS	ATGTCAGCCAGAAAGGGCTAT	CTCTCCGAGCATGACATTGTT
Hoxa10_c7	+1.35kb	GCAGATAGCACGGATGTTTGT	GGGCTTATTTATTGGCTCTGG
Meis1_c2	-1.2kb	CTCTTCTTGCTCTGGCTTTGA	GGTGATGCCAAAAGTACTGGA
Meis1_c4	TSS	GGGGGAGTTTGCATATTTGTT	CTCTGGCTCCCTTCCTACTTC
Meis1_c6	+2.3kb	GAGTGGCCGTCTAAAGATTCC	CGAGCTAAGTCTAGCGAGCAA

References

Argiropoulos B, Humphries RK. 2007. Hox genes in hematopoiesis and leukemogenesis. *Oncogene* **26**: 6766-6776.

Ayton PM, Cleary ML. 2001. Molecular mechanisms of leukemogenesis mediated by MLL fusion proteins. *Oncogene* **20**: 5695-5707.

Barry ER, Krueger W, Jakuba CM, Veilleux E, Ambrosi DJ, Nelson CE, Rasmussen TP. 2009. ES cell cycle progression and differentiation require the action of the histone methyltransferase Dot1L. *Stem Cells* **27**: 1538-1547.

Bitoun E, Oliver PL, Davies KE. 2007. The mixed-lineage leukemia fusion partner AF4 stimulates RNA polymerase II transcriptional elongation and mediates coordinated chromatin remodeling. *Hum Mol Genet* **16**: 92-106.

Caslini C, Yang Z, El-Osta M, Milne TA, Slany RK, Hess JL. 2007. Interaction of MLL amino terminal sequences with menin is required for transformation. *Cancer Res* **67**: 7275-7283.

Chang MJ, Wu H, Achille NJ, Reisenauer MR, Chou CW, Zeleznik-Le NJ, Hemenway CS, Zhang W. 2010. Histone H3 lysine 79 methyltransferase Dot1 is required for immortalization by MLL oncogenes. *Cancer Res* **70**: 10234-10242.

Chen YX, Yan J, Keeshan K, Tubbs AT, Wang H, Silva A, Brown EJ, Hess JL, Pear WS, Hua X. 2006. The tumor suppressor menin regulates hematopoiesis and myeloid transformation by influencing Hox gene expression. *Proc Natl Acad Sci U S A* **103**: 1018-1023.

Daser A, Rabbitts TH. 2004. Extending the repertoire of the mixed-lineage leukemia gene MLL in leukemogenesis. *Genes Dev* **18**: 965-974.

Erfurth F, Hemenway CS, de Erkenez AC, Domer PH. 2004. MLL fusion partners AF4 and AF9 interact at subnuclear foci. *Leukemia* **18**: 92-102.

Faber J, Krivtsov AV, Stubbs MC, Wright R, Davis TN, van den Heuvel-Eibrink M, Zwaan CM, Kung AL, Armstrong SA. 2009. HOXA9 is required for survival in human MLL-rearranged acute leukemias. *Blood* **113**: 2375-2385.

Feng Q, Wang H, Ng HH, Erdjument-Bromage H, Tempst P, Struhl K, Zhang Y. 2002. Methylation of H3-lysine 79 is mediated by a new family of HMTases without a SET domain. *Curr Biol* **12**: 1052-1058.

Feng Y, Yang Y, Ortega MM, Copeland JN, Zhang M, Jacob JB, Fields TA, Vivian JL, Fields PE. 2010. Early mammalian erythropoiesis requires the Dot1L methyltransferase. *Blood*.

Guenther MG, Jenner RG, Chevalier B, Nakamura T, Croce CM, Canaani E, Young RA. 2005. Global and Hox-specific roles for the MLL1 methyltransferase. *Proc Natl Acad Sci U S A* **102**: 8603-8608.

Guenther MG, Lawton LN, Rozovskaia T, Frampton GM, Levine SS, Volkert TL, Croce CM, Nakamura T, Canaani E, Young RA. 2008. Aberrant chromatin at genes encoding stem cell regulators in human mixed-lineage leukemia. *Genes Dev* **22**: 3403-3408.

Hess JL. 2004. MLL: a histone methyltransferase disrupted in leukemia. *Trends Mol Med* **10**: 500-507.

Hsieh JJ, Cheng EH, Korsmeyer SJ. 2003a. Taspase1: a threonine aspartase required for cleavage of MLL and proper HOX gene expression. *Cell* **115**: 293-303.

Hsieh JJ, Ernst P, Erdjument-Bromage H, Tempst P, Korsmeyer SJ. 2003b. Proteolytic cleavage of MLL generates a complex of N- and C-terminal fragments that confers protein stability and subnuclear localization. *Mol Cell Biol* **23**: 186-194.

Jones B, Su H, Bhat A, Lei H, Bajko J, Hevi S, Baltus GA, Kadam S, Zhai H, Valdez R et al. 2008. The histone H3K79 methyltransferase Dot1L is essential for mammalian development and heterochromatin structure. *PLoS Genet* **4**: e1000190.

Kouzarides T. 2007. Chromatin modifications and their function. *Cell* **128**: 693-705.

Krivtsov AV, Armstrong SA. 2007. MLL translocations, histone modifications and leukaemia stem-cell development. *Nat Rev Cancer* **7**: 823-833.

Krivtsov AV, Feng Z, Lemieux ME, Faber J, Vempati S, Sinha AU, Xia X, Jesneck J, Bracken AP, Silverman LB et al. 2008. H3K79 methylation profiles define murine and human MLL-AF4 leukemias. *Cancer Cell* **14**: 355-368.

Krivtsov AV, Twomey D, Feng Z, Stubbs MC, Wang Y, Faber J, Levine JE, Wang J, Hahn WC, Gilliland DG et al. 2006. Transformation from committed progenitor to leukaemia stem cell initiated by MLL-AF9. *Nature* **442**: 818-822.

Krogan NJ, Dover J, Wood A, Schneider J, Heidt J, Boateng MA, Dean K, Ryan OW, Golshani A, Johnston M et al. 2003. The Paf1 complex is required for histone H3 methylation by COMPASS and Dot1p: linking transcriptional elongation to histone methylation. *Mol Cell* **11**: 721-729.

Lacoste N, Utley RT, Hunter JM, Poirier GG, Cote J. 2002. Disruptor of telomeric silencing-1 is a chromatin-specific histone H3 methyltransferase. *J Biol Chem* **277**: 30421-30424.

Li ZY, Liu DP, Liang CC. 2005. New insight into the molecular mechanisms of MLL-associated leukemia. *Leukemia* **19**: 183-190.

Lin C, Smith ER, Takahashi H, Lai KC, Martin-Brown S, Florens L, Washburn MP, Conaway JW, Conaway RC, Shilatifard A. 2010. AFF4, a component of the ELL/P-TEFb elongation complex and a shared subunit of MLL chimeras, can link transcription elongation to leukemia. *Mol Cell* **37**: 429-437.

Lukas J, Parry D, Aagaard L, Mann DJ, Bartkova J, Strauss M, Peters G, Bartek J. 1995. Retinoblastoma-protein-dependent cell-cycle inhibition by the tumour suppressor p16. *Nature* **375**: 503-506.

Martin C, Zhang Y. 2005. The diverse functions of histone lysine methylation. *Nat Rev Mol Cell Biol* **6**: 838-849.

Medema RH, Herrera RE, Lam F, Weinberg RA. 1995. Growth suppression by p16ink4 requires functional retinoblastoma protein. *Proc Natl Acad Sci U S A* **92**: 6289-6293.

Milne TA, Kim J, Wang GG, Stadler SC, Basrur V, Whitcomb SJ, Wang Z, Ruthenburg AJ, Elenitoba-Johnson KS, Roeder RG et al. 2010. Multiple interactions recruit MLL1 and MLL1 fusion proteins to the HOXA9 locus in leukemogenesis. *Mol Cell* **38**: 853-863.

Mohan M, Herz HM, Takahashi YH, Lin C, Lai KC, Zhang Y, Washburn MP, Florens L, Shilatifard A. 2010. Linking H3K79 trimethylation to Wnt signaling through a novel Dot1-containing complex (DotCom). *Genes Dev* **24**: 574-589.

Monroe SC, Jo SY, Sanders DS, Basrur V, Elenitoba-Johnson KS, Slany RK, Hess JL. 2011. MLL-AF9 and MLL-ENL alter the dynamic association of transcriptional regulators with genes critical for leukemia. *Exp Hematol* **39**: 77-86 e71-75.

Mueller D, Bach C, Zeisig D, Garcia-Cuellar MP, Monroe S, Sreekumar A, Zhou R, Nesvizhskii A, Chinnaiyan A, Hess JL et al. 2007. A role for the MLL fusion partner ENL in transcriptional elongation and chromatin modification. *Blood* **110**: 4445-4454.

Mueller D, Garcia-Cuellar MP, Bach C, Buhl S, Maethner E, Slany RK. 2009. Misguided transcriptional elongation causes mixed lineage leukemia. *PLoS Biol* **7**: e1000249.

Muntean AG, Tan J, Sitwala K, Huang Y, Bronstein J, Connelly JA, Basrur V, Elenitoba-Johnson KS, Hess JL. 2010. The PAF complex synergizes with MLL fusion proteins at HOX loci to promote leukemogenesis. *Cancer Cell* **17**: 609-621.

Okada Y, Feng Q, Lin Y, Jiang Q, Li Y, Coffield VM, Su L, Xu G, Zhang Y. 2005. hDOT1L links histone methylation to leukemogenesis. *Cell* **121**: 167-178.

Okada Y, Jiang Q, Lemieux M, Jeannotte L, Su L, Zhang Y. 2006. Leukaemic transformation by CALM-AF10 involves upregulation of Hoxa5 by hDOT1L. *Nat Cell Biol* **8**: 1017-1024.

Schubeler D, MacAlpine DM, Scalzo D, Wirbelauer C, Kooperberg C, van Leeuwen F, Gottschling DE, O'Neill LP, Turner BM, Delrow J et al. 2004. The histone modification pattern of active genes revealed through genome-wide chromatin analysis of a higher eukaryote. *Genes Dev* **18**: 1263-1271.

Singer MS, Kahana A, Wolf AJ, Meisinger LL, Peterson SE, Goggin C, Mahowald M, Gottschling DE. 1998. Identification of high-copy disruptors of telomeric silencing in Saccharomyces cerevisiae. *Genetics* **150**: 613-632.

Slany RK. 2005. When epigenetics kills: MLL fusion proteins in leukemia. *Hematol Oncol* **23**: 1-9.

Somervaille TC, Cleary ML. 2006. Identification and characterization of leukemia stem cells in murine MLL-AF9 acute myeloid leukemia. *Cancer Cell* **10**: 257-268.

Srinivasan RS, Nesbit JB, Marrero L, Erfurth F, LaRussa VF, Hemenway CS. 2004. The synthetic peptide PFWT disrupts AF4-AF9 protein complexes and induces apoptosis in t(4;11) leukemia cells. *Leukemia* **18**: 1364-1372.

Steger DJ, Lefterova MI, Ying L, Stonestrom AJ, Schupp M, Zhuo D, Vakoc AL, Kim JE, Chen J, Lazar MA et al. 2008. DOT1L/KMT4 recruitment and H3K79 methylation are ubiquitously coupled with gene transcription in mammalian cells. *Mol Cell Biol* **28**: 2825-2839.

Thiel AT, Blessington P, Zou T, Feather D, Wu X, Yan J, Zhang H, Liu Z, Ernst P, Koretzky GA et al. 2010. MLL-AF9-induced leukemogenesis requires coexpression of the wild-type Mll allele. *Cancer Cell* **17**: 148-159.

Thorsteinsdottir U, Sauvageau G, Hough MR, Dragowska W, Lansdorp PM, Lawrence HJ, Largman C, Humphries RK. 1997. Overexpression of HOXA10 in murine hematopoietic cells perturbs both myeloid and lymphoid differentiation and leads to acute myeloid leukemia. *Mol Cell Biol* **17**: 495-505.

van Leeuwen F, Gafken PR, Gottschling DE. 2002. Dot1p modulates silencing in yeast by methylation of the nucleosome core. *Cell* **109**: 745-756.

Ventura A, Kirsch DG, McLaughlin ME, Tuveson DA, Grimm J, Lintault L, Newman J, Reczek EE, Weissleder R, Jacks T. 2007. Restoration of p53 function leads to tumour regression in vivo. *Nature* **445**: 661-665.

Wong P, Iwasaki M, Somervaille TC, So CW, Cleary ML. 2007. Meis1 is an essential and rate-limiting regulator of MLL leukemia stem cell potential. *Genes Dev* **21**: 2762-2774.

Wood A, Schneider J, Dover J, Johnston M, Shilatifard A. 2003. The Paf1 complex is essential for histone monoubiquitination by the Rad6-Bre1 complex, which signals for histone methylation by COMPASS and Dot1p. *J Biol Chem* **278**: 34739-34742.

Yokoyama A, Lin M, Naresh A, Kitabayashi I, Cleary ML. 2010. A higher-order complex containing AF4 and ENL family proteins with P-TEFb facilitates oncogenic and physiologic MLL-dependent transcription. *Cancer Cell* **17**: 198-212.

Yokoyama A, Somervaille TC, Smith KS, Rozenblatt-Rosen O, Meyerson M, Cleary ML. 2005. The menin tumor suppressor protein is an essential oncogenic cofactor for MLL-associated leukemogenesis. *Cell* **123**: 207-218.

Zeisig DT, Bittner CB, Zeisig BB, Garcia-Cuellar MP, Hess JL, Slany RK. 2005. The eleven-nineteen-leukemia protein ENL connects nuclear MLL fusion partners with chromatin. *Oncogene* **24**: 5525-5532.

Zhang W, Xia X, Reisenauer MR, Hemenway CS, Kone BC. 2006. Dot1a-AF9 complex mediates histone H3 Lys-79 hypermethylation and repression of ENaCalpha in an aldosterone-sensitive manner. *J Biol Chem* **281**: 18059-18068.

Chapter 4

PERSPECTIVES AND FUTURE DIRECTIONS

DOT1L and the mammalian cell cycle

The studies herein provide a small glimpse of the many functions of mammalian DOT1L. Without a doubt DOT1L is a critical enzyme for both normal biological and oncogenic processes. However, a great deal of information remains to be elucidated. For instance, exactly what part does DOT1L play in regulating cell cycle progression and the DNA damage response in mammalian cells? In yeast, Dot1 is a vital component of DNA damage repair pathways, but does this role translate into mammals?

Thus far, several observations suggest mechanisms exist in mammalian cells involving DOT1L-mediated H3K79 methylation in checkpoint response and DNA replication. DOT1L knockout (KO) mouse embryonic stem (ES) cells exhibit a G2 arrest (Jones, Su et al. 2008) and aneuploidy, while KO erythroid progenitor cells undergo G1 arrest (Feng, Yang et al. 2010). On the other hand, loss of DOT1L in cardiomyocytes and C2C12 myoblasts did not impair cell proliferation (Nguyen, Xiao et al. 2011). Of noteworthy, H3K79me2 patterns are also different between yeast and human. In HeLa cells, H3K79me2 is high in G1, decreases in S, reaches lowest point in G2, and increases again in M phase (Feng, Wang et al. 2002). However, in yeast, H3K79me2 is low in G1 and S, begins to increase in late S, and is maintained in G2 and M phases (Schulze, Jackson et al. 2009). It is apparent that mammalian DOT1L plays distinct cell type specific roles in regulating cell cycle progression. Additionally, these data suggest that not all functions of Dot1 are evolutionarily conserved from yeast to humans. Further studies are required to determine which DNA repair mechanisms involving DOT1L are conserved and to dissect the role of every H3K79 methylation state during each phase of the mammalian cell cycle.

Maintaining telomere length in DOT1L-deficient cells

A second area of divergence between yeast Dot1 and mammalian DOT1L is their role in telomere silencing. In yeast, Dot1 and its associated H3K79 methylation mark block SIR protein binding. In the absence of Dot1, SIR protein spreading occurs, diluting their ability to effectively maintain telomere silencing and, subsequently, reducing telomere lengths (Singer, Kahana et al. 1998; Ng, Feng et al. 2002; Ng, Ciccone et al. 2003). Surprisingly, ES cells derived from DOT1L KO embryos have longer, heterogeneous telomeres compared to wild type and heterozygote cells (Jones, Su et al. 2008). The aberrant telomere elongation observed in KO cells was attributed to activation of the alternative lengthening of telomere (ALT) pathway (Jones, Su et al. 2008). The ALT pathway utilizes homologous recombination for maintaining telomeres and can be activated in a number of human somatic cells and immortalized cells in response to reduced telomerase activity and to by-pass the end-replication problem (Bryan, Englezou et al. 1995; Bryan, Englezou et al. 1997; Henson, Neumann et al. 2002).

Yeast cells that lack telomerase for maintaining telomere length die within 50-100 cell divisions. However, a small fraction of these cells can survive through two different mechanisms. Type I survivors use amplification of subtelomeric regions to maintain short telomeres (Lundblad and Blackburn 1993). Alternatively, type II survivors use the ALT pathway, acquiring a heterogeneous pool of long telomeres (Teng and Zakian 1999). In addition, Teng and Zakian demonstrate that type I survivors often convert to the ALT pathway to maintain telomere length (Teng and Zakian 1999). If the ALT pathway exists in yeast, it is unclear why it is not activated to by-pass the effects of Dot1 deletion for

regulating telomere length as is observed in DOT1L KO mouse ES cells. The inconsistency in telomere regulation upon loss of yeast Dot1 and mouse DOT1L signifies the need for more in-depth analysis of mammalian DOT1L.

DOT1L as a therapeutic target to treat MLL-related leukemias

Chromosomal rearrangement of the Philadelphia chromosome in chronic myeloid leukemia (CML) was first identified in 1973, and the protein product, Bcr-Abl, was demonstrated to be the causative agent in 1990. The oncogenic function of Bcr-Abl is mediated by the constitutively active tyrosine kinase domain of Abl. In 1996, Imatinib (also known as Gleevec), a 2-phenyaminopyrimidine derivative, was discovered as a selective inhibitor of tyrosine kinase activity of Bcr-Abl, platelet-derived growth factor (PDGF-R), and c-Kit. Surprisingly, the drug had no effect on normal cells and is well tolerated with minor side effects. Therefore, in December of 2002, Imatinib was FDA approved for targeted therapy to treat human CML (Deininger and Druker 2003).

The first 11q23 rearrangement in acute leukemia was identified in 1985. In 1992, several labs mapped the chromosomal breakpoint region at 11q23 to the *MLL* gene, a homolog of the *Drosophila* gene *trithorax* (Gu, Nakamura et al. 1992; McCabe, Burnett et al. 1992; Tkachuk, Kohler et al. 1992). Although it has been almost two decades since the discovery of *MLL* rearrangements as a cause of acute leukemias, no effective target-based therapy has been developed. The lack of targeted therapeutics to treat MLL-related leukemias may be due to the large heterogeneity of *MLL* rearrangements (over 50 different translocation partners). Mounting evidence supports a universal mechanism by which oncogenic MLL-fusion

proteins mistarget DOT1L to *Hoxa* and *Meis1* genes for H3K79 hypermethylation, up-regulation, and leukemogenesis. In this dissertation, I demonstrated for the first time that DOT1L activity is essential for acute myeloid leukemia development and progression in the mouse. These data suggest that targeting DOT1L may be an effective therapeutic to treat the majority of MLL-related leukemias.

Due to the unique structure of DOT1L's catalytic domain compared to all other histone lysine methyltransferases (Min, Feng et al. 2003), the ability to generate specific inhibitors of DOT1L HMTase activity is feasible. Unfortunately, at least in the mouse, DOT1L is an essential enzyme required for development (Jones, Su et al. 2008), ES cell maintenance (Jones, Su et al. 2008; Barry, Krueger et al. 2009), cardiac function (Nguyen, Xiao et al. 2011), and hematopoiesis (Feng, Yang et al. 2010). Leukemia patients treated with DOT1L inhibitors may develop adverse side effects, including anemia and heart disease. Therefore, any drug designed to inhibit DOT1L enzymatic activity for the treatment of MLL-related leukemias must be carefully and thoroughly characterized both *in vitro* and *in vivo* long term. It is my hope that one day, a drug will be developed that specifically targets DOT1L in leukemic cells, leaving normal cells unscathed, reminiscent of Imatinib.

References

Barry, E. R., W. Krueger, et al. (2009). "ES cell cycle progression and differentiation require the action of the histone methyltransferase Dot1L." Stem Cells **27**(7): 1538-1547.

Bryan, T. M., A. Englezou, et al. (1997). "Evidence for an alternative mechanism for maintaining telomere length in human tumors and tumor-derived cell lines." Nat Med **3**(11): 1271-1274.

Bryan, T. M., A. Englezou, et al. (1995). "Telomere elongation in immortal human cells without detectable telomerase activity." EMBO J **14**(17): 4240-4248.

Deininger, M. W. and B. J. Druker (2003). "Specific targeted therapy of chronic myelogenous leukemia with imatinib." Pharmacol Rev **55**(3): 401-423.

Feng, Q., H. Wang, et al. (2002). "Methylation of H3-lysine 79 is mediated by a new family of HMTases without a SET domain." Curr Biol **12**(12): 1052-1058.

Feng, Y., Y. Yang, et al. (2010). "Early mammalian erythropoiesis requires the Dot1L methyltransferase." Blood.

Gu, Y., T. Nakamura, et al. (1992). "The t(4;11) chromosome translocation of human acute leukemias fuses the ALL-1 gene, related to Drosophila trithorax, to the AF-4 gene." Cell **71**(4): 701-708.

Henson, J. D., A. A. Neumann, et al. (2002). "Alternative lengthening of telomeres in mammalian cells." Oncogene **21**(4): 598-610.

Jones, B., H. Su, et al. (2008). "The histone H3K79 methyltransferase Dot1L is essential for mammalian development and heterochromatin structure." PLoS Genet **4**(9): e1000190.

Lundblad, V. and E. H. Blackburn (1993). "An alternative pathway for yeast telomere maintenance rescues est1- senescence." Cell **73**(2): 347-360.

McCabe, N. R., R. C. Burnett, et al. (1992). "Cloning of cDNAs of the MLL gene that detect DNA rearrangements and altered RNA transcripts in human leukemic cells with 11q23 translocations." Proc Natl Acad Sci U S A **89**(24): 11794-11798.

Min, J., Q. Feng, et al. (2003). "Structure of the catalytic domain of human DOT1L, a non-SET domain nucleosomal histone methyltransferase." Cell **112**(5): 711-723.

Ng, H. H., D. N. Ciccone, et al. (2003). "Lysine-79 of histone H3 is hypomethylated at silenced loci in yeast and mammalian cells: a potential mechanism for position-effect variegation." Proc Natl Acad Sci U S A **100**(4): 1820-1825.

Ng, H. H., Q. Feng, et al. (2002). "Lysine methylation within the globular domain of histone H3 by Dot1 is important for telomeric silencing and Sir protein association." Genes Dev **16**(12): 1518-1527.

Nguyen, A. T., B. Xiao, et al. (2011). "DOT1L regulates dystrophin expression and is critical for cardiac function." Genes Dev **25**(3): 263-274.

Schulze, J. M., J. Jackson, et al. (2009). "Linking cell cycle to histone modifications: SBF and H2B monoubiquitination machinery and cell-cycle regulation of H3K79 dimethylation." Mol Cell **35**(5): 626-641.

Singer, M. S., A. Kahana, et al. (1998). "Identification of high-copy disruptors of telomeric silencing in Saccharomyces cerevisiae." Genetics **150**(2): 613-632.

Teng, S. C. and V. A. Zakian (1999). "Telomere-telomere recombination is an efficient bypass pathway for telomere maintenance in Saccharomyces cerevisiae." Mol Cell Biol **19**(12): 8083-8093.

Tkachuk, D. C., S. Kohler, et al. (1992). "Involvement of a homolog of Drosophila trithorax by 11q23 chromosomal translocations in acute leukemias." Cell **71**(4): 691-700.